AD-A084 661 NEWMARK (NATHAN M) CONSULTING ENGINEERING SERVICES U--ETC F/G 13/13
BEHAVIOR OF RESTRAINED TWO-WAY SLABS.(U)
FEB 79 J D HALTIWANGER, W J HALL, N M NEWMARK DNA001-78-C-0300

UNCLASSIFIED DNA-4959Z NL

1 OF 1
AD
A084661

END
DATE
FILMED
6-80
DTIC

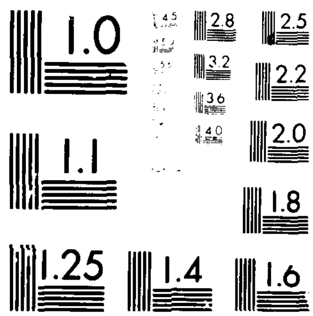

MICROCOPY RESOLUTION TEST CHART
NATIONAL BUREAU OF STANDARDS-1963-A

LEVEL III

AD-E300756

(12)

DNA 4959Z

ADA084661

BEHAVIOR OF RESTRAINED TWO-WAY SLABS

J. D. Haltiwanger
In Cooperation with
W. J. Hall and N. M. Newmark
Nathan M. Newmark
Consulting Engineering Services
1211 Civil Engineering Building
Urbana, Illinois 61801

22 February 1979

Interim Report for Period 1 September 1978—22 February 1979

CONTRACT No. DNA 001-78-C-0300

APPROVED FOR PUBLIC RELEASE;
DISTRIBUTION UNLIMITED.

THIS WORK SPONSORED BY THE DEFENSE NUCLEAR AGENCY
UNDER RDT&E RMSS CODE B344078464 V99QAXSC06163 H2590D.

Prepared for
Director
DEFENSE NUCLEAR AGENCY
Washington, D. C. 20305

DDC FILE COPY

DTIC
ELECTE
MAY 27 1980
S D
D

80 4 4 066

Destroy this report when it is no longer needed. Do not return to sender.

PLEASE NOTIFY THE DEFENSE NUCLEAR AGENCY, ATTN: STTI, WASHINGTON, D.C. 20305, IF YOUR ADDRESS IS INCORRECT, IF YOU WISH TO BE DELETED FROM THE DISTRIBUTION LIST, OR IF THE ADDRESSEE IS NO LONGER EMPLOYED BY YOUR ORGANIZATION.

REPORT DOCUMENTATION PAGE

READ INSTRUCTIONS BEFORE COMPLETING FORM

1. REPORT NUMBER: DNA 4959Z	2. GOVT ACCESSION NO.: AD-A084 661
3. RECIPIENT'S CATALOG NUMBER:	
4. TITLE (and Subtitle): BEHAVIOR OF RESTRAINED TWO-WAY SLABS	5. TYPE OF REPORT & PERIOD COVERED: Interim Report for Period 1 Sep 78—22 Feb 79
	6. PERFORMING ORG. REPORT NUMBER
7. AUTHOR(s): J. D. Haltiwanger, in cooperation with W. J. Hall and N. M. Newmark	8. CONTRACT OR GRANT NUMBER(s): DNA 001-78-C-0300
9. PERFORMING ORGANIZATION NAME AND ADDRESS: Nathan M. Newmark, Consulting Engineering Services, 1211 Civil Engineering Building, Urbana, Illinois 61801	10. PROGRAM ELEMENT, PROJECT, TASK AREA & WORK UNIT NUMBERS: Subtask V99QAXSC061-63
11. CONTROLLING OFFICE NAME AND ADDRESS: Director, Defense Nuclear Agency, Washington, D.C. 20305	12. REPORT DATE: 22 February 1979
	13. NUMBER OF PAGES: 80
14. MONITORING AGENCY NAME & ADDRESS (if different from Controlling Office)	15. SECURITY CLASS (of this report): UNCLASSIFIED
	15a. DECLASSIFICATION/DOWNGRADING SCHEDULE

16. DISTRIBUTION STATEMENT (of this Report)

Approved for public release; distribution unlimited.

17. DISTRIBUTION STATEMENT (of the abstract entered in Block 20, if different from Report)

18. SUPPLEMENTARY NOTES

This work sponsored by the Defense Nuclear Agency under RDT&E RMSS Code B344078464 V99QAXSC06163 H2590D.

19. KEY WORDS (Continue on reverse side if necessary and identify by block number)

Reinforced Concrete	Large Deformation Behavior
Two-Way Slabs	Membrane Behavior
Resistance-Displacement Functions	Edge Restraint Effects

20. ABSTRACT (Continue on reverse side if necessary and identify by block number)

In many DOD applications, reinforced concrete slab-type structures are frequently not considered to have failed until deflections have reached values far beyond those that correspond to maximum resistance, but present analytical procedures, especially for dynamic loading conditions, do not adequately reflect the actual resistance deformation relations of slabs under large deflection conditions.

20. ABSTRACT (Continued)

The purpose of this work was to study the results of an earlier series of tests of small scale, laterally restrained two-way slabs, whose behaviors under uniform transverse load were measured out to the point of collapse, in an effort to formulate procedures for the prediction of the resistance functions for such slabs throughout their total response histories. While this objective was not fully met, it was found that present procedures are generally adequate to define the maximum resistance levels of such slabs. Additionally, detailed analysis of the experimental data suggests strongly the existence of systematic relationships which, when evaluated, will provide a basis for the prediction of large deflection slab behavior.

Summary

The purpose of this study was to investigate our ability, on the basis of presently available theory and experimental data, to define the resistance-deformation relationships of reinforced concrete slabs throughout their response histories to uniformly applied transverse loads, up to the point of final collapse. To accomplish this, currently available procedures for the prediction of the resistance-deflection relationships for two-way slabs were compared with the experimental results obtained from a series of small-scale slab tests that were conducted in 1965 at M.I.T. by Brotchie, Jacobson, and Okubo under contract with the U.S. Naval Civil Engineering Laboratory. In that test series, load-deflection data were taken throughout the response histories, up to and including collapse.

It is concluded from this study that the load-deflection of a two-way slab can be reasonably approximated by a multi-linear function that is defined by initial elastic behavior, followed successively by regions of constant *maximum resistance*, plastic decay resistance and, finally, by the development of resistance in the domain of membrane response of large deflection. However, while present procedures do generally define adequately the small-deflection portions of such a resistance function, they are inadequate as a basis for the prediction of large deflection behavior. But the nature of the observed response in the large deflection domain suggested strongly the existence of systematic relationships which, when defined, will permit the reliable prediction of large deflection response.

Accession For
NTIS GRA&I X
DDC TAB
Unannounced
Justification

By
Distribution/
Availability Codes
Dist. | Avail and/or special
A

DTIC
ELECTE
MAY 27 1980
S D
D

Preface

This report was prepared in summary of a part of the work accomplished by Nathan M. Newmark, Consulting Engineering Services, under Contract No. DNA 001-78-C-0300 for the Defense Nuclear Agency under RDT&E RMSS Code B344078464 V99QAXSC061-63 H2590D. The work reported herein was done by J. D. Haltiwanger, with the advice and cooperation of W. J. Hall and N. M. Newmark.

For background data, this work draws heavily on material contained in Report R65-25, "Effect of Membrane Action on Slab Behavior", by John F. Brotchie, Ammon Jacobson, and Sadaji Okubo, of the Department of Civil Engineering, Massachusetts Institute of Technology, which was published in August 1965. That research was supported by the U.S. Naval Civil Engineering Laboratory under Contract No. NBy-32243. For convenience of reference, and with the verbal approval of Dr. Warren A. Shaw, Head, Department of Civil Engineering, U.S. Naval Civil Engineering Laboratory, portions of the referenced report are reproduced herein. Such reproduced segments are specifically identified where they occur.

Conversion Factors for U.S. Customary to Metric (SI) Units of Measurement

To Convert from	To	Multiply by
inch	meter	2.540 000 x E-2
pounds/inch	newton/meter	1.751 268 x E+2
kips/sq in. (ksi)	kilo pascal	6.894 757 x E+3
pounds/sq in. (psi)	kilo pascal	6.894 757

Table of Contents

Behavior of Restrained Two-Way Slabs

Introduction:

In many DOD applications, reinforced concrete slab-type structures are frequently not considered to have failed until deflections have reached values far beyond those that correspond to maximum flexural resistance. Hence, to analyze slabs that are expected to sustain such large deflections, it is necessary that their load-deflection curves be defined throughout their response histories. Unfortunately, however, very little is known of the large-deflection behavior of slabs.

Perhaps the most extensive such study was conducted by Holley and Brotchie at M.I.T. in 1965 (Ref. 1). While the primary objective of that study was to investigate the effects of in-plane edge restraint on the maximum resistance of square two-way slabs, load-deflection data were also taken in the plastic decay and tensile membrane recovery domains of response. Because of the edge-restraint conditions imposed on these slabs, it is clear that they are not "typical" of a panel in a continuous slab structure. Nevertheless, they constitute a relatively large series of comparable slabs, tested under comparable conditions, the data from which might be useful as a basis for the study of large deflection slab behavior.

The slabs being studied were square, two-way slabs, 15" x 15" in clear span, with thicknesses of 0.75", 1.50" and 3.00", and with positive moment reinforcement ratios of 0.00, 0.005, 0.01, 0.02, and 0.03 for each of the three thicknesses. Complete descriptions of the slab specimens and the test apparatus and procedures used are given in the Appendix, which includes Chap. II, Table I, and Figs. 1, 2 and 3 of Ref. 1.

The slabs of particular interest here are those that are identified as being of Types I and II in the MIT study. Within the limits of experimental variations, the slabs of these two types were identical except that, for slabs of Type II, half of the reinforcement (alternate bars) was bent up near the supports to provide greater resistance to shear failure. In both cases, resistance to lateral (in-plane) displacement of the slabs was provided near the bottoms of the slabs approximately at the locations of the reinforcement. Except for the provision of resistance to lateral deformation, the slabs were all simply supported and they were tested under uniformly distributed hydrostatic pressures.

The properties of these slabs, together with a summary of the significant data taken in the tests conducted on them, are given in Table I, and their measured load-center deflection curves are reproduced herein as Figs. 1 through 6, which are, respectively, Figs. 5, 6, 9, 10, 13 and 14 of Ref. 1. The objective of the study reported herein was to formulate a procedure whereby the load-deflection curves could be reasonably but simply defined in terms of their properties.

To facilitate the individual study of these load-deflection curves, they are plotted separately in Figs. 7 through 37. As is evident, these curves are of the general shape shown in Fig. 38, and can be represented adequately by the following four straight-line segments:

OA - A linear rise from 0 to maximum resistance

AB - A short horizontal segment for which the resistance is constant at its maximum value

BC - A linear decay segment

and CD - A straight line that represents the development of increased strength as the slab responds in tensile membrane action under large deflections

Procedures now in common use attempt to define only the initial linear rise to maximum resistance (OA) and the short horizontal segment (AB) during which the resistance is assumed to remain constant. And, as will be demonstrated subsequently, these presently used procedures represent adequately only the maximum resistances of the slabs, test results of which are being reviewed herein.

Maximum Resistance

The procedures presented in Ref. (2) for the prediction of the ultimate flexural capacities of two-way slabs, including the effects of in-plane forces, were applied to slabs considered herein and the results are identified as q_{yf} in Table II. The ratios of the measured resistances to these theoretical flexural capacities, q_y/q_{yf}, are also tabulated, and a review of these ratios confirms the reasonableness of the prediction methods of Ref. (2), at least when applied to simply supported square slabs in which lateral displacement of the sides of the slabs are prevented. The average of these comparative ratios for the 29 slabs for which such ratios could be computed was 1.04, and, if one ratio of 1.45 is neglected, the ratios varied within the range from 0.71 to 1.28.

Without intending to draw a conclusion that may not be justified, it is worth noting that the ultimate capacities of these slabs appear to be given within acceptable limits by the flexural resistance prediction procedures of Ref. (2), regardless of the mode of failure of the slabs. For the 12 slabs that were identified by the authors of Ref. (1) as having failed in flexure, the resistance ratio, q_y/q_{yf}, varied between 0.71 and 1.28 with an average value of 0.98, while for the remaining 16 slabs that were identified as having failed in shear (again excluding slab No. 37), the range was from 0.72 to 1.24, with an average value of 1.06.

Stiffness:

While, as indicated in the preceding section, the procedures of Ref. (2) can be used with reasonable confidence to predict the ultimate strengths of the slabs under review, it appears that the same cannot be said in regard to the use of these procedures to predict the effective stiffnesses of these slabs. These effective stiffnesses are the slopes of the linear rise portions (Line OA in Fig. 38) of the load-deflection diagrams of Figs. 7 through 37.

To study the predictability of the relative stiffnesses of these slabs, a straight line which reasonably approximated the nonlinear rise was drawn from the origin to the maximum resistance of each of the slabs, and the resulting effective elastic yield deflections, x_{ye}, were determined. These values and their corresponding effective stiffnesses, $K_{eff} = q_y/x_{ye}$, are tabulated in Table III. While these effective slab stiffnesses were established by eye and are, therefore, subject to some error, calculations demonstrated clearly that they are not reasonably approximated by the procedures that are now commonly used.

Consider, for example, the VAS procedures of Ref. (2), which do not compute slab stiffnesses directly, but have such stiffnesses implicit in expressions given for determination of natural periods of vibration. Using those natural period expressions and recognizing the relationships that exist between period, mass and stiffness for a single-degree-of-freedom system, the slab stiffness implicit in the period expressions of Ref. (2) is found to be

$$K = (\text{constant})\ M\rho d^2$$

where "M" is the effective mass per unit slab area, "ρ" is the reinforcement ratio, and "d" is the effective slab depth. For a slab of given thickness, the quantities "M" and "d" also become constants, and the stiffness would appear to vary linearly with reinforcement percentage. A review of the effective slab stiffnesses, K_{eff}-values, of Table III, shows conclusively that this was not the case for these slabs. Indeed, for any given group of slabs of constant thickness, the actual effective stiffnesses appear to be virtually insensitive to the reinforcement ratios used in them.

The experimental effective stiffnesses, K_{eff}, were also compared to the stiffness values as determined from the methods of Ref. (3). That reference proposes, essentially, that the stiffness be determined as for an elastic slab, but with an average or effective moment of inertia which acknowledges the cracked condition of the concrete. If "I" is taken as the average of the moments of inertia of the gross section and of the cracked transformed section (neglecting the effects of in-plane forces), the resulting stiffness values are identified as K_e in Table III.

The ratios between the observed effective stiffnesses, K_{eff}, and the values of K_e as determined above are also tabulated in Table III, and inspection of these ratios reveals some interesting, if not readily explainable, relationships. For example, acknowledging the degree of approximation in the values of K_{eff} (which were determined by eye), the K_{eff}/K_e ratios within each slab group are remarkably uniform. Furthermore, it is observed that the K_{eff}/K_e ratio tends generally to decrease as the slab thickness increases, which suggests that the ratios might be made essentially constant for all of the slabs, regardless of thickness, by including the effects of shear deformation. Unfortunately, an attempt to do this proved to be largely ineffective because the computed shear deformations, even for the 3-inch slabs, were so small in comparison with the computed flexural deformations as to be relatively insignificant. Of course, only elastic shear deformations were considered (because we don't know how to predict inelastic or plastic shear deformations), and this almost certainly underestimated the real contribution of shearing deformation to the total deflection.

In this regard, we observe another rather interesting relationship. It will be remembered that the Type II slabs were identical to the Type I slabs except for the fact that, for Type II, half of the reinforcement was bent up near the edges of the slabs to provide increased shear resistance. It is interesting to note, however, that the effective stiffnesses of the 1.5" and 3.00" Type II slabs are noticeably less than are those of the equivalent Type I slabs. A probable explanation for this behavior might be an increased inelastic ductility in shear for the Type II slabs as a result of the shear reinforcement in them.

Plastic Decay Domain

The plastic decay domain is shown in Fig. 38 as the straight-line segment BC, which represents that region in which the resistance of the slab diminishes with increasing deflection, until it completely fails or until its resistance mechanism changes from flexure to a quasi-membrane action. If it is assumed that the internal ultimate moment capacity of a slab, which corresponds to the slab yield resistance, q_y, can be sustained under deflections greater than x_{ye}, then some insight into slab behavior in the plastic decay domain can be obtained by considering the effect on the external moment of changes in the eccentricity of the in-plane forces as the deflection increases.

Consider, for example, a one-way slab element as shown in Fig. 39, in which the internal resisting moment, m_u', is defined and computed as in Ref. (2) to be the ultimate moment capacity of the section, including the effects of a concentrically applied in-plane force, N. If, then, the in-plane compressive force is applied at an eccentricity, e, it effectively increases the slab's internal moment resistance by an amount Ne. However, as the slab deflects at center, the eccentricity of N with respect to the center of the slab is reduced by an amount equal to this deflection, and the moment augmentation produced by N is correspondingly reduced by (N)(Δ), where Δ is the center deflection.

But the preceding discussion presumes that "N" existed when Δ was zero, which was clearly not the case for the slabs considered herein, in which N developed as a consequence of slab deflection, and reached a maximum at or near a deflection corresponding to maximum slab resistance. It might thus be assumed that, at a deflection, x_{yp}, as shown in Fig. 38, the slab resistance is as yet undiminished and that the effective resisting moment is the same as that which defined its maximum resistance, or

$$m_u = m'_u + Ne$$

in which m'_u includes the effect of a concentrically applied force, N, and "e" is the maximum eccentricity of N with respect to mid-depth of the slab. As the deflection increases beyond x_{yp}, the effective eccentricity of N is decreased, and the total resisting moment becomes

$$m_u = (m'_u + Ne) - N(\Delta - x_{yp})$$

in which Δ is the total deflection at the center of the slab.

If this reduced moment is then used in the expression of Ref. (2) for the flexural resistance of a two-way slab, it is found that, for the slabs studied herein, the plastic decay resistance is given by

$$\begin{aligned} q &= 0.1067\,[m'_u + N(e + x_{yp}) - N\Delta] \\ &= 0.1067(m'_u + Ne) = 0.1067N(\Delta - x_{yp}) \\ &= q_y - 0.1067N(\Delta - x_{yp}) \\ &= q_y - K_p(\Delta - x_{yp}) \end{aligned}$$

from which it is observed that, for deflection greater than x_{yp}, the resistance decays from its maximum value, q_y, on a slope, K_p, which, for a given slab, is a constant times the maximum in-plane force, N. Observation of the experimental data studied herein indicates that this concept checks very well the plastic decay response of most of the slabs that were identified by the experimenters as having failed in flexure. Confirmation of this agreement is given in Table IV in which the measured plastic decay slope, K_p, is compared with the theoretical value, 0.1067 N, the slope of the decay that would be given by the above equation.

It is obvious that the expression given above is significant primarily in that the procedure used to arrive at it yields a decay slope that is confirmed by tests for slabs in which premature failure in shear has been prevented by appropriate edge shear reinforcement. It obviously presumes that the yield resistance of the slab, q_y, the in-plane force, N, and the plastic decay deflection, x_{yp}, are known. It has been shown previously that the procedures of Ref. (2) can be used to predict q_y with generally acceptable levels of reliability, but methods of predicting x_{yp} have yet to be developed, and, of course, in a real structure, the magnitude of the maximum in-plane force, N, will almost certainly be subject to substantial uncertainty.

Constant Resistance Domain:

The constant resistance domain of the load-deflection curve is defined by the line segment AB in Fig. 38, for which the resistance can be taken as being constant at its maximum value, q_y, between the elastic yield deflection, x_{ye}, and the plastic decay deflection, x_{yp}. Obviously, to define this segment, it is necessary only to define q_y, x_{ye}, and x_{yp}.

As noted in the preceding section, procedures currently in use appear to predict q_y within generally acceptable limits of error. Similarly, the elastic yield deflection, x_{ye}, will be given by q_y/K_{eff}, and while present procedures do not represent K_{eff}, the effective elastic slab stiffness, very well, comparisons drawn herein suggest strongly the existence of relationship which, with further research, can be identified and used to define K_{eff} within acceptable limits.

But the value of x_{yp} is now an unknown quantity, and the experimental data reviewed in this study provide little basis for its prediction. The experimentally determined values of x_{yp} are tabulated in Table IV, and one is struck by the very low sensitivity of these values (especially for Type II slabs) to the effects of increasing slab thickness. One would normally expect the decay in resistance at deflections greater than x_{yp} to be associated not only with a reduction in the moment-augmentation effect of the eccentric in-plane force, N, but also with the development of crushing strains in the concrete on its compressive face and the associated reductions in internal slab moment capacities. If the decay were associated with compressive crushing of the concrete, then the onset of such decay should occur, in slabs of constant span, at much smaller deflections in thick slabs than in thinner ones. Some evidence does exist in the data of Table IV that this occurred in the Type I slabs (without shear reinforcement), but the x_{yp} values for the Type II slabs (with shear reinforcement) appeared to be generally insensitive to the depth-span ratios of the slabs.

This observed insensitivity of x_{yp} to the depth-span ratio of a slab suggests that the common premise that the internal moment capacity of a slab begins to diminish when the extreme fiber of the concrete reaches its crushing strain and/or that the crushing strain of concrete was, for a given f'_c, a constant may not be correct. A possible explanation for the observed behavior of the slabs being studied here might be given by relating the crushing strain of concrete to the transverse confining pressure to which it is subjected. As the slab depth increases, for a given span, so does its resistance, q_y, to transverse pressure. And if this transverse pressure effectively increases the crushing strain of the concrete, then it might not be unreasonable to find the values of x_{yp} to be relatively insensitive to the depth-span ratio for slabs loaded as these slabs were loaded, since the crushing strain would increase as the confining pressure, q_y, increased.

Although the values of x_{yp} appear to be relatively insensitive to slab depth, there does seem to be a relationship between x_{yp} and the tension reinforcement ratio. The general nature of this relationship is shown in Fig. 40, in which it appears that x_{yp} could be reasonably represented as a simple linear function of the reinforcement ratio, ρ. But these limited data are hardly adequate as a basis for the empirical definition of such a relationship, despite the systematic nature of the data, especially for the Type II slabs.

One further observation concerning the values of x_{yp} is worth noting. In Table IV the ratios of the experimental x_{yp} values to the x_{ye} values shown in Table III are tabulated. While not yet rationally explainable, the relative constancy of this ratio at a value of about 2.0 for all slabs tested should not be overlooked. This degree of uniformity can hardly be a matter of chance.

Membrane Action Domain:

The membrane action domain of slab response is represented by the straight-line segment CD of Fig. 38. It is suggested in Ref. (1) that, in this region, the behavior of the slab can be represented as a simple tensile net, for which the resistance is given, for a square slab, by

$$q = \frac{16\ \rho d f_y}{\ell^2} (\Delta)$$

where Δ is the deflection at the center.

The resistance given by this expression is compared with the experimental results in Table V. It is interesting to note, by inspection of this table, that this simple expression represents quite well the membrane behavior of the 0.75-inch thick Type II slabs and that the slopes of the experimental curves for the 1.50-inch thick Type II slabs are checked exactly by this equation, although these curves are displaced upward by a significant, but as yet unexplainable amount. For this latter group of slabs, the resistance is given by:

$$q = q_{mo} + \frac{16\ \rho d f_y}{\ell^2} (\Delta)$$

in which q_{mo} is the as-yet undefined resistance increment.

For the unreinforced slabs and for most of the slabs that failed in shear, no membrane region developed, and the membrane region for the few shear-failure slabs, in which such a region did develop (principally the 0.75" and 1.5" Type 1 slabs), is not reasonably approximated by the above expression. But one would not expect a simple tensile net to represent reasonably the behavior of a slab that has failed in shear.

Conclusions

While recognizing that their validity may be called into question because they have their bases in test results of small-scale models, the following conclusions may be tentatively drawn from the preceding discussions:

(1) The load-deflection behavior of a two-way slab can be reasonably approximated by a multilinear function of the type shown in Fig. 38.

(2) The maximum resistance, q_y, is reasonably predicted by the procedures proposed for this purpose in Ref. (2).

(3) The slope of the equivalent linear rise from zero to maximum resistance is substantially overestimated by the procedures of Ref. (2). However, the ratios of the experimental values of the effective stiffnesses to effective elastic stiffnesses (computed as in Ref. (3) using "averaged" or "effective" moments of inertia to account for the cracked condition of the concrete) were sufficiently uniform to suggest strongly that, through further research, the effective stiffness could be adequately predicted by a modification of the methods of Ref. (3), especially if the effects of inelastic shear deformation can be included.

(4) The plastic decay region for slabs that have been reinforced in such a way as to preclude premature failure in shear can be expressed quite simply by an equation of the form,

$$q = q_y - KN(\Delta - x_{yp})$$

$$= q_y - K_p(\Delta - x_{yp})$$

in which q_y is the maximum resistance, N is the in-plane force, Δ is the deflection at the center of the slab, x_{yp} is the deflection at which plastic decay begins, and K is a factor (constant for any given slab) whose value is determined by the slab dimensions and internal moment resistances at the center and edges.

No similar systematic relationship to define this response domain for slabs that failed in shear appears to exist.

(5) The deflection, x_{yp}, at which plastic decay of the resistance function begins is not rationally definable. However, the experimental data indicate that it bears sufficiently systematic relationships to the effective elastic yield deflection, and to such slab properties as their reinforcement ratio, as to suggest that, with further research, it can be defined. For the slabs studied herein, an adequate approximation is given by $x_{yp} = 2x_{ye}$.

(6) The large deflection, membrane action domain of response for slabs so reinforced as to preclude failure in shear can probably be adequately defined by the behavior of a tension steel net represented by the primary slab reinforcement. For very thin slabs (span/depth ratio of 20) of this type, the experimental membrane domain response is checked exactly by this theory, and for similar thicker slabs (span/depth ratio of 10), the slope of the resistance function in this domain is checked exactly by this theory. However, in the latter case, the experimental function is displaced vertically through a distance (resistance increment) that is not yet rationally explained.

For slabs that failed completely in shear early in their response histories, there are no membrane phases of response. For slabs that failed in shear, but in which the reinforcement net maintained its integrity, there is a pseudo-membrane region of response, but systematic relationships which might be presumed to govern it were not in evidence in the test data studied herein.

Recommendations

(1) Study more systematically the available slab test data to define better an equivalent, or effective, elastic stiffness, K_{eff} of Fig. 38.

(2) Undertake additional research, including further tests, on slabs adequately reinforced to prevent a shear failure, in an effort to define the deflection, x_{yp}, at which plastic decay of resistance begins, and to confirm or correct the method suggested herein for the definition of the plastic decay slope.

(3) Extend the research suggested in (2) to include also the tensile membrane response domain in order to complete or to correct the definition of this response region as suggested herein for slabs whose dominant failure mode is flexure.

(4) Recognizing that the observations and resulting recommendations made herein are based on the results of static tests of slabs, investigate the possibility that the failure mode of a slab might be influenced by the nature of a dynamically applied load. Is it possible that a slab which failed in flexure under a statically applied load might fail in shear under a near-instantaneously applied dynamic load?

(5) While undertaking studies to develop structural details that will eliminate (minimize?) the possibility of shear failure in slabs, endeavor (primarily through further experiments) also to understand better the nature of shear failures and the circumstances under which it might occur.

Table I. Summary of Slab Properties and Significant Response Data

Slab	(1) d_c"	(2) d"	(3) ρ	f'_c, psi	f_y, ksi	(4) N, lbs/in.	(5) e, in.	(6) q_y, psi
Type I Slabs								
5	0.75	0.75	0	3509	-	576	0.19	35
6	"	0.56	.005	4528	60	845	"	34
4	"	"	.01	4261	"	?	"	37
7	"	"	.02	4413	"	755	"	44
10	"	"	.03	4043	"	1009	"	44
11	1.50	1.50	0	4365	-	1673	0.38	180
17	"	1.22	.005	3554	55	1911	"	190
13	"	"	.01	4223	"	1545	"	193
14	"	"	.02	4585	"	612(?)	"	240
16	"	"	.03	3473	"	1227	"	220
18	3.00	3.00	0	3421	-	2015	1.00	570
26	"	3.00	0	4387	-	3006(?)	"	800
24	"	2.59	.005	3551	53	2100	"	625
20	"	"	.01	2925	"	2345	"	720
21	"	"	.02	3341	"	3145	"	1075
22	"	"	.03	4123	"	2108	"	1150
Type II Slabs								
32	0.75	0.75	0	4721	-	1092	0.19	36
33	"	0.56	.005	"	60	576	"	40
34	"	"	.01	5041	"	1059	"	41
35	"	"	.02	"	"	915	"	50
36	"	"	.03	5540	"	731	"	62
27	1.50	1.50	0	4205	-	1917	0.38	154
28	"	1.22	.005	4774	55	2135	"	190
29	"	"	.01	4487	"	2118	"	226
31	"	"	.02	3620	"	1834	"	259
30	"	"	.03	4510	"	1525	"	276
37	3.00	3.00	0	3738	-	3581	1.00	1070
38	"	2.59	.005	"	53	3260	"	920
39	"	"	.01	4159	"	4391	"	1155
40	"	"	.02	"	"	3641	"	1310
41	"	"	.03	3378	"	?	"	1620

Notes: (1) Total thickness of slab.

(2) Effective depth of slab.

(3) Reinforcement ratio, each direction, bottom face only.

(4) Maximum measured average lateral restraining force.

(5) Distance from mid-depth of slab and location of N.

(6) Maximum measured transverse pressure sustained by slab.

Table II. Comparison of Theoretical and Measured Yield (Max) Resistances

Slab	d, in.	ρ	(1) q_y, psi	(2) q_{yf}	q_y/q_{yf}
Type I Slabs					
5	0.75	0	35	29	1.21
6	0.56	.005	34	47	0.72
4	"	.01	37	?	?
7	"	.02	44	53	0.83
10	"	.03	44	53	0.83
11	1.50	0	180	161	1.12
17	1.22	.005	190	183	1.04
13	"	.01	193	201	0.96
14	"	.02	240	208	1.15
16	"	.03	220	197	1.12
18	3.00	0	570	463	1.23
26	3.00	0	800	673	1.19
24	2.59	.005	625	612	1.02
20	"	.01	720	708	1.02
21	"	.02	1075	872	1.18
22	"	.03	1150	1045	1.10
Type II Slabs					
32	0.75	0	36	50	0.72
33	0.56	.005	40	37	1.08
34	"	.01	41	58	0.71
35	"	.02	50	60	0.83
36	"	.03	62	64	0.97
27	1.50	0	154	176	0.88
28	1.22	.005	190	221	0.86
29	"	.01	226	231	0.98
31	"	.02	259	202	1.28
30	"	.03	276	246	1.12
37	3.00	0	1070	740	1.45
38	2.59	.005	920	798	1.15
39	"	.01	1155	1028	1.12
40	"	.02	1310	1054	1.24
41	"	.03	1620	?	?
					Avg = 1.04

Notes: (1) As obtained by experiment.

(2) As computed using the procedures of Ref. (2).

Table III. Comparison of Experimental and Theoretical Effective Stiffnesses

Slab	d, in.	ρ	(1) q_y, psi	(2) x_{ye}, in.	(3) K_{eff}, psi	(4) K_e	K_{eff}/K_e
Type I Slabs							
5	0.75	0	35	0.19	184	302	0.61
6	0.56	.005	34	0.19	179	382	0.47
4	"	.01	37	0.16	231	407	0.57
7	"	.02	44	0.18	244	452	0.54
10	"	.03	44	0.18	244	487	0.50
11	1.50	0	180	0.12	1500	2643	0.57
17	1.22	.005	190	0.12	1583	2825	0.56
13	"	.01	193	0.12	1608	3393	0.47
14	"	.02	240	0.12	2000	4020	0.50
16	"	.03	220	0.12	1833	3963	0.46
18	3.00	0	570	0.06	9500	18670	0.51
26	3.00	0	800	0.15	5333	24567	0.22
24	2.59	.005	625	0.08	7813	23318	0.34
20	"	.01	720	0.08	9000	24478	0.37
21	"	.02	1075	0.12	8958	30360	0.30
22	"	.03	1150	0.12	9583	36492	0.26
Type II Slabs							
32	0.75	0	36	0.19	189	351	0.54
33	0.56	.005	40	0.17	235	390	0.60
34	"	.01	41	0.17	241	443	0.54
35	"	.02	50	0.18	278	483	0.58
36	"	.03	62	0.18	344	548	0.63
27	1.50	0	154	0.14	1100	2594	0.42
28	1.22	.005	190	0.18	1056	3215	0.33
29	"	.01	226	0.17	1329	3478	0.38
31	"	.02	259	0.18	1439	3670	0.39
30	"	.03	276	0.19	1453	4383	0.33
37	3.00	0	1070	0.17	6294	19516	0.32
38	2.59	.005	920	0.13	7077	23836	0.30
39	"	.01	1155	0.17	6794	28125	0.24
40	"	.02	1310	0.19	6895	32955	0.21
41	"	.03	1620	0.24	6750	33923	0.20

Notes:

(1) As measured.

(2) As determined by eye to define a good approximation of the experimental data by a linear rise from zero to yield resistance, q_y.

(3) $K_{eff} = q_y/x_{ye}$

(4) Elastic stiffness with "I" = average of gross and cracked transformed section values for N = 0, per Ref. (3).

Table IV. Comparison of Theoretical and Experimental Plastic Decay Responses

Slab	d_c, in.	d, in.	(a) Theo, K_p	(b) Exp, K_p	(c) x_{yp}, in.	(d) x_{yp}/x_{ye}	(e) Failure
Type I Slabs							
5	0.75	0.75	-62	Data questionable		-	Flexure
6	"	0.56	-90	-109	0.35	1.8	Shear & Bond
4	"	"	?	-53	0.38	2.4	" "
7	"	"	-81	-98	0.35	1.9	Shear
10	"	"	-108	-55	0.40	2.0	"
11	1.50	1.50	-179	-431	0.21	1.8	Flexure
17	"	1.22	-204	-528	0.24	2.0	Shear
13	"	"	-165	-1608	0.28	2.3	"
14	"	"	?	-377	0.28	2.3	"
16	"	"	-131	-1222	0.22	1.8	"
18	3.00	3.00	-215	-6353	0.08	1.3	Shear
26	"	"	?	Failed before decay			"
24	"	2.59	-224	" " "			"
20	"	"	-250	-2414	0.14	1.8	"
21	"	"	-336	-3162	0.20	1.7	"
22	"	"	-225	-1120	0.25	2.1	Edge Reinf.
Type II Slabs							
32	0.75	0.75	-117	-118	0.35	1.8	Flexure
33	"	0.56	-61	-146	0.34	2.0	"
34	"	"	-113	-116	0.36	2.1	"
35	"	"	-98	-99	0.38	2.1	"
36	"	"	-78	-76	0.43	2.4	"
27	1.50	1.50	-205	-555	0.28	2.0	Flexure
28	"	1.22	-229	-221	0.28	1.6	"
29	"	"	-226	-231	0.32	1.9	"
31	"	"	-196	-198	0.37	2.1	"
30	"	"	-163	-164	0.40	2.1	"
37	3.00	3.00	-382	Failed before decay			Shear
38	"	2.59	-348	" " "			"
39	"	"	-469	-1470	0.36	2.1	"
40	"	"	-388	-220	0.36	1.9	"
41	"	"	?	Failed before decay			Loading Membrane

Notes: (a) K_p = -0.1067 N (See Table I for N)

(b) Slope of experimental decay curves.

(c) Intersection of experimental q_y and plastic decay slopes.

(d) Ratio of experimental x_{yp} to x_{ye} from Table III.

(e) Mode of failure as reported in Ref. (1).

Table V. Comparison of Theoretical and Experimental Response in the Membrane Action Domain

Slab	d_c, in.	d, in.	ρ	(c) Theo. Resist., psi	(d) Exper. Resist., psi	(a) Failure
Type I Slabs						
5	0.75	0.75	0	0	(b) 0	Flexure
6	"	0.56	.005	11.95Δ	5 + 7.0Δ	Shear & Bond
4	"	"	.01	23.89Δ	5 + 15.0Δ	" "
7	"	"	.02	47.79Δ	(uncertain)	Shear
10	"	"	.03	71.68Δ	0	"
11	1.50	1.50	0	0	0	Flexure
17	"	1.22	.005	23.86Δ	50 - 22Δ	Shear
13	"	"	.01	47.72Δ	20 + 10Δ	"
14	"	"	.02	95.43Δ	92 + 34Δ	"
16	"	"	.03	143.15Δ	122 + 24Δ	"
18	3.00	3.00	0	0	0	Shear
26	"	3.00	0	0	0	"
24	"	2.59	.005	48.81Δ	0	"
20	"	"	.01	97.61Δ	0	"
21	"	"	.02	195.23Δ	0	"
22	"	"	.03	292.84Δ	900 + 60Δ	Edge Reinf.
Type II Slabs						
32	0.75	0.75	0	0	0	Flexure
33	"	0.56	.005	11.95Δ	2 + 11.95Δ	"
34	"	"	.01	23.89Δ	0 + 23.89Δ	"
35	"	"	.02	47.78Δ	0 + 40.0Δ	"
36	"	"	.03	71.68Δ	0 + 45.0Δ	"
27	1.50	1.50	0	0	0	Flexure
28	"	1.22	.005	23.86Δ	50 + 13Δ	"
29	"	"	.01	47.72Δ	62 + 47.72Δ	"
31	"	"	.02	95.43Δ	76 + 95.43Δ	"
30	"	"	.03	143.15Δ	75 + 143.15Δ	"
37	3.00	3.00	0	0	0	Shear
38	"	2.59	.005	48.81Δ	0	"
39	"	"	.01	97.61Δ	0	"
40	"	"	.02	195.23Δ	0	"
41	"	"	.03	292.84Δ	0	Loading Membrane

Notes: (a) As reported in Ref. (1).

(b) No membrane domain developed.

(c) Computed from Eq. (29) of Ref. (1).

(d) As determined by eye from data published in Ref. (1).

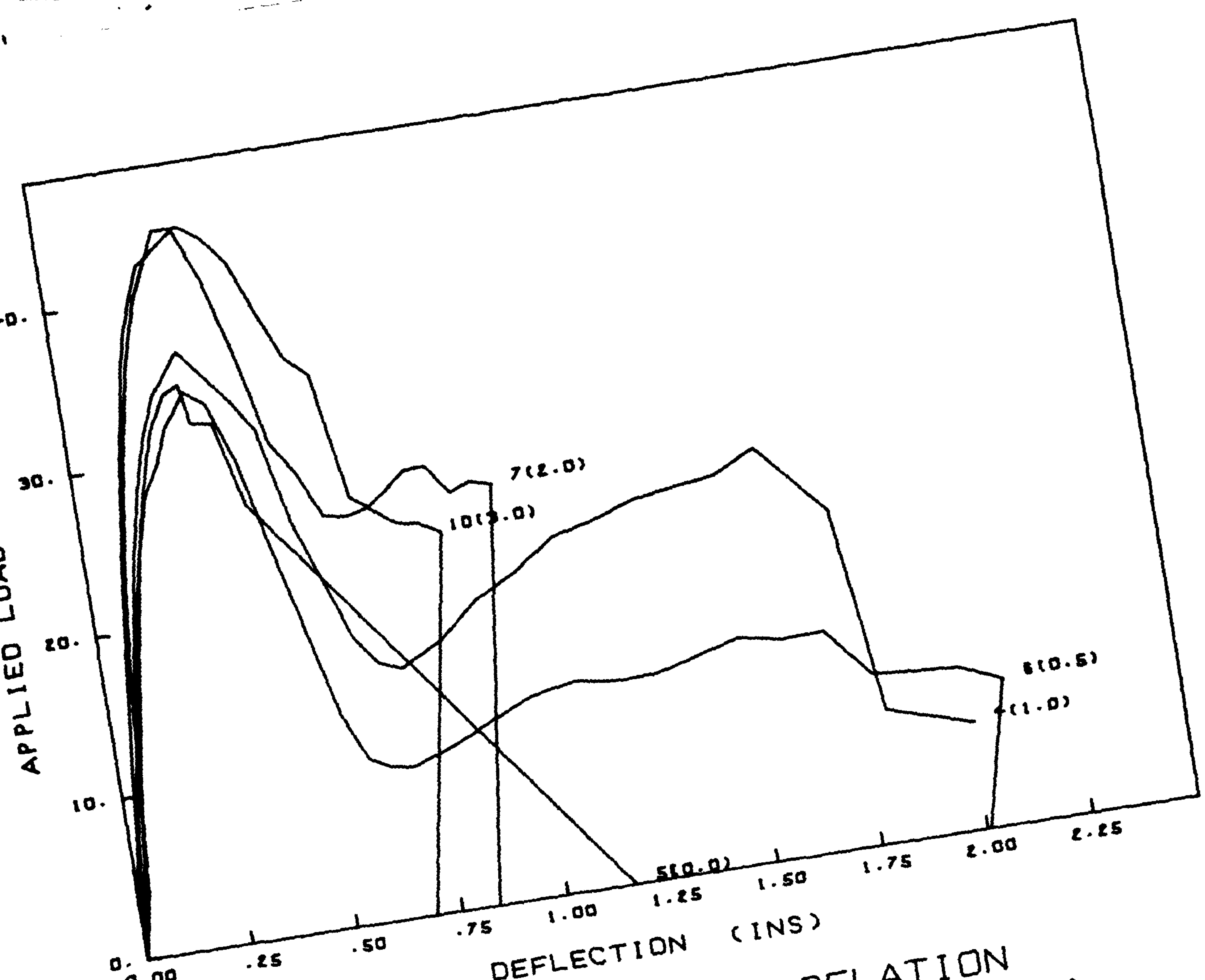

FIG. 1 : LOAD-DEFLECTION RELATION
(3/4 INCH THICKNESS RESTRAINED SLABS I)
(SAME AS FIG. 5 OF REF. 1)

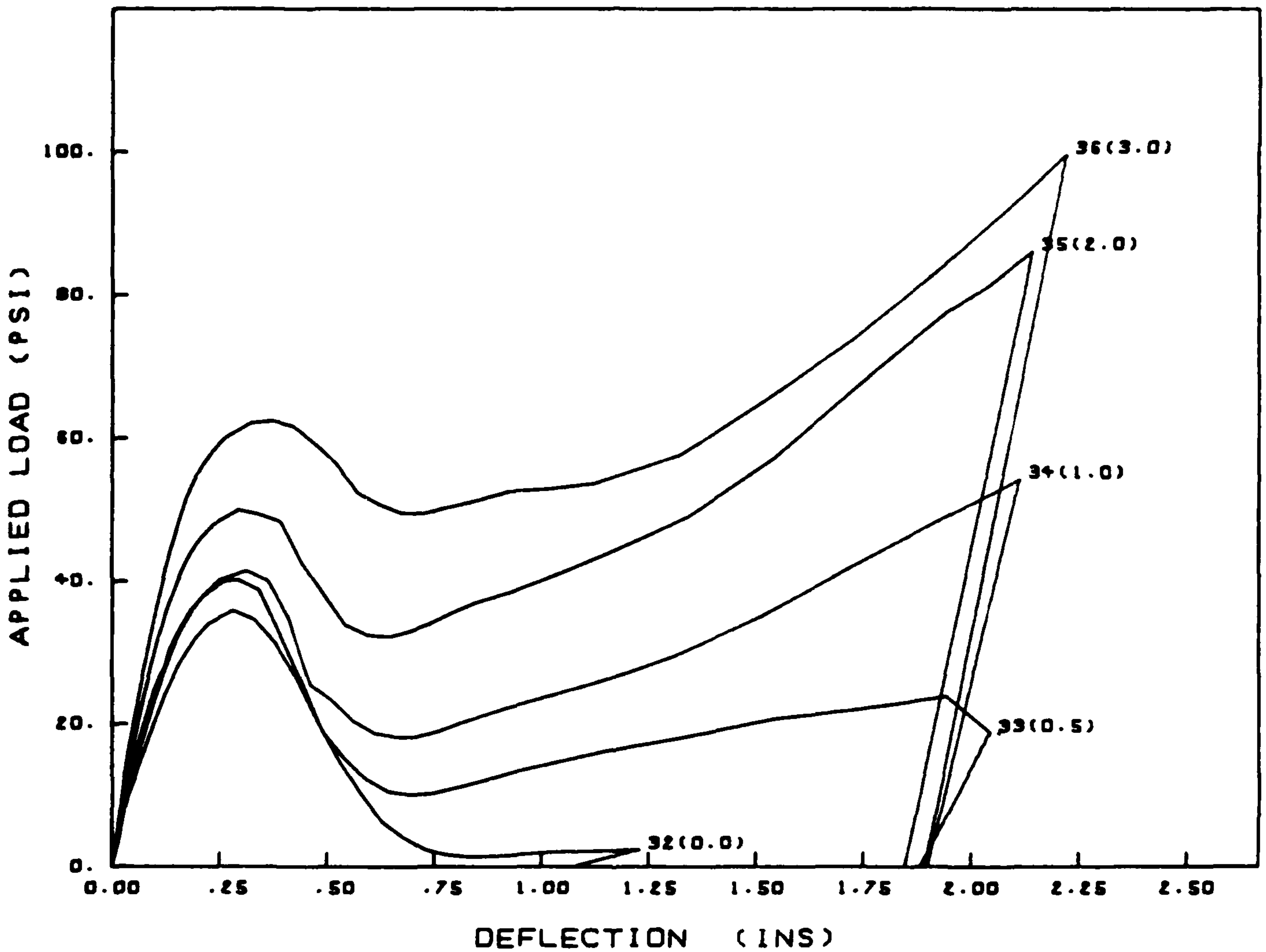

FIG. 2 : LOAD-DEFLECTION RELATION
(3/4 INCH THICKNESS RESTRAINED SLABS II)
(SAME AS FIG. 6 OF REF. 1)

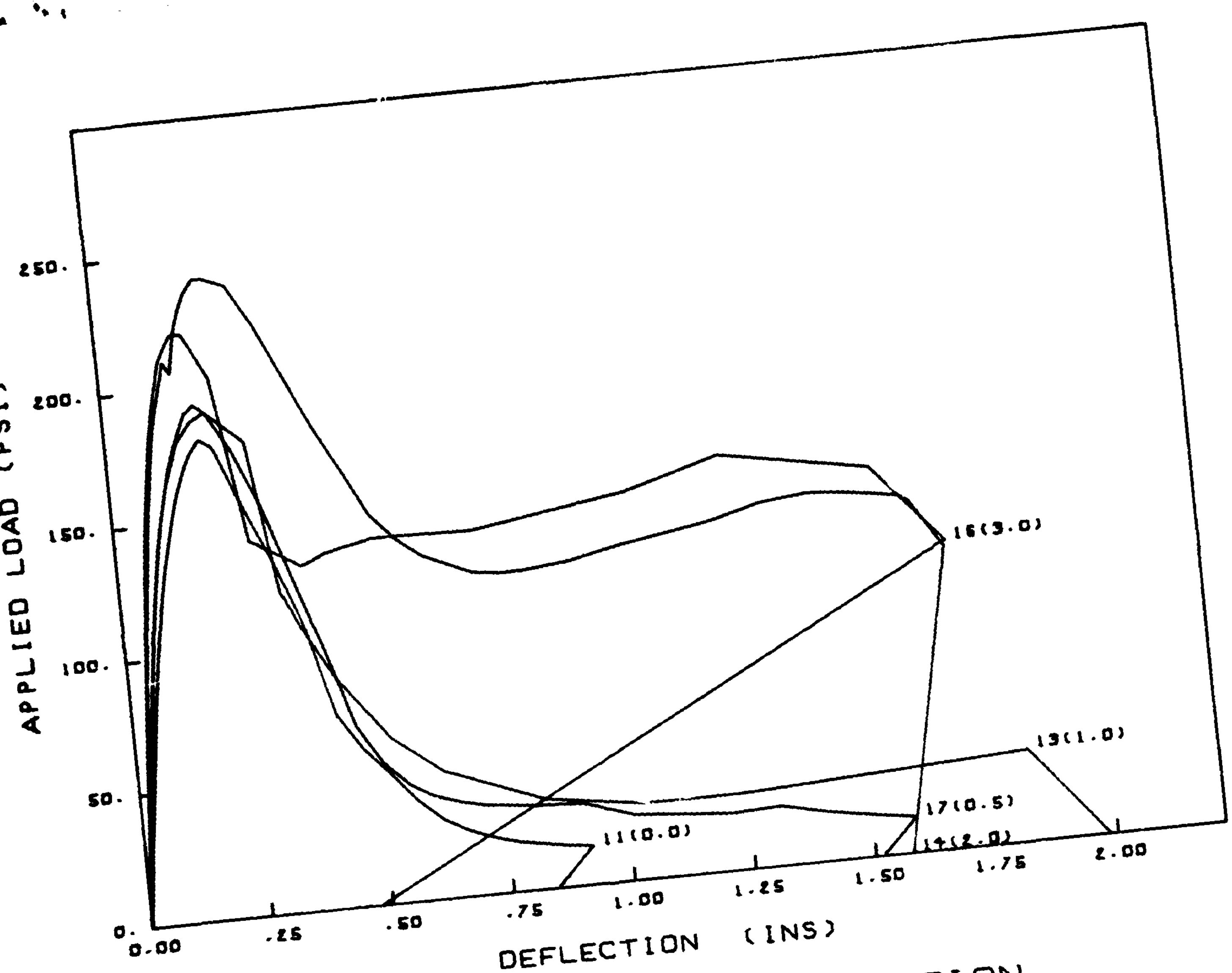

FIG. 3 : LOAD-DEFLECTION RELATION
(1.5 INCH THICKNESS RESTRAINED SLABS I)
(SAME AS FIG. 9 OF REF. 1)

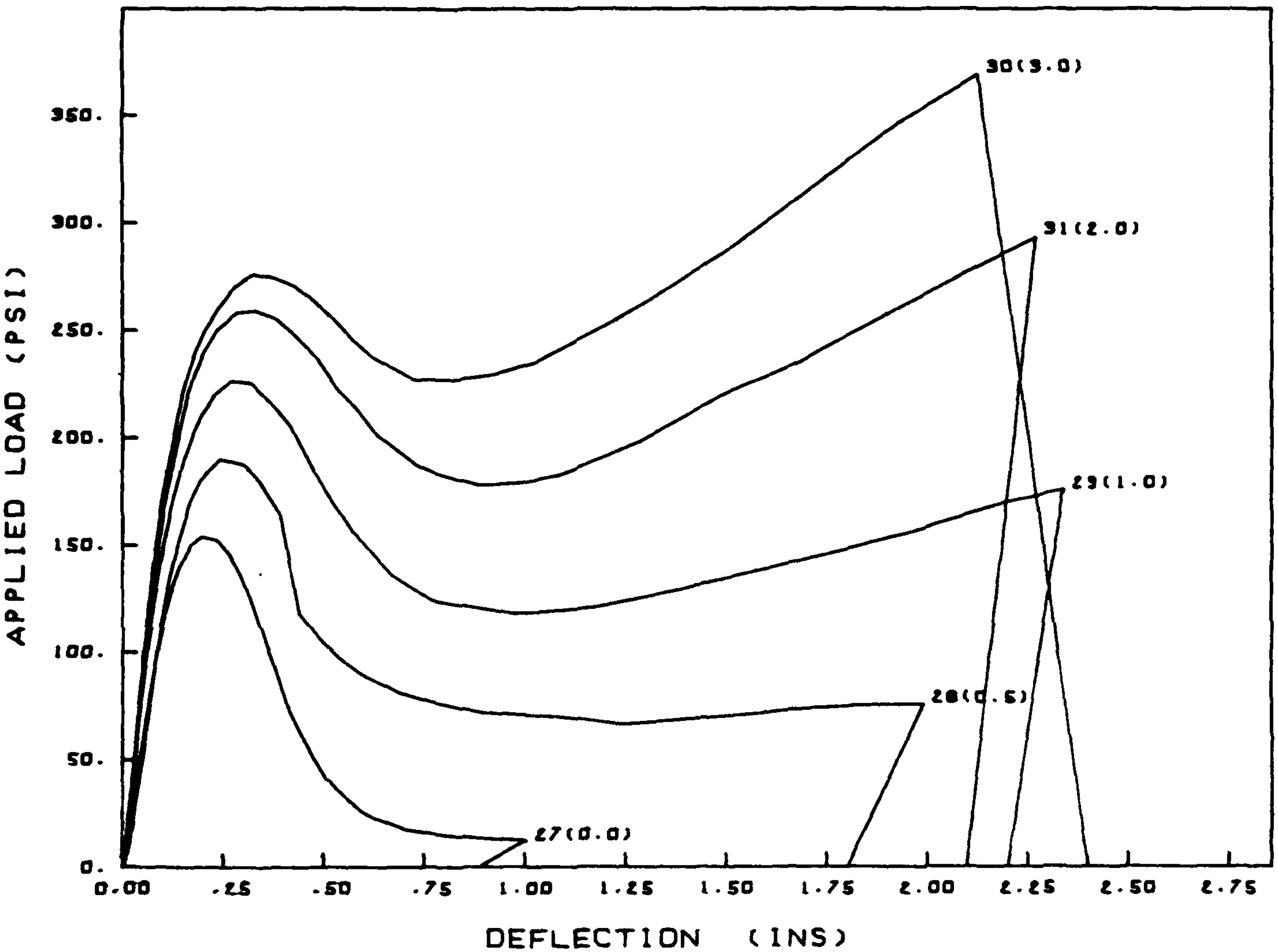

FIG. 4 : LOAD-DEFLECTION RELATION
(1.5 INCH THICKNESS RESTRAINED SLABS II)
(SAME AS FIG. 10 OF REF. 1)

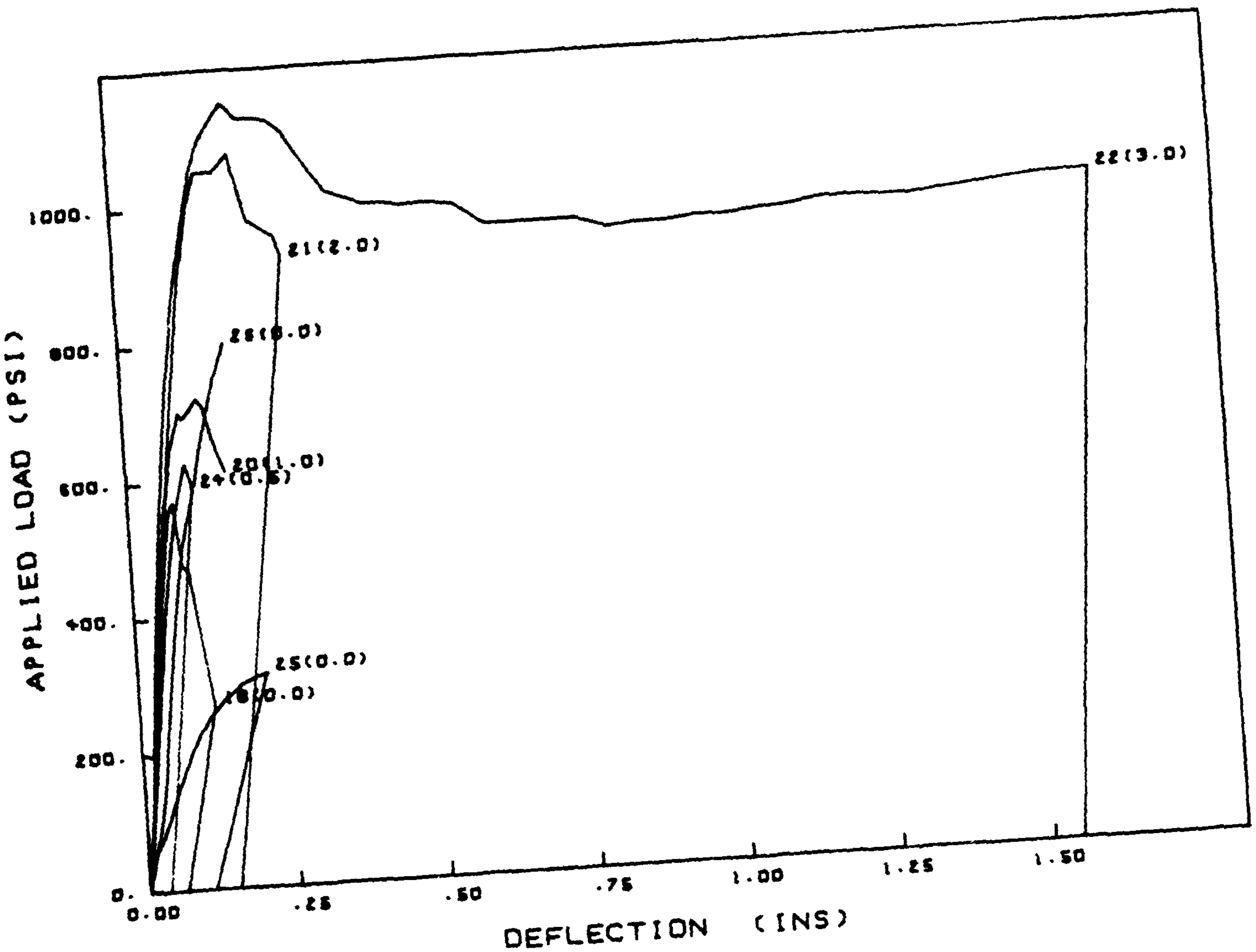

FIG. 5 : LOAD-DEFLECTION RELATION
(3.0 INCH THICKNESS RESTRAINED SLABS I)
(SAME AS FIG. 13 OF REF. 1)

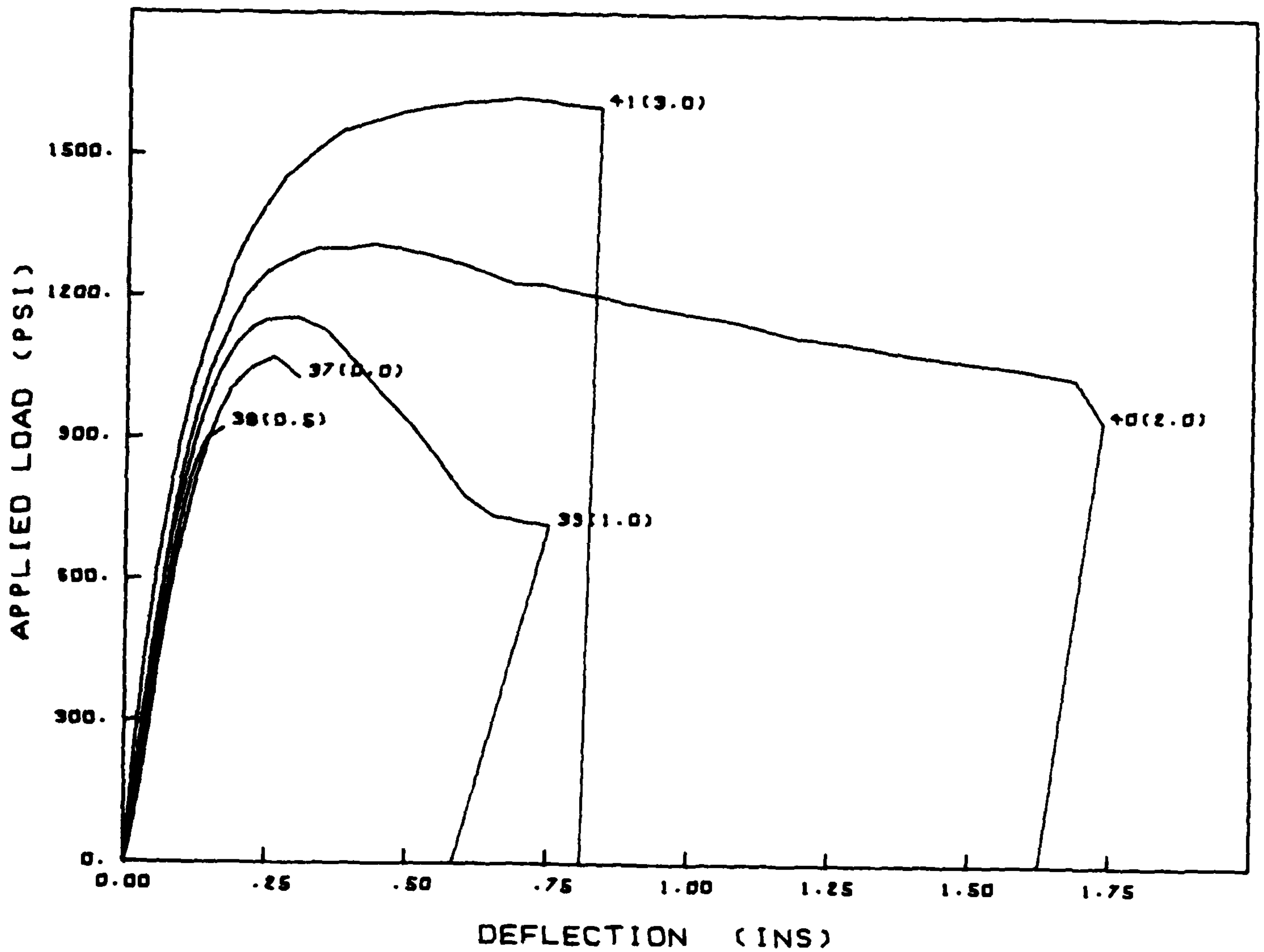

FIG. 6 : LOAD-DEFLECTION RELATION
(3.0 INCH THICKNESS RESTRAINED SLABS II)
(SAME AS FIG. 14 OF REF. 1)

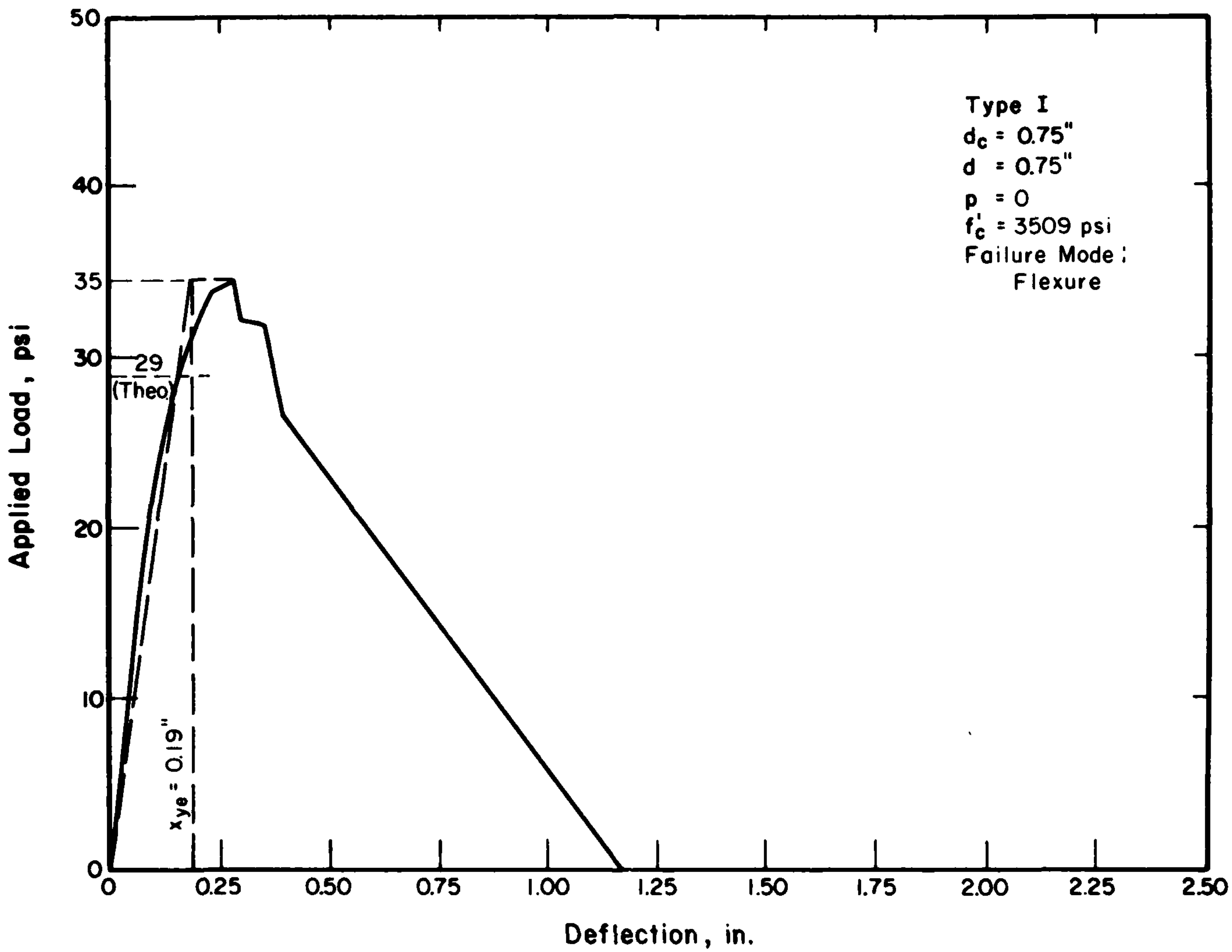

FIG. 7 LOAD-DEFLECTION CURVE FOR SLAB NO. 5

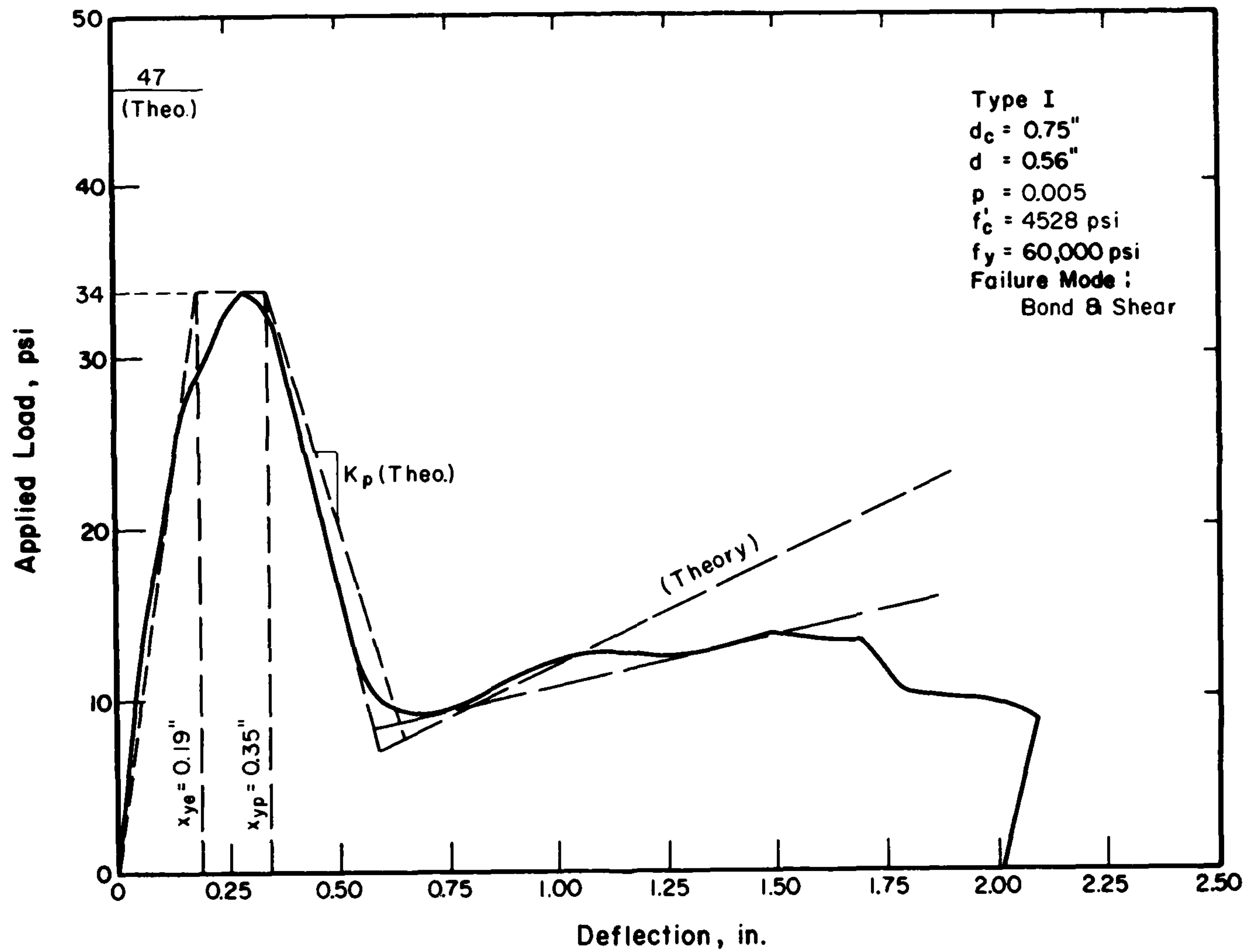

FIG. 8 LOAD-DEFLECTION CURVE FOR SLAB NO. 6

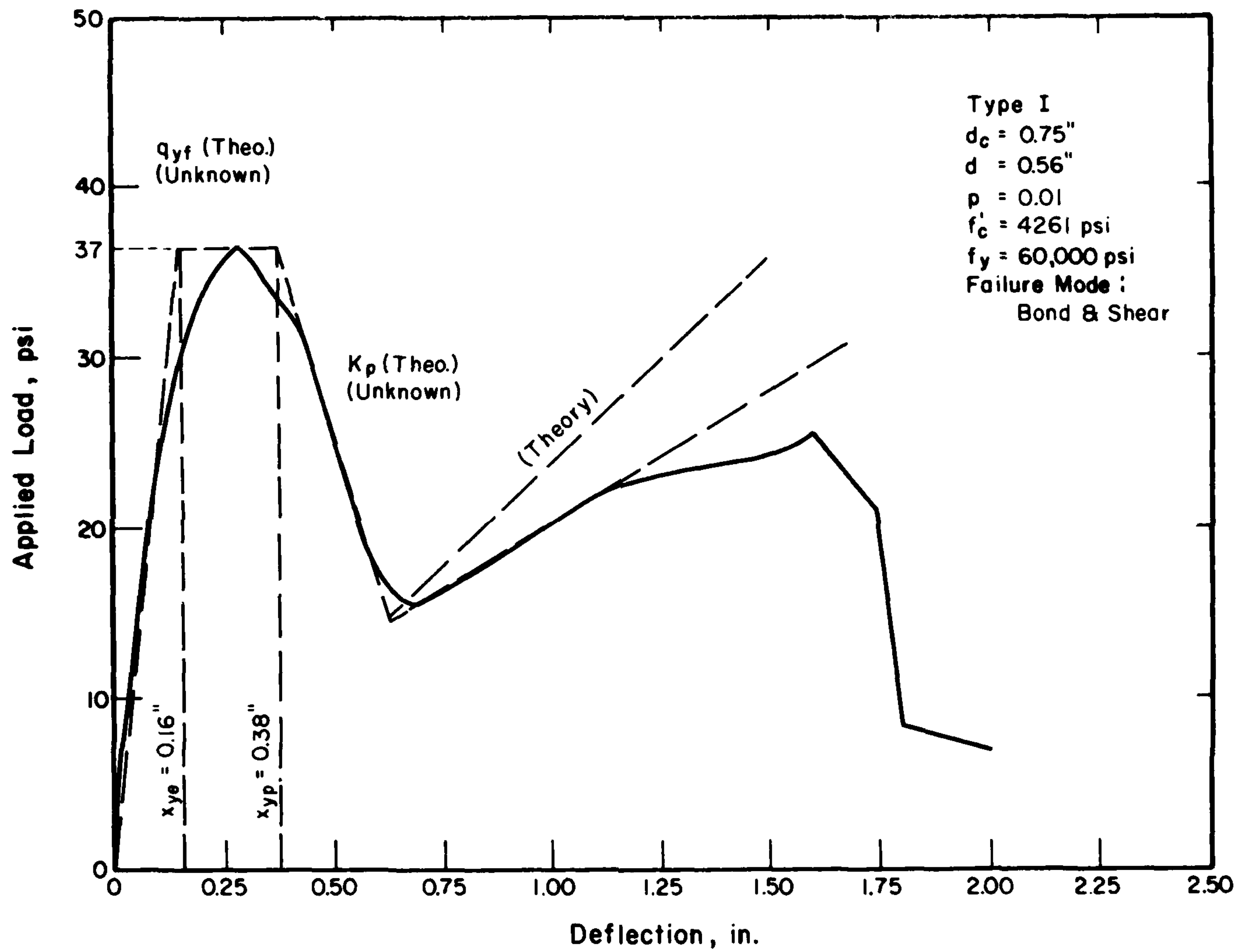

FIG. 9 LOAD-DEFLECTION CURVE FOR SLAB NO. 4

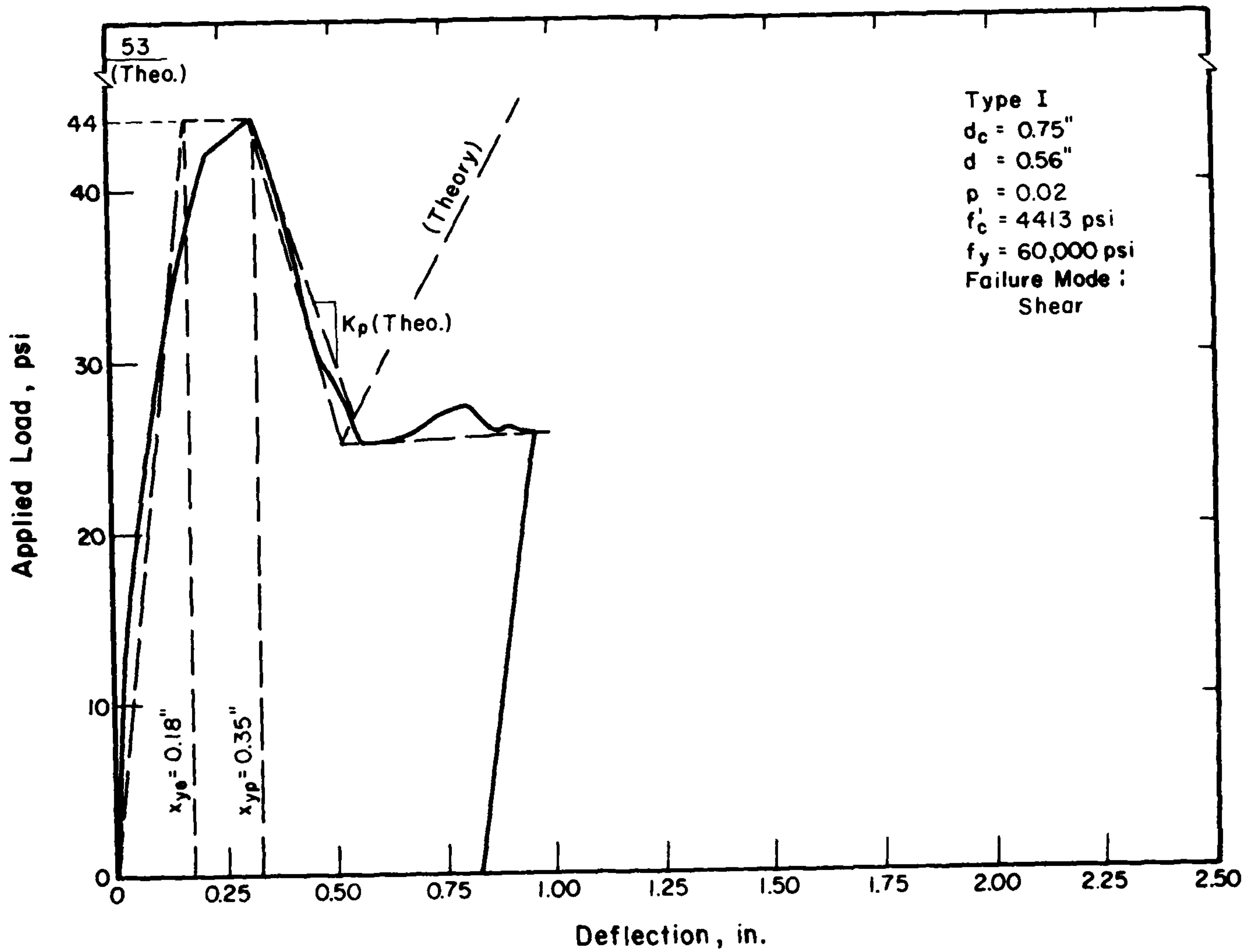

FIG. 10 LOAD-DEFLECTION CURVE FOR SLAB NO. 7

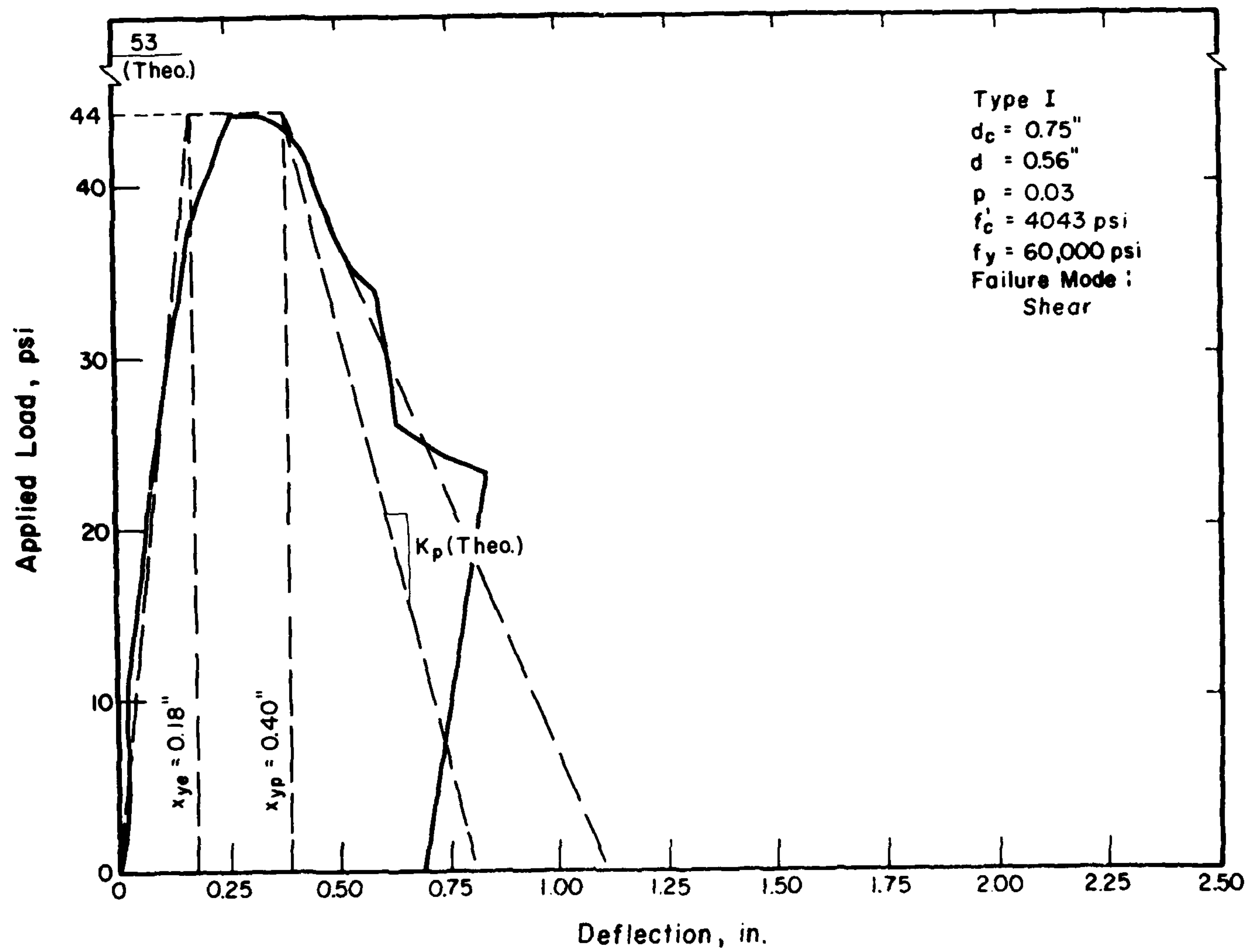

FIG. 11 LOAD-DEFLECTION CURVE FOR SLAB NO. 10

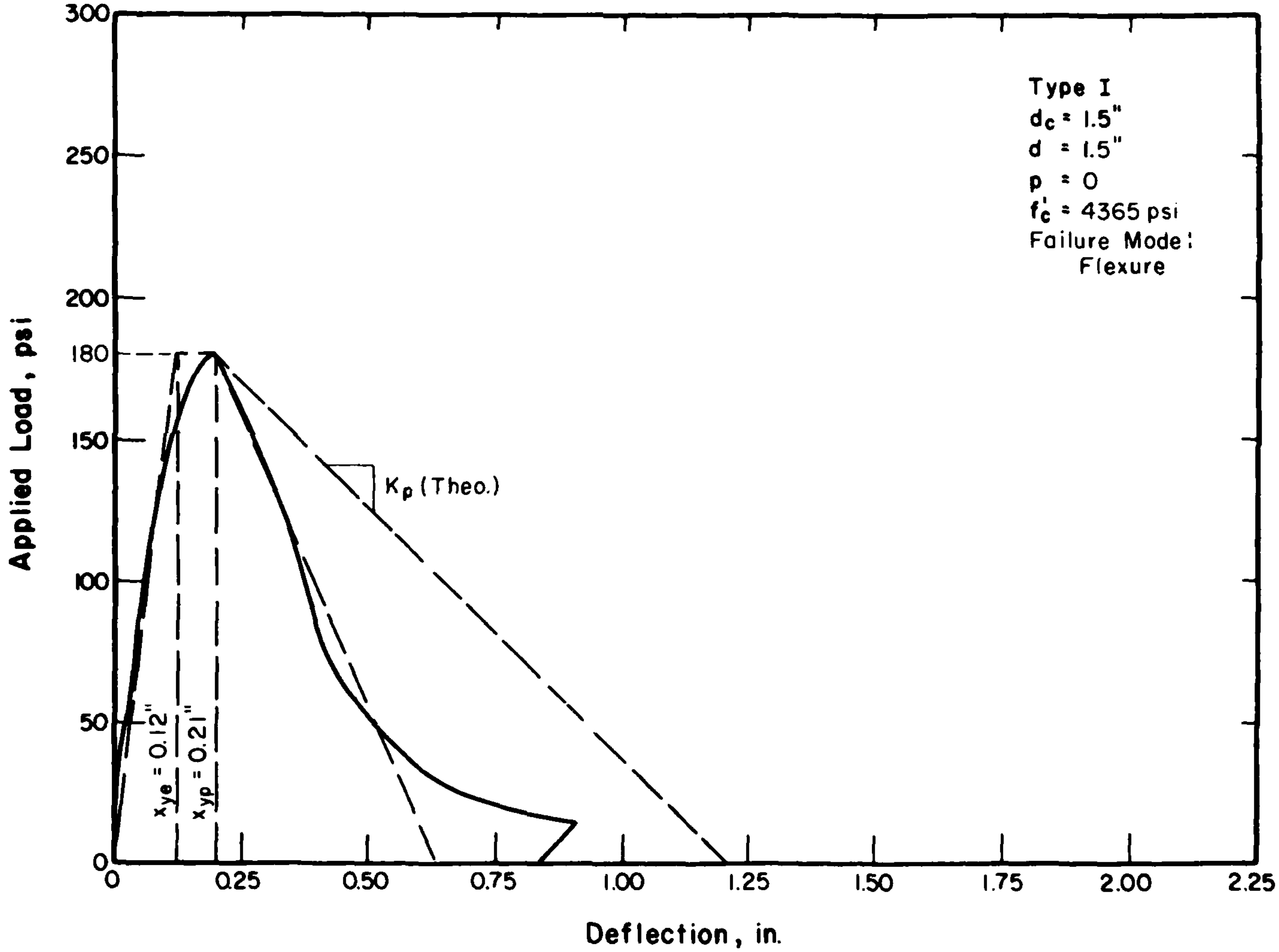

FIG. 12 LOAD-DEFLECTION CURVE FOR SLAB NO. 11

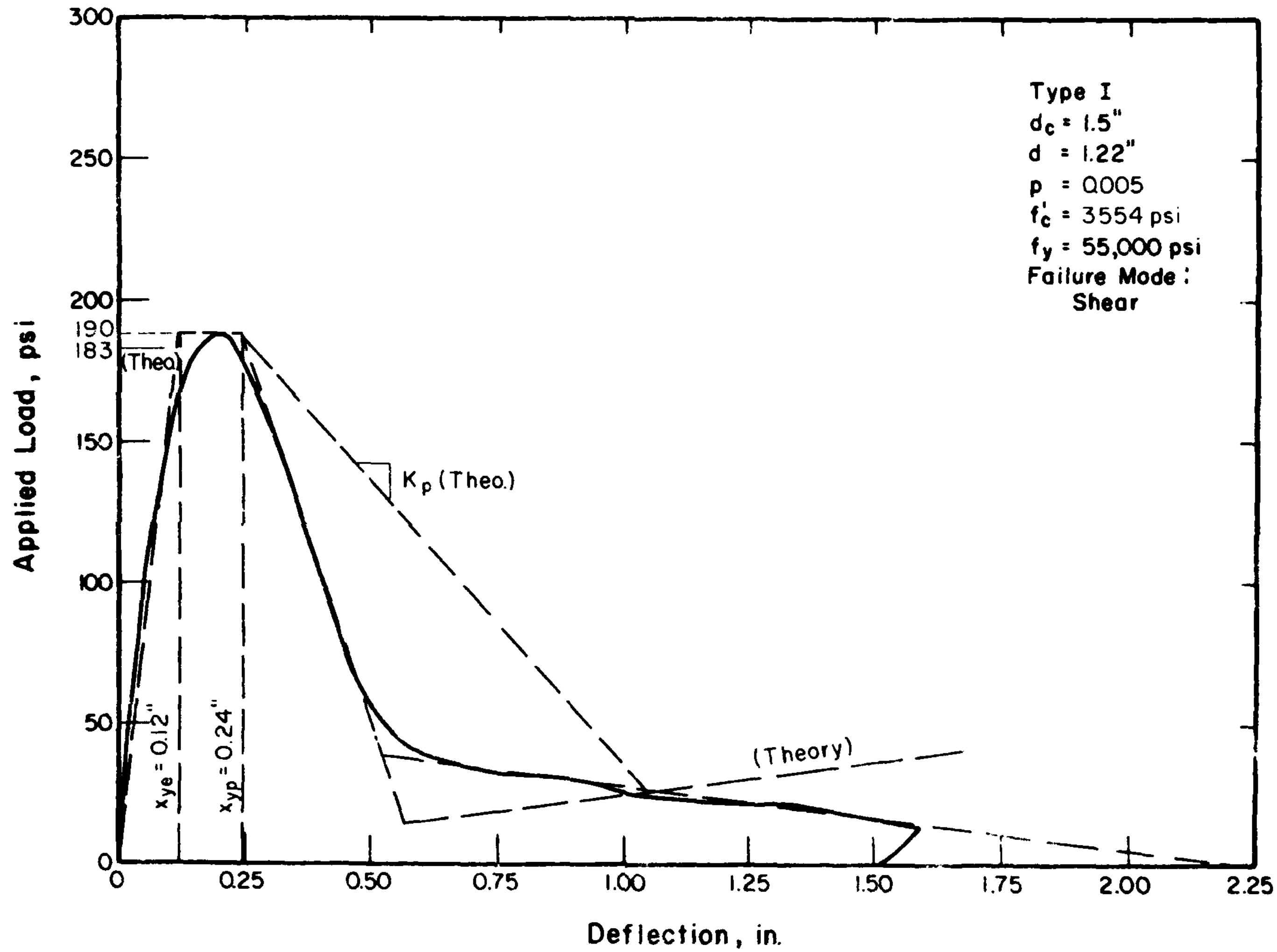

FIG. 13 LOAD-DEFLECTION CURVE FOR SLAB NO. 17

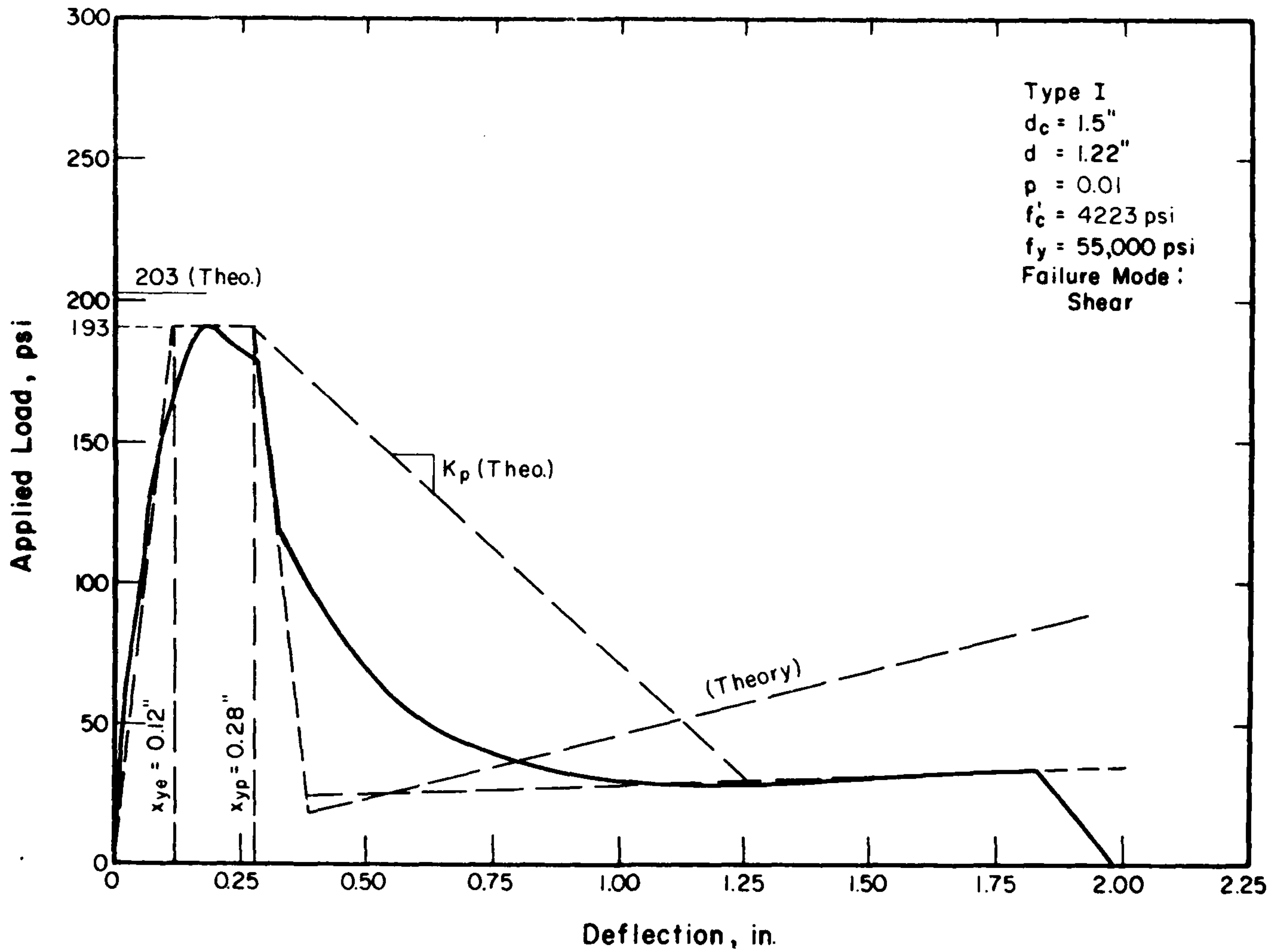

FIG. 14 LOAD-DEFLECTION CURVE FOR SLAB NO. 13

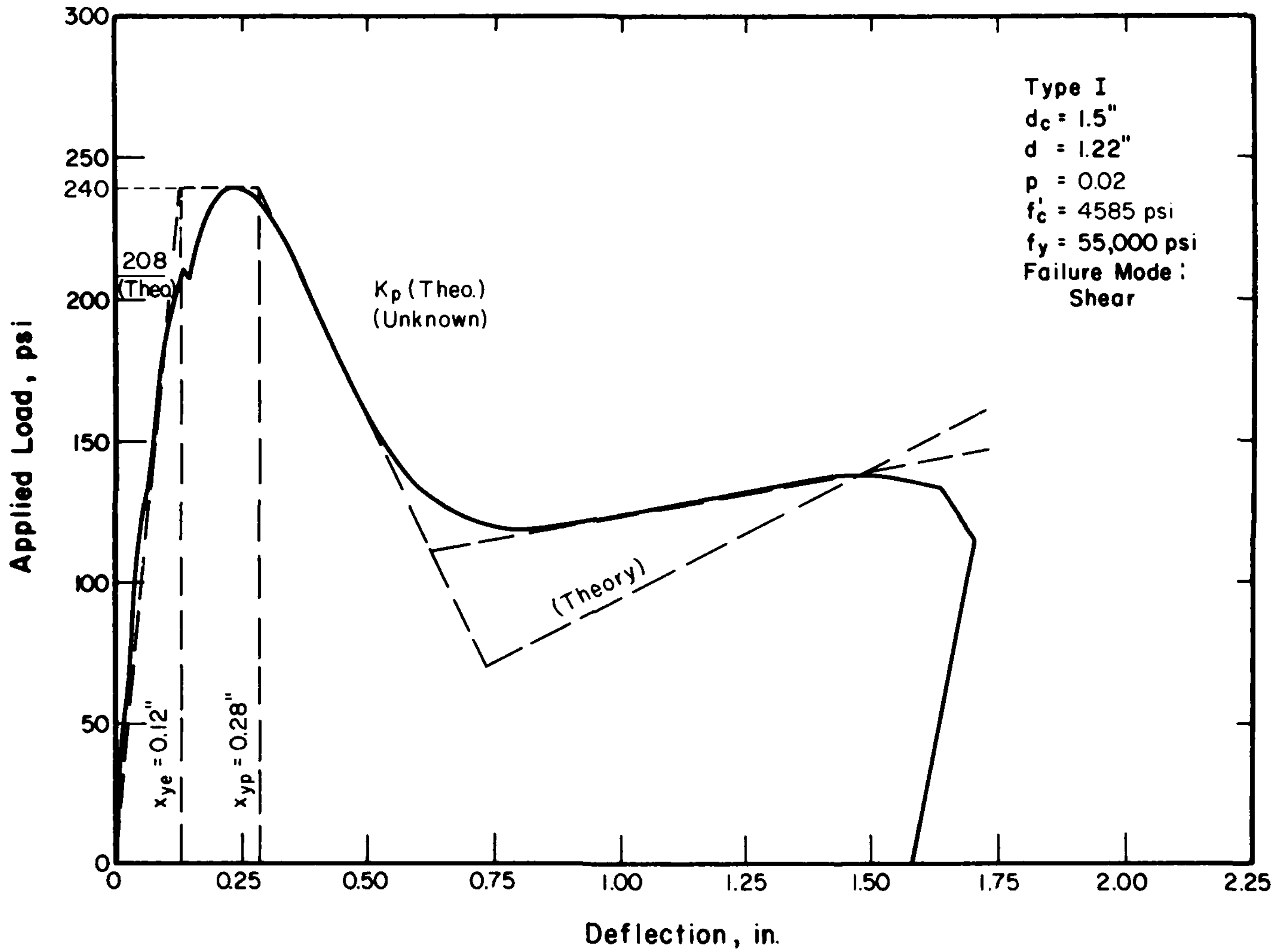

FIG. 15 LOAD-DEFLECTION CURVE FOR SLAB NO. 14

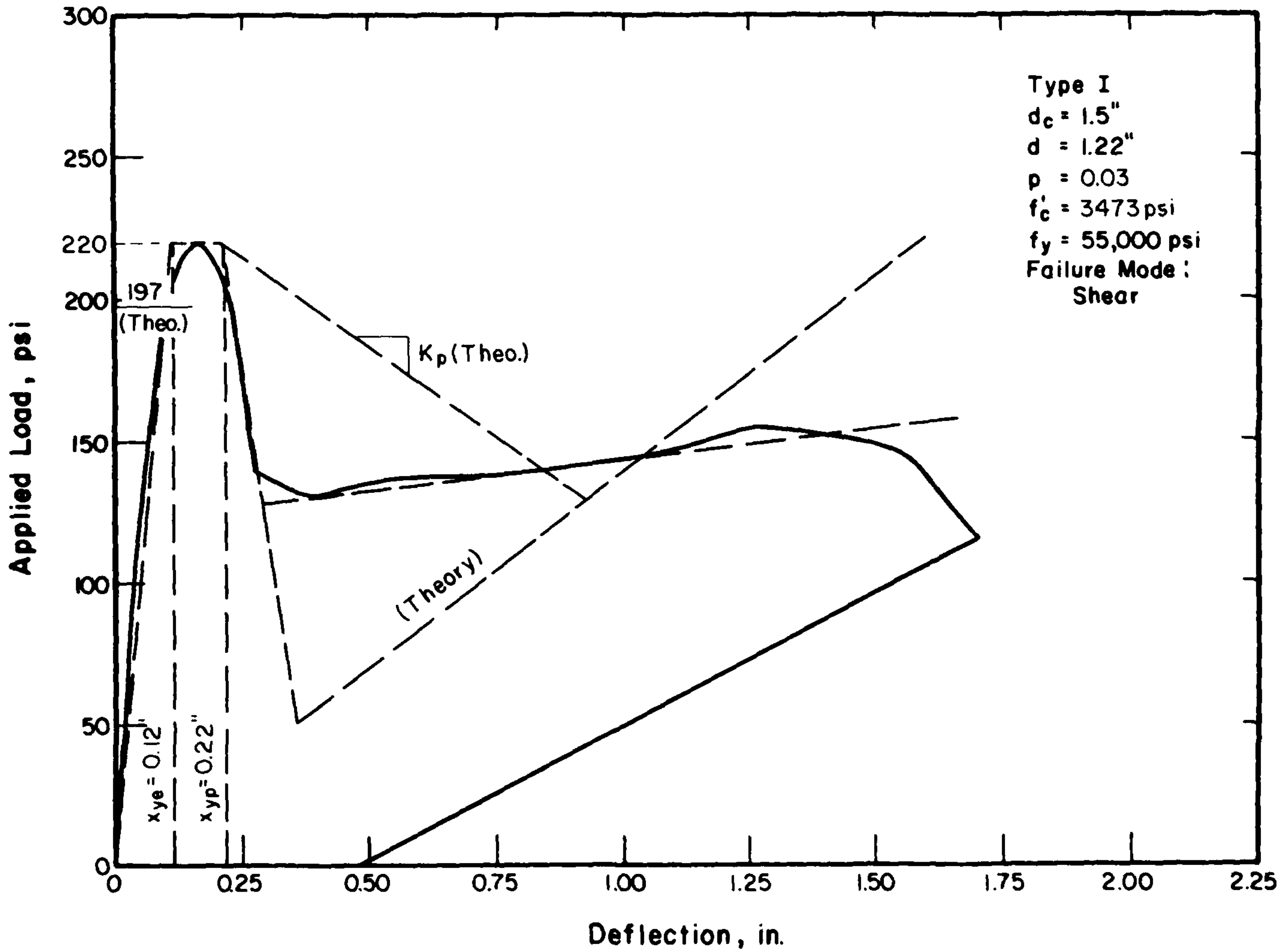

FIG. 16 LOAD-DEFLECTION CURVE FOR SLAB NO. 16

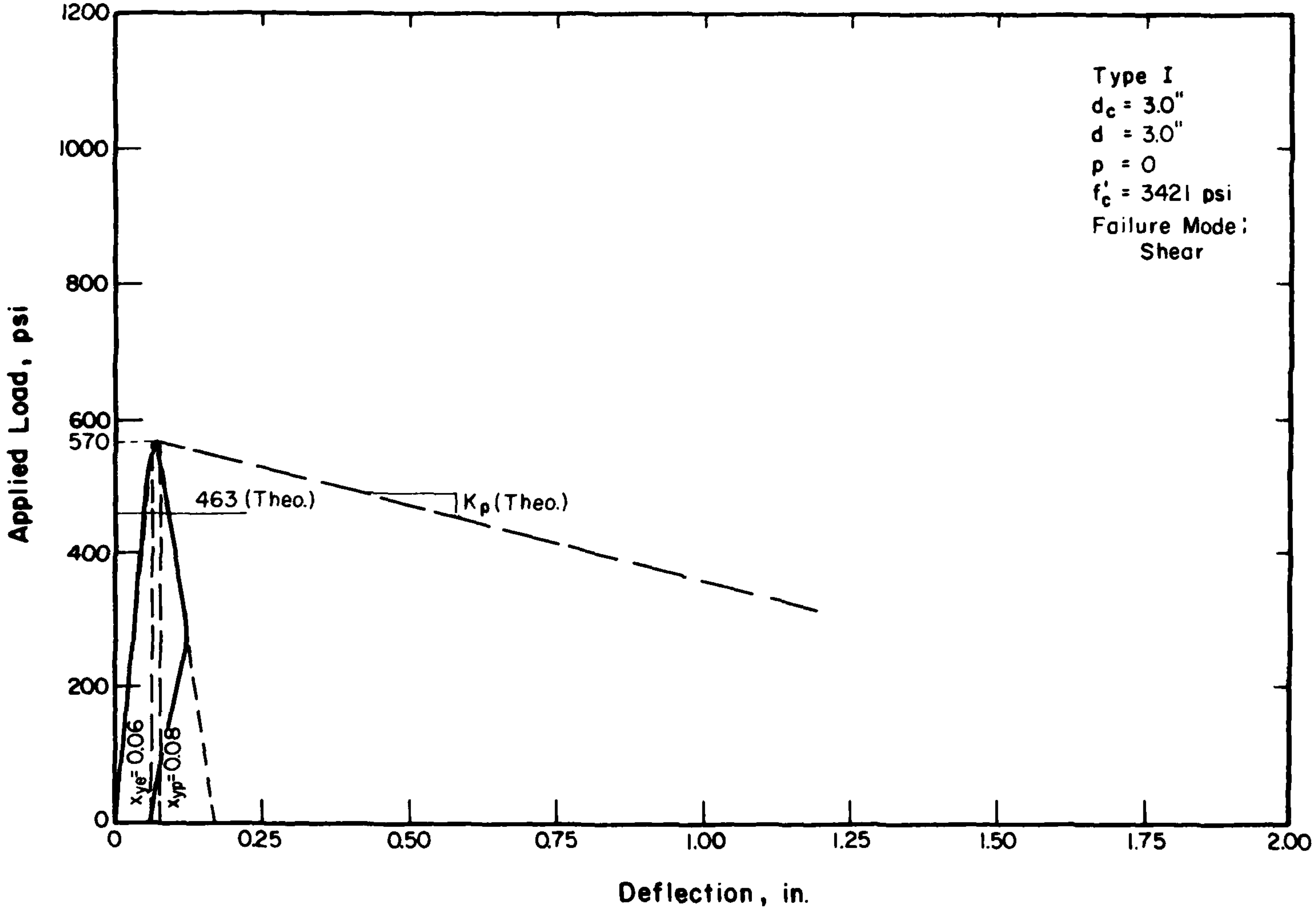

FIG. 17 LOAD-DEFLECTION CURVE FOR SLAB NO. 18

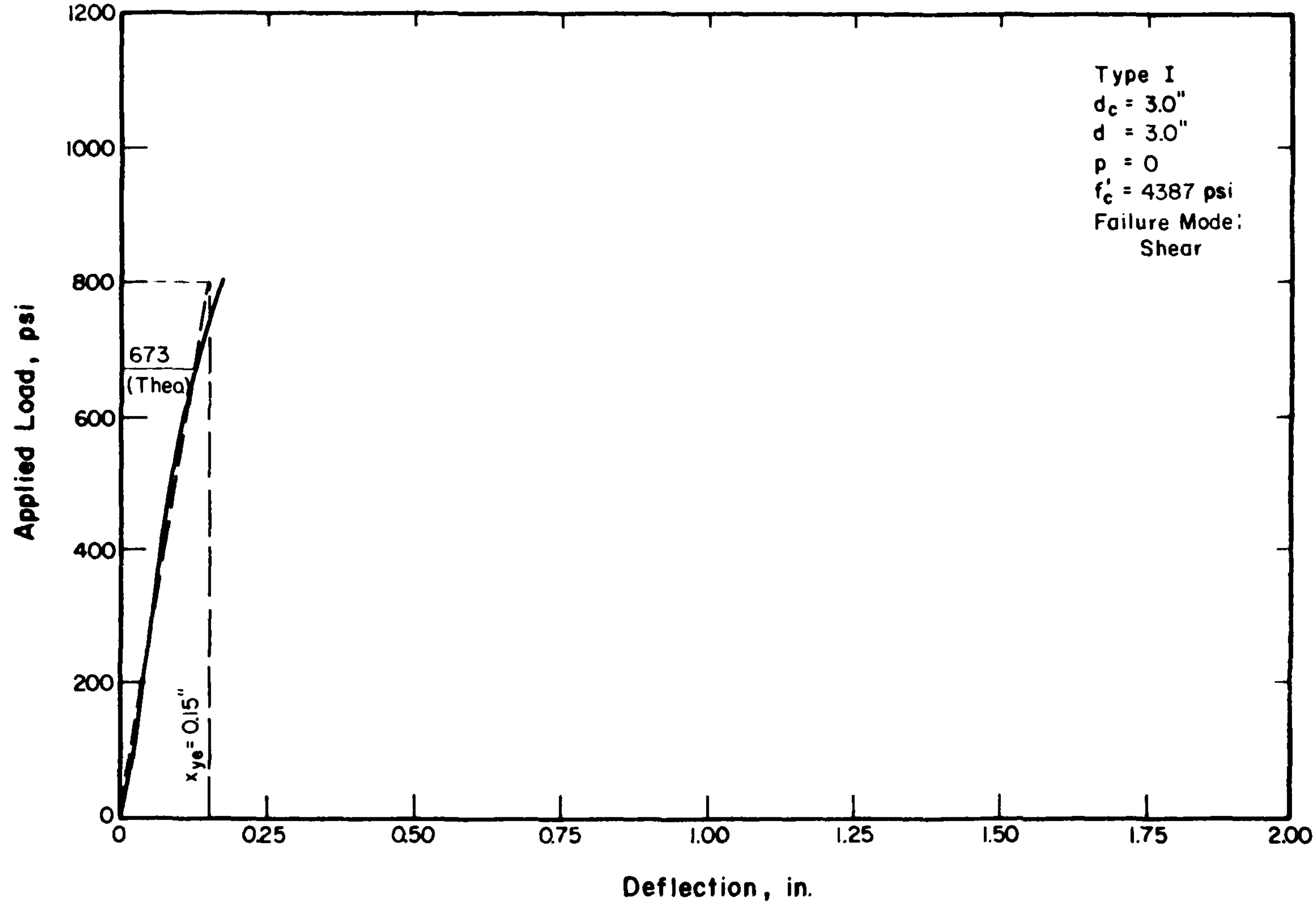

FIG. 18 LOAD-DEFLECTION CURVE FOR SLAB NO. 26

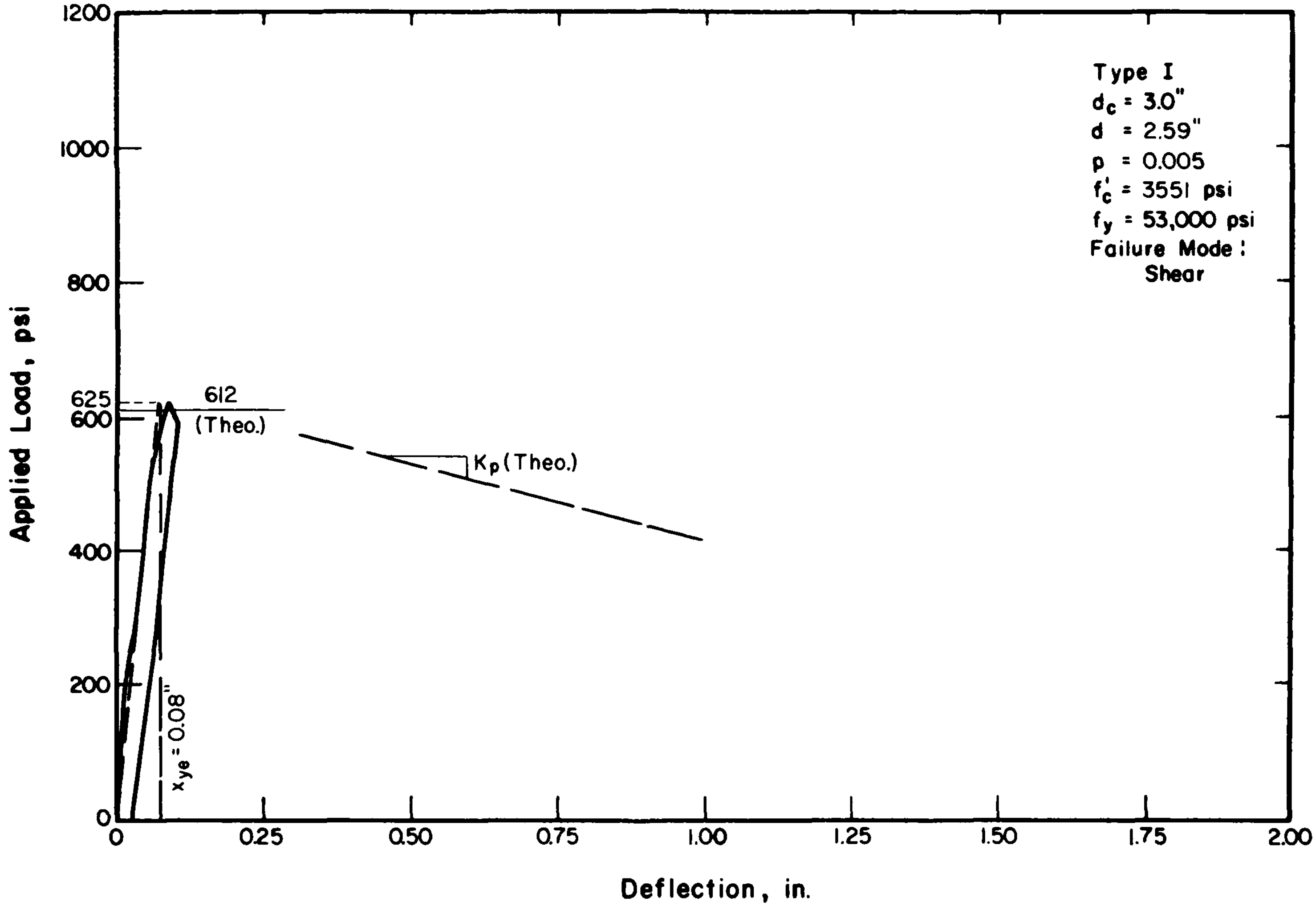

FIG. 19 LOAD-DEFLECTION CURVE FOR SLAB NO. 24

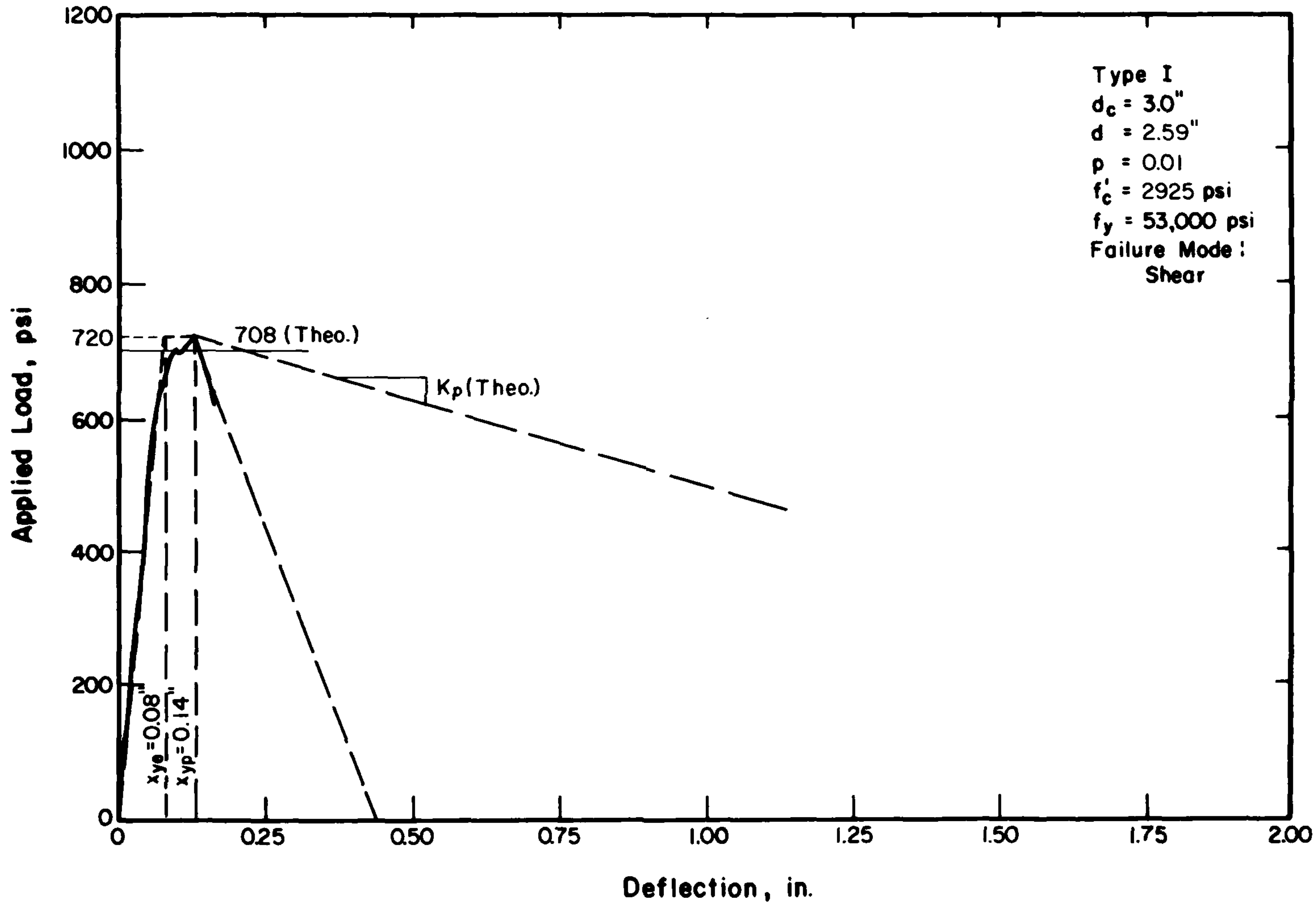

FIG. 20 LOAD-DEFLECTION CURVE FOR SLAB NO. 20

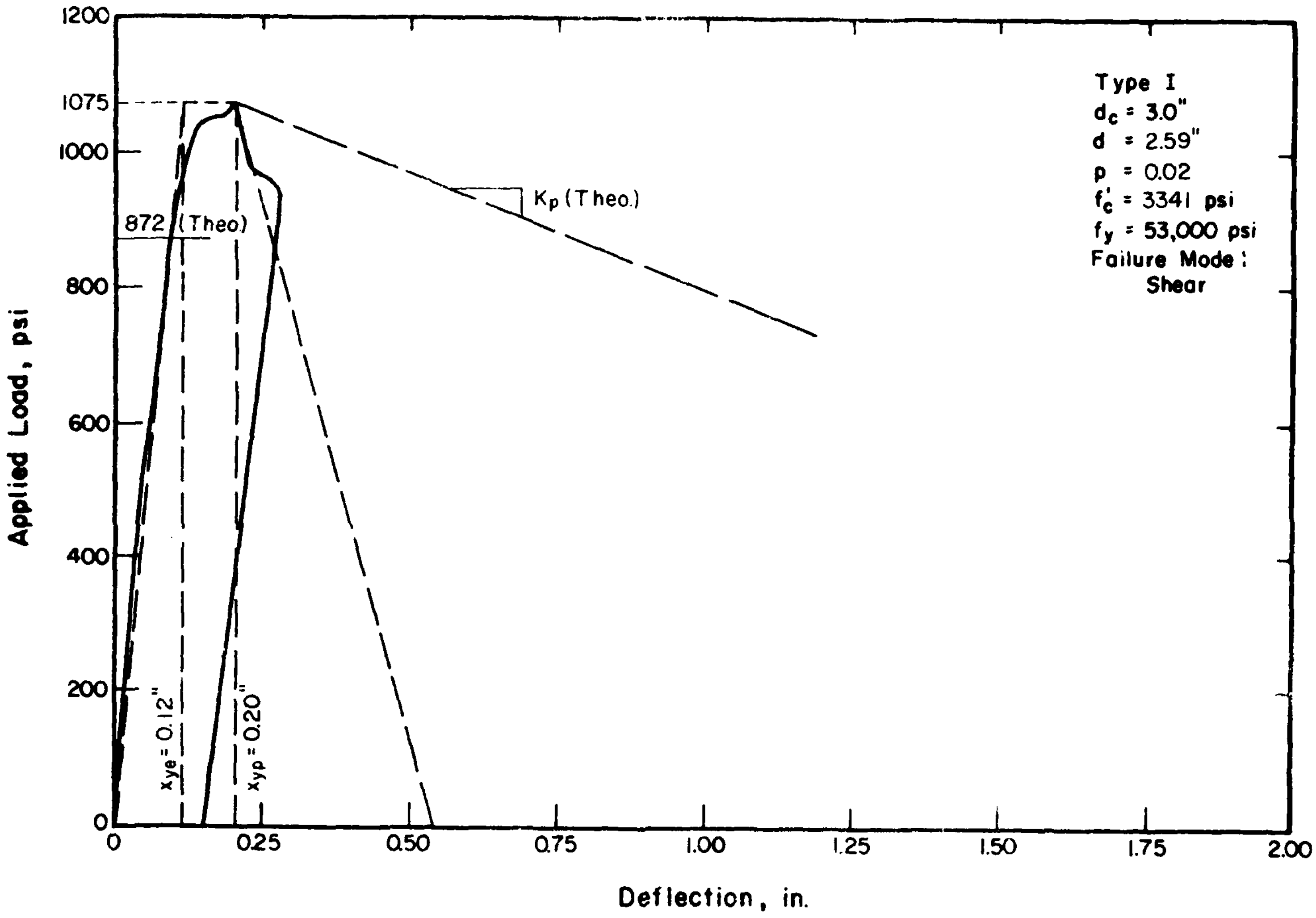

FIG. 21 LOAD-DEFLECTION CURVE FOR SLAB NO. 21

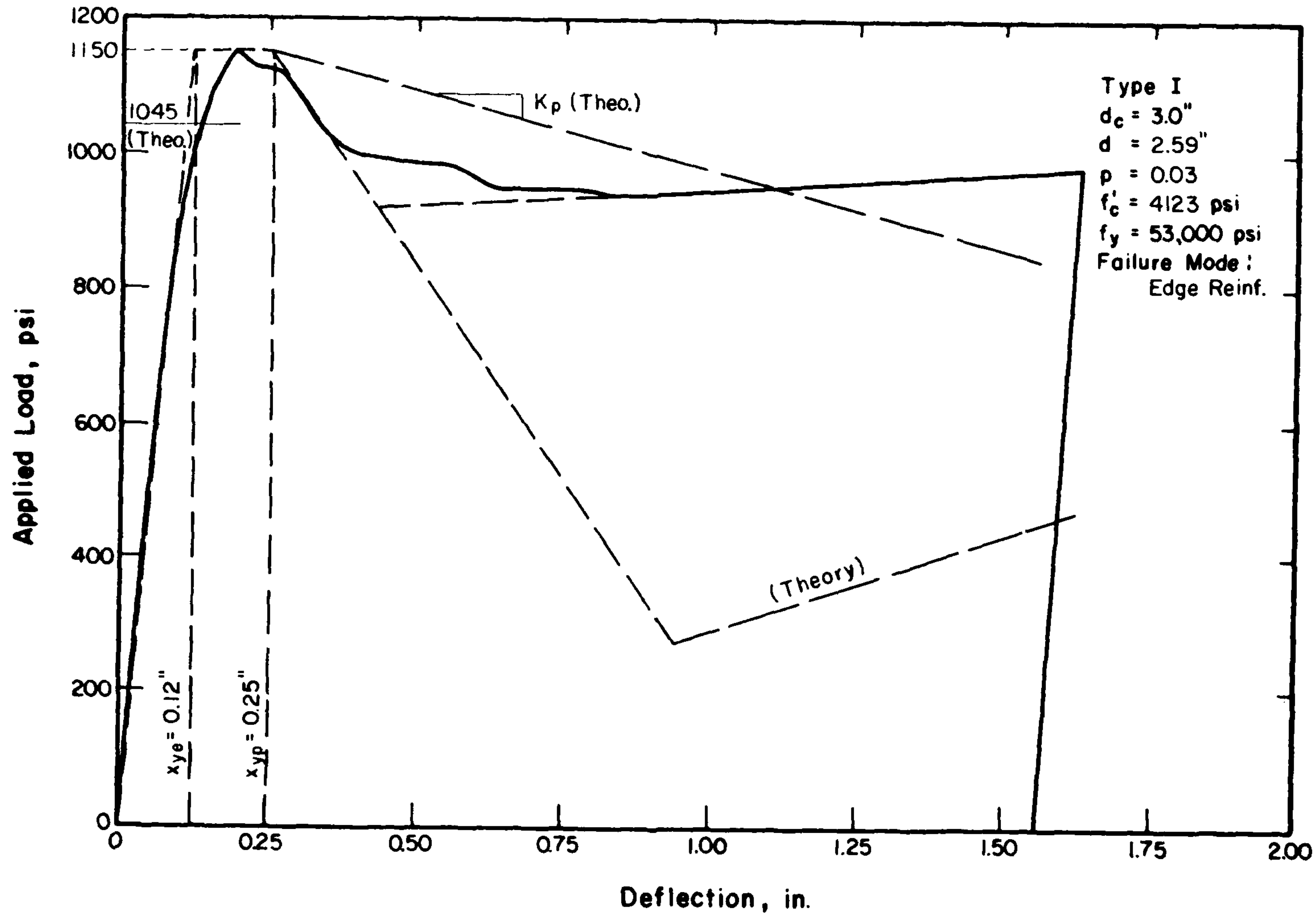

FIG. 22 LOAD-DEFLECTION CURVE FOR SLAB NO. 22

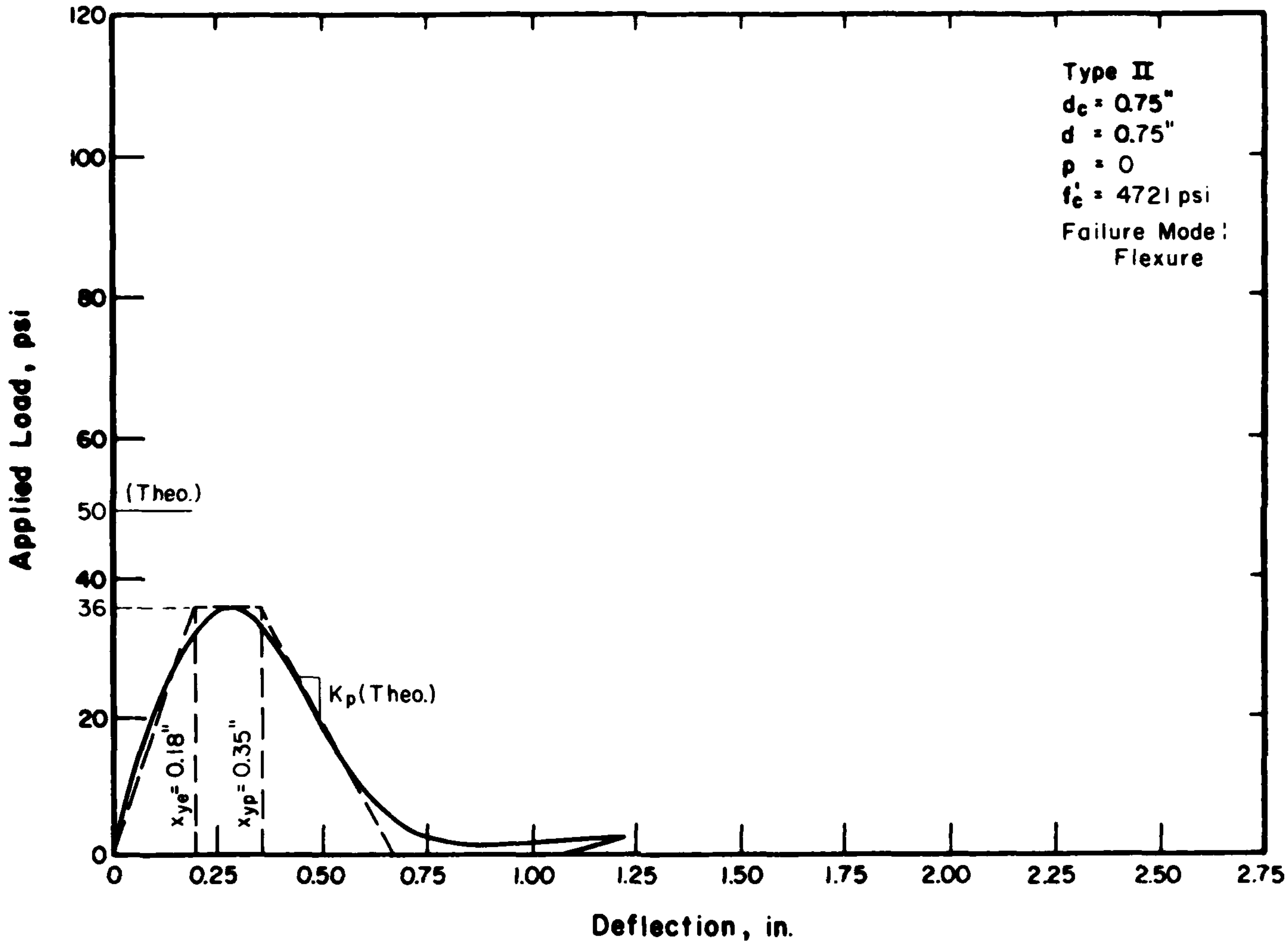

FIG. 23 LOAD-DEFLECTION CURVE FOR SLAB NO. 32

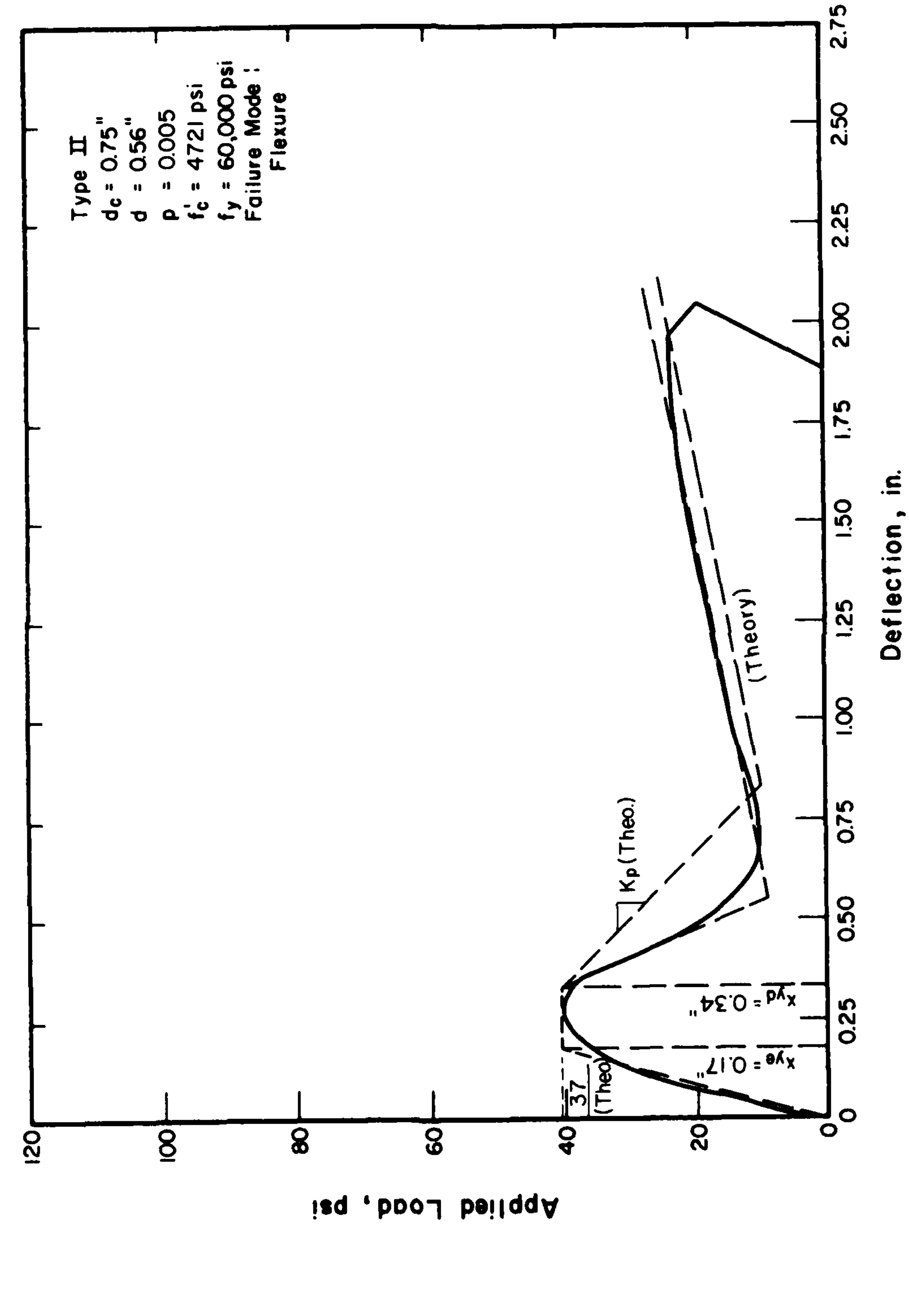

FIG. 24 LOAD-DEFLECTION CURVE FOR SLAB NO. 33

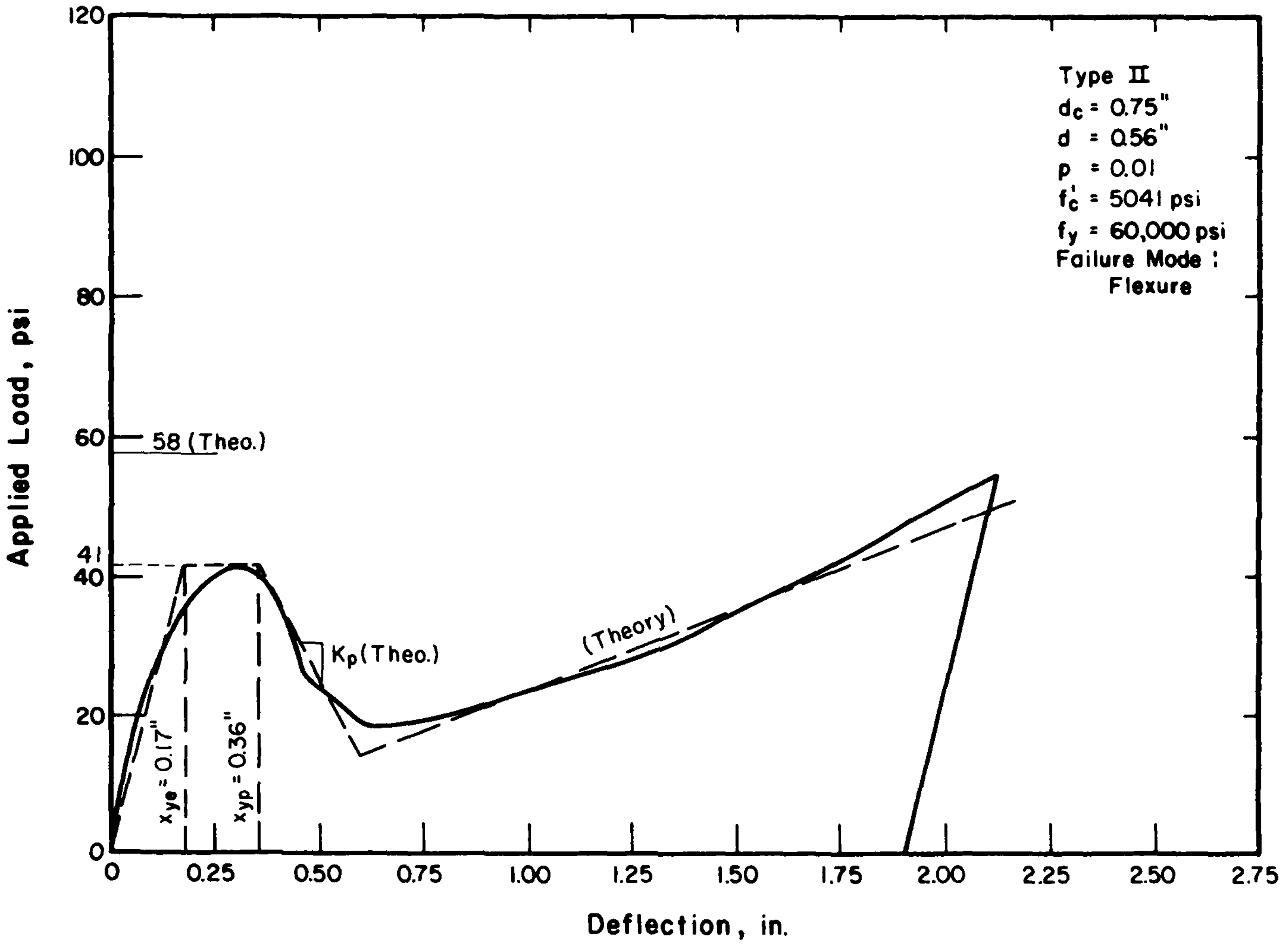

FIG. 25 LOAD-DEFLECTION CURVE FOR SLAB NO. 34

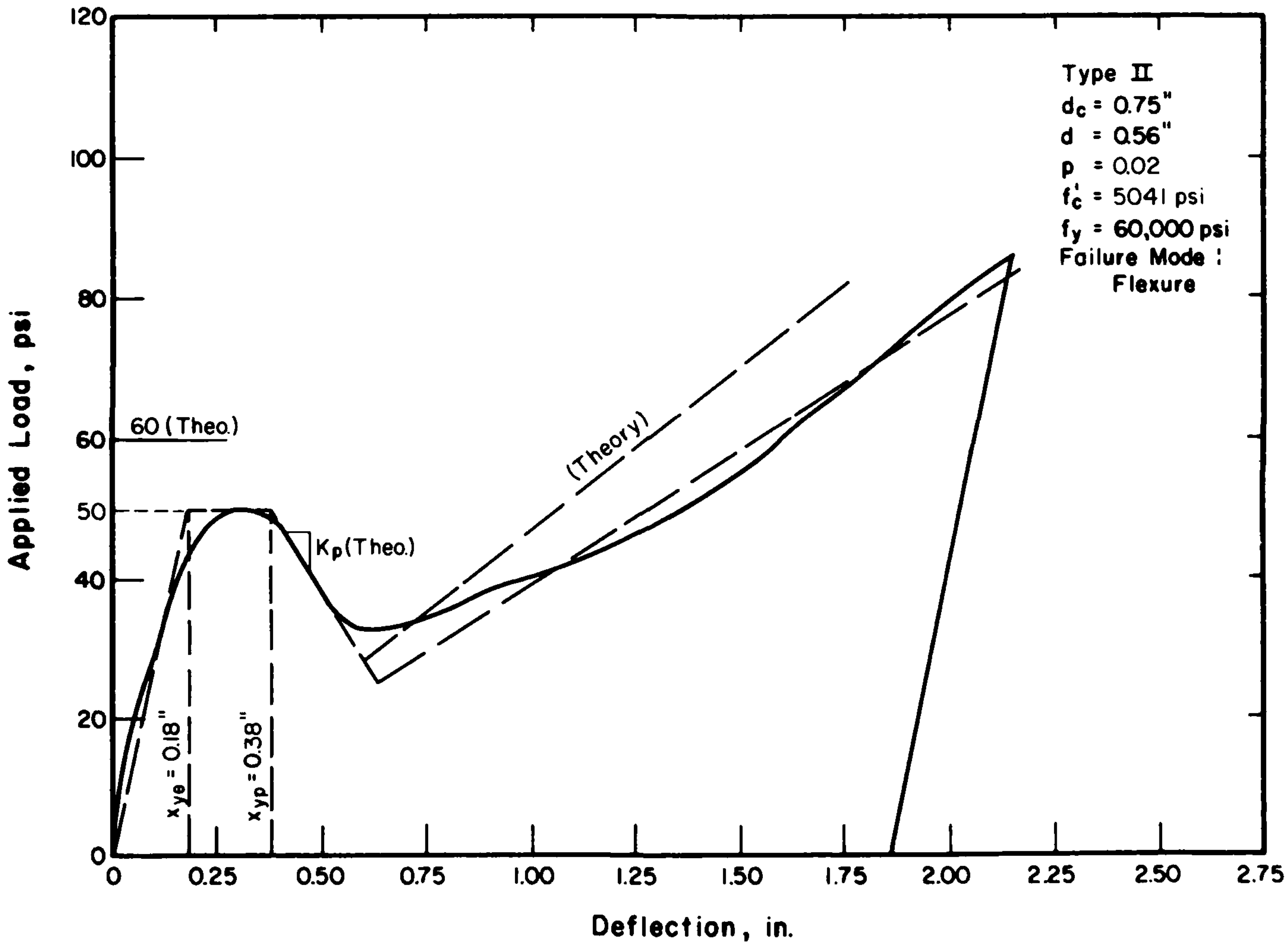

FIG. 26 LOAD-DEFLECTION CURVE FOR SLAB NO. 35

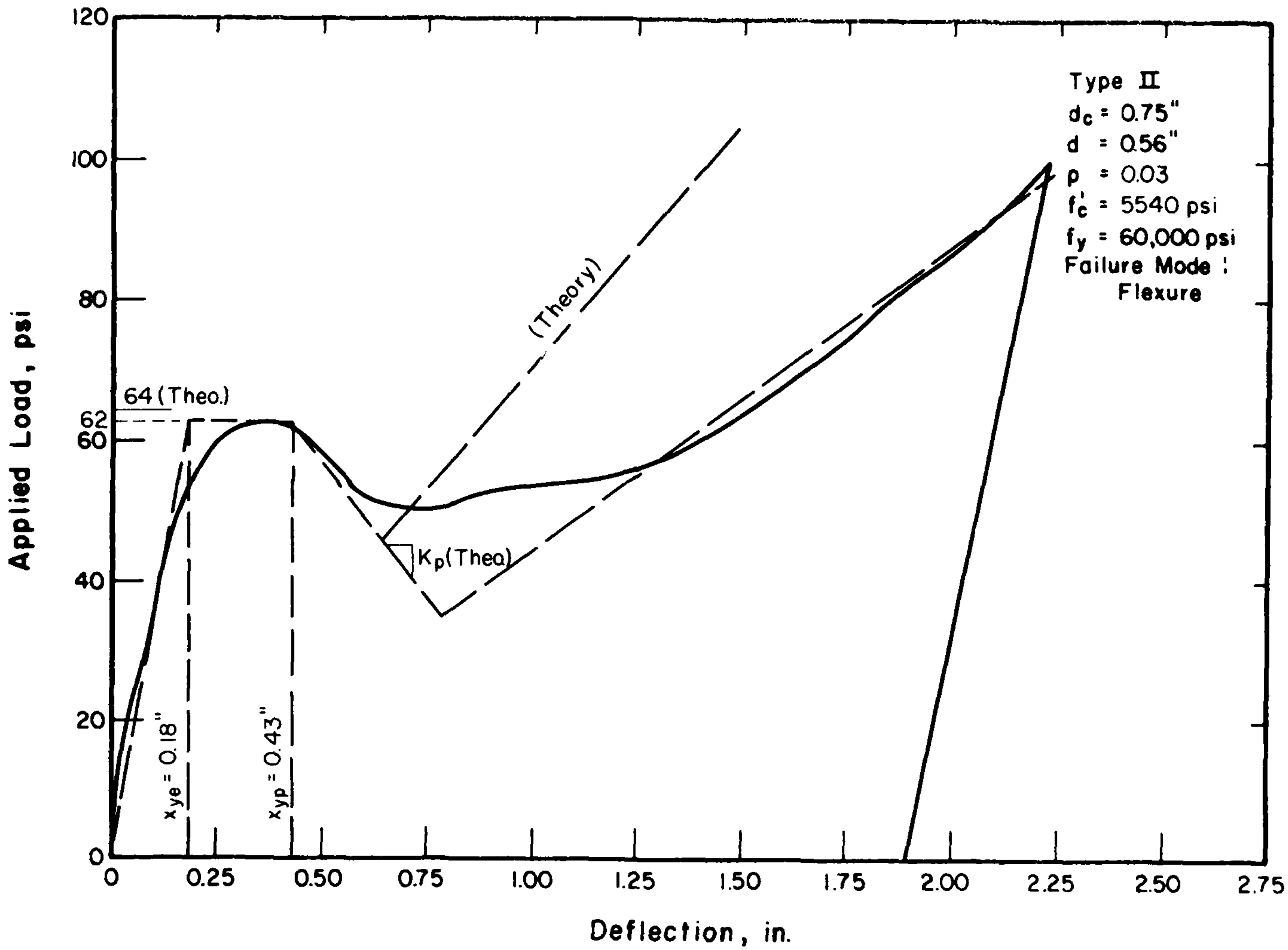

FIG. 27 LOAD-DEFLECTION CURVE FOR SLAB NO. 36

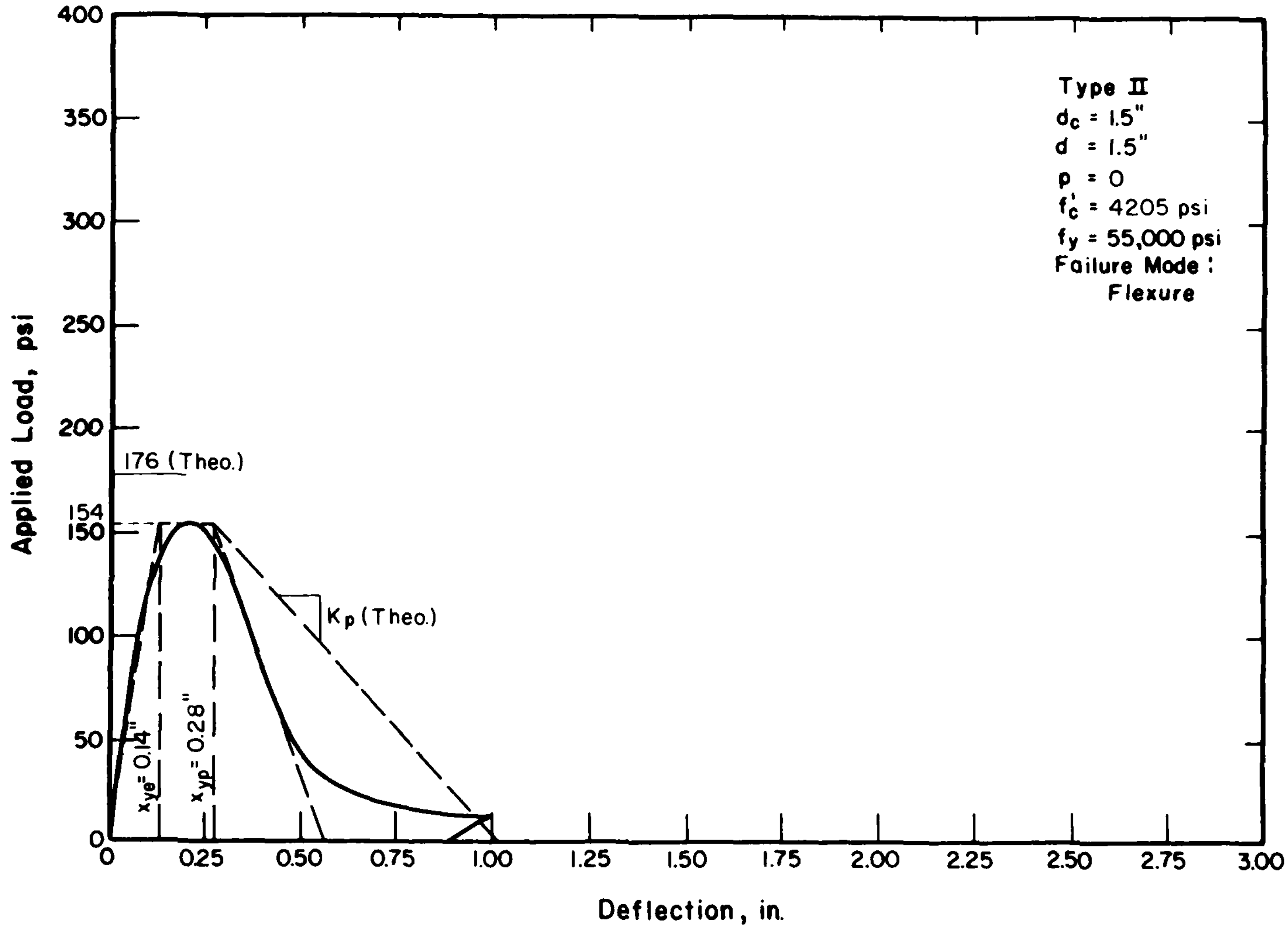

FIG. 28 LOAD-DEFLECTION CURVE FOR SLAB NO. 27

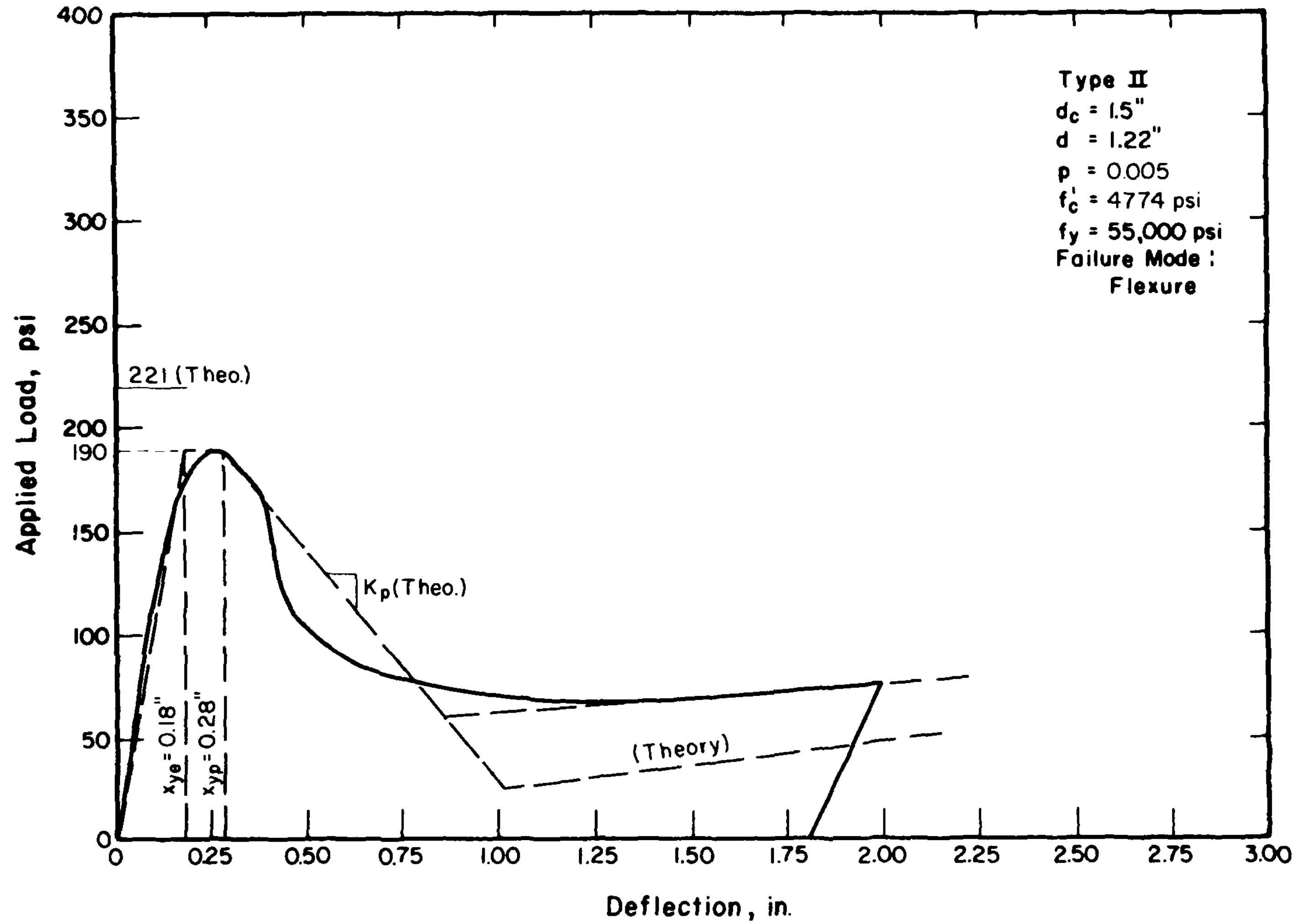

FIG. 29 LOAD-DEFLECTION CURVE FOR SLAB NO. 28

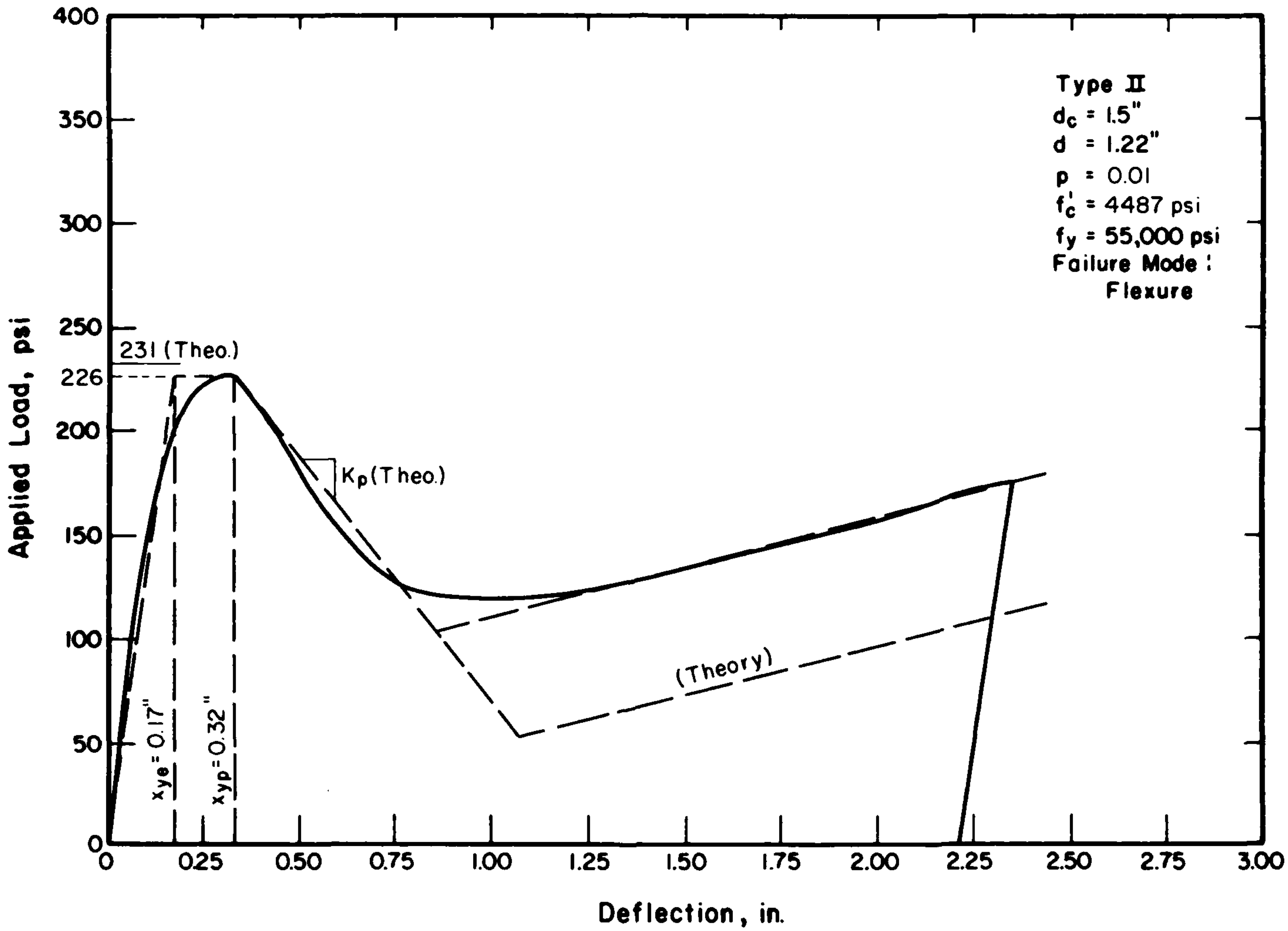

FIG. 30 LOAD-DEFLECTION CURVE FOR SLAB NO. 29

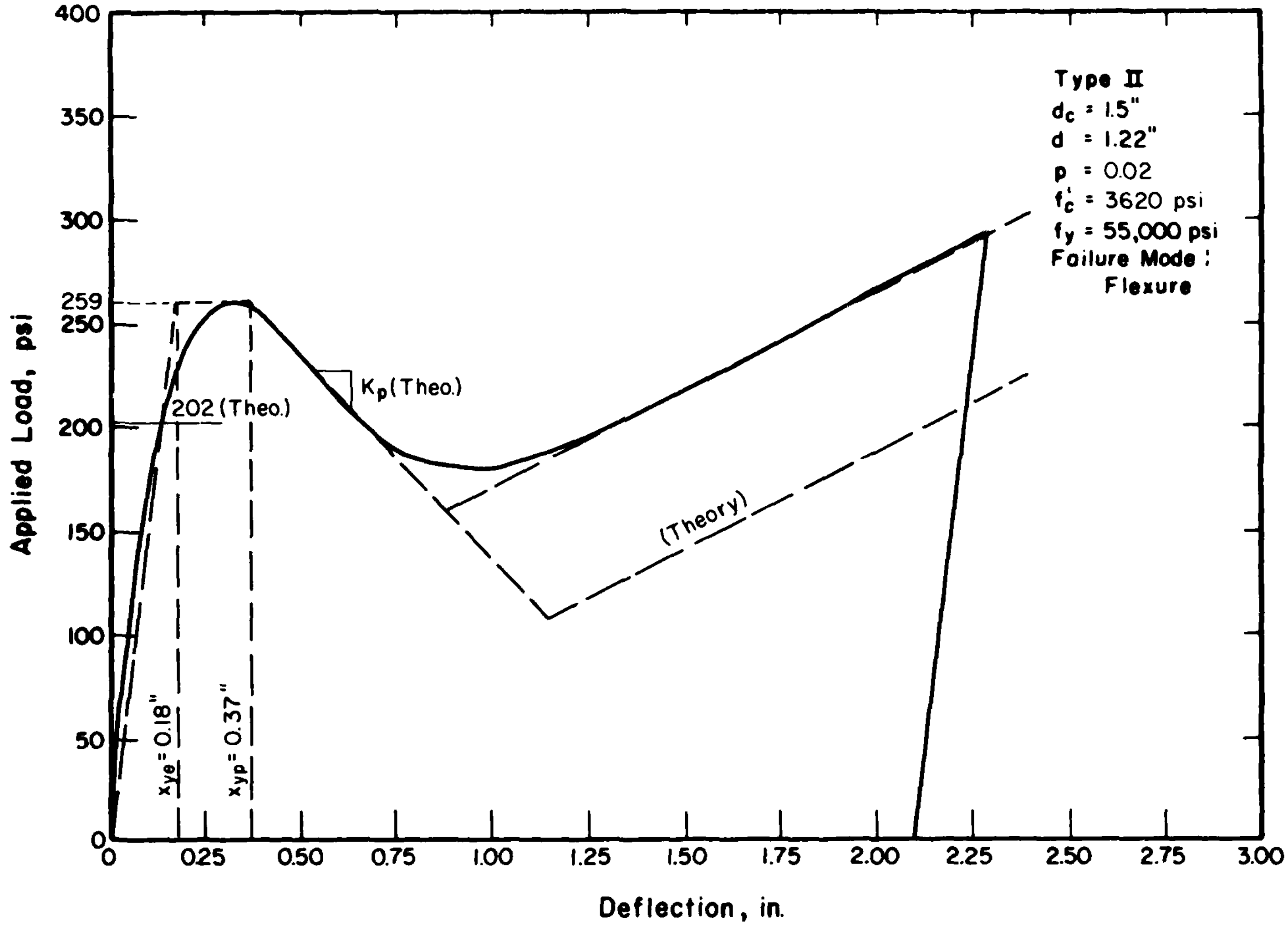

FIG. 31 LOAD-DEFLECTION CURVE FOR SLAB NO. 31

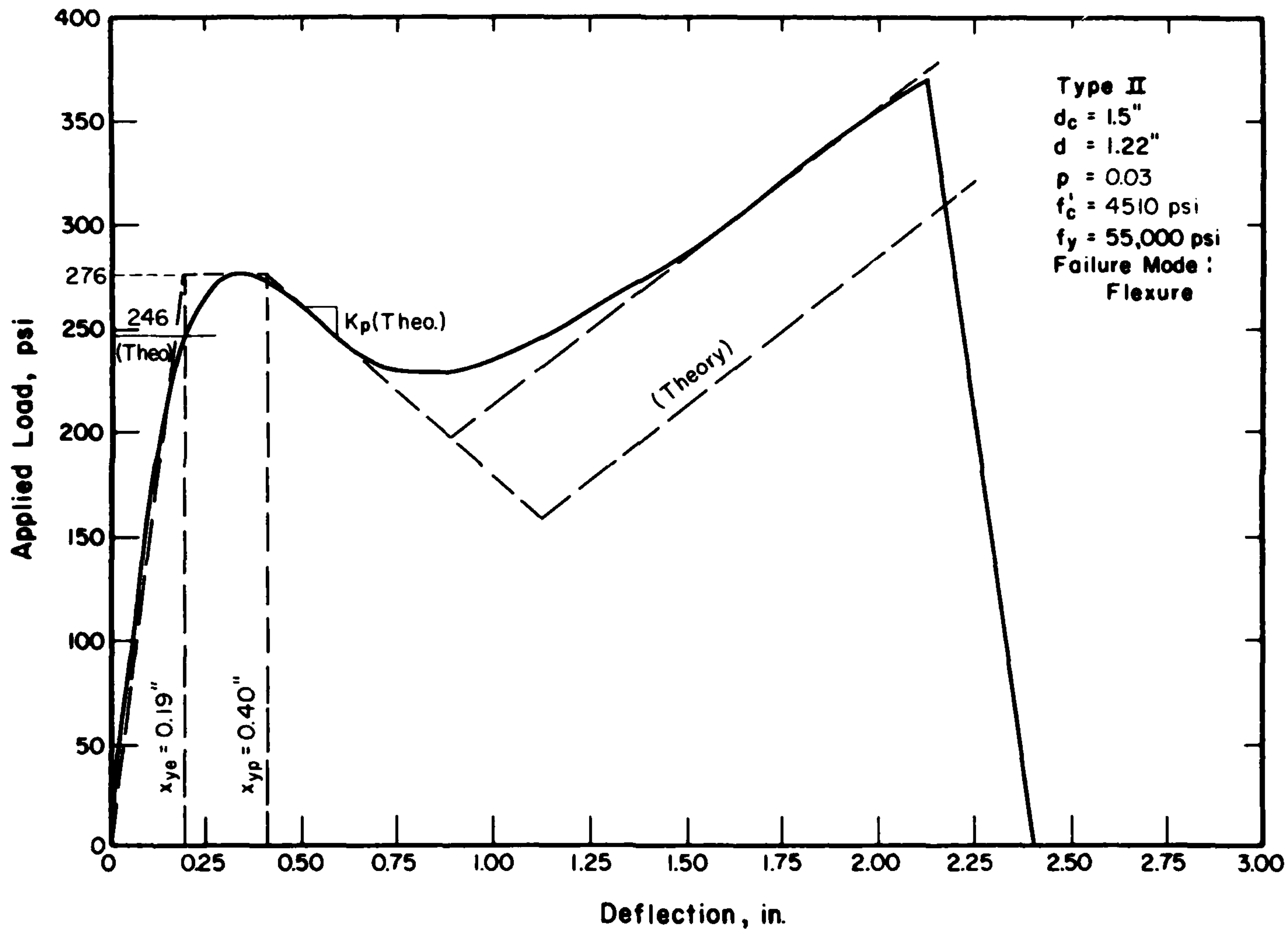

FIG. 32 LOAD-DEFLECTION CURVE FOR SLAB NO. 30

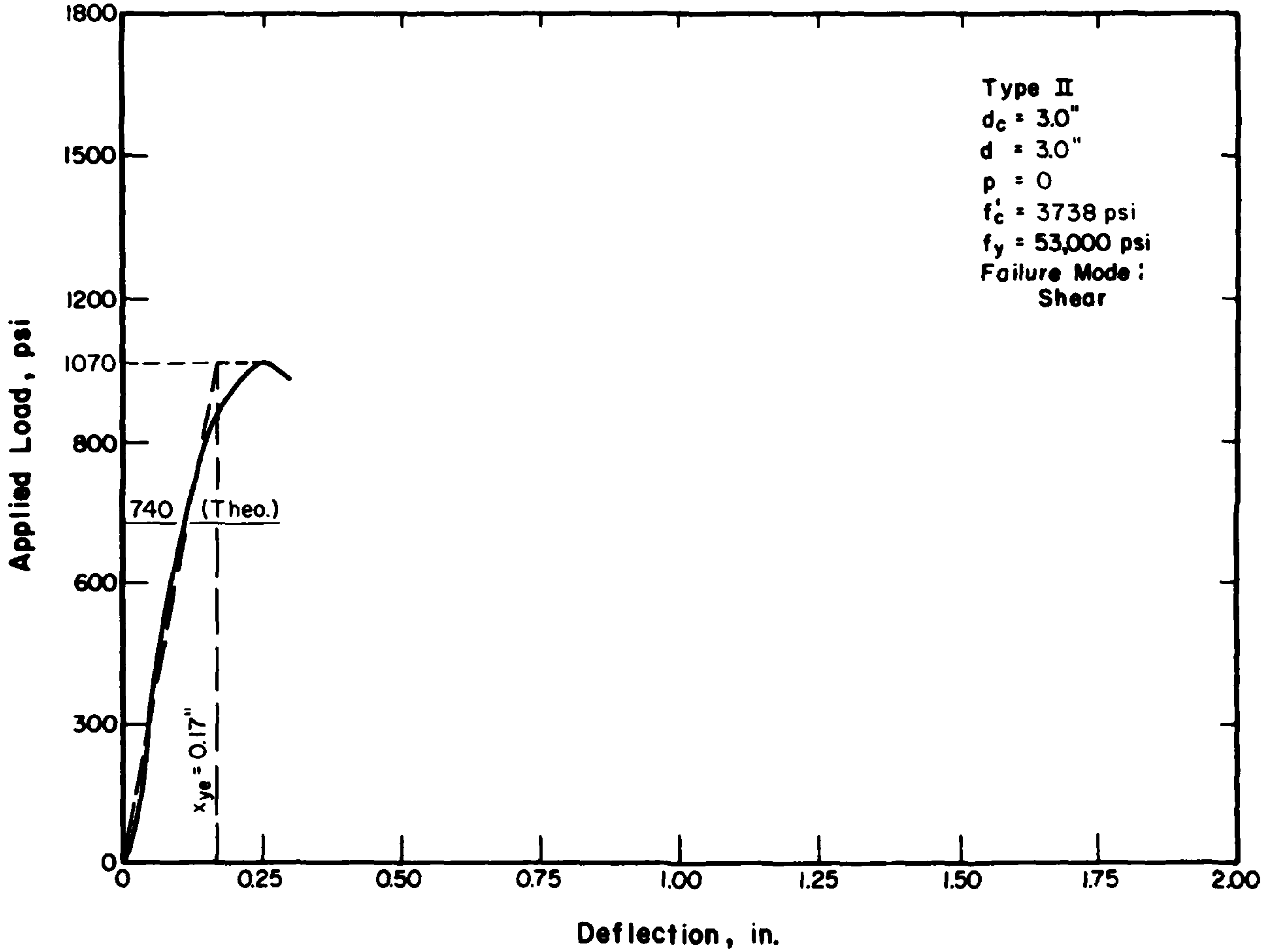

FIG. 33 LOAD-DEFLECTION CURVE FOR SLAB NO. 37

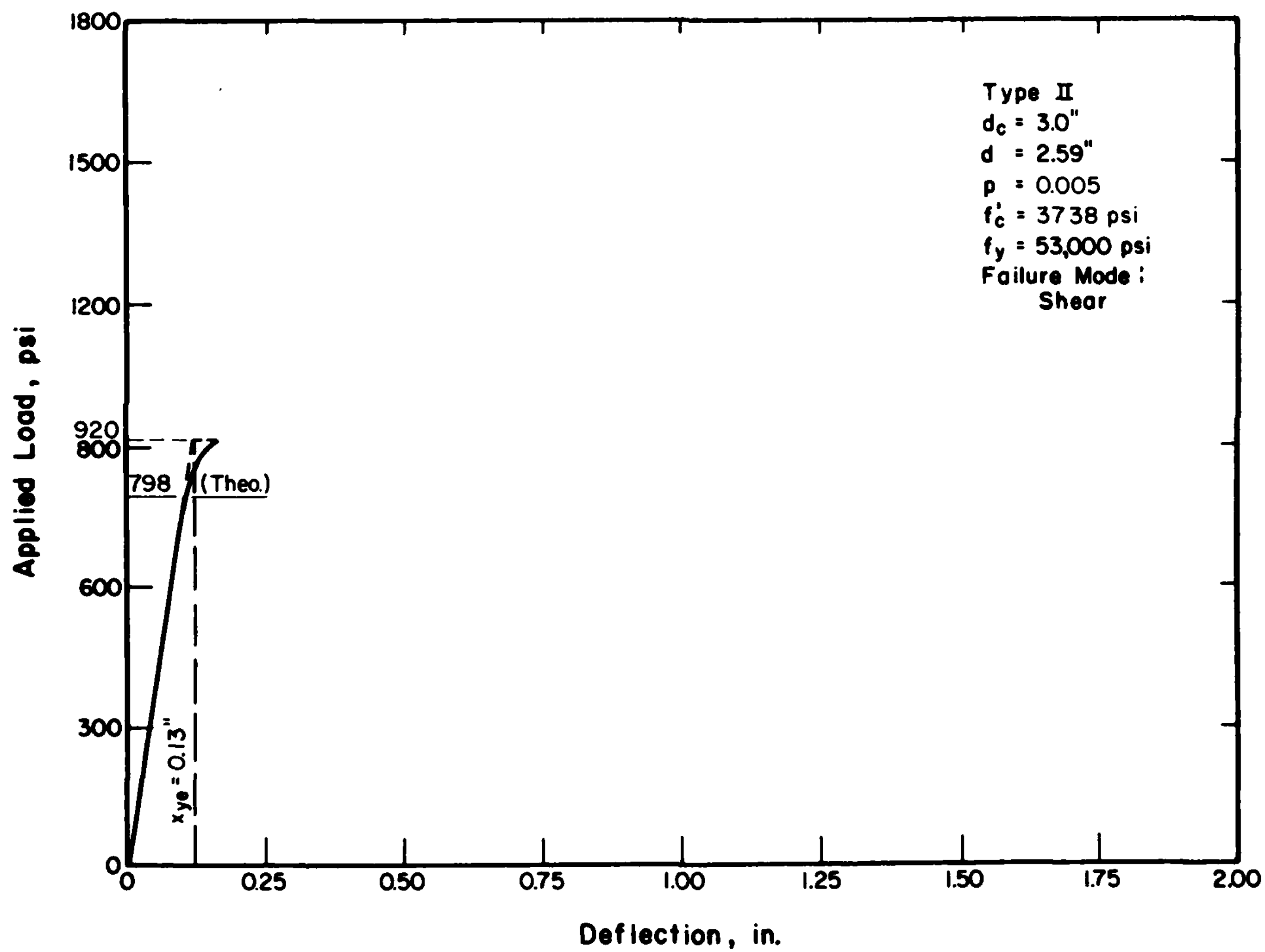

FIG. 34 LOAD-DEFLECTION CURVE FOR SLAB NO. 38

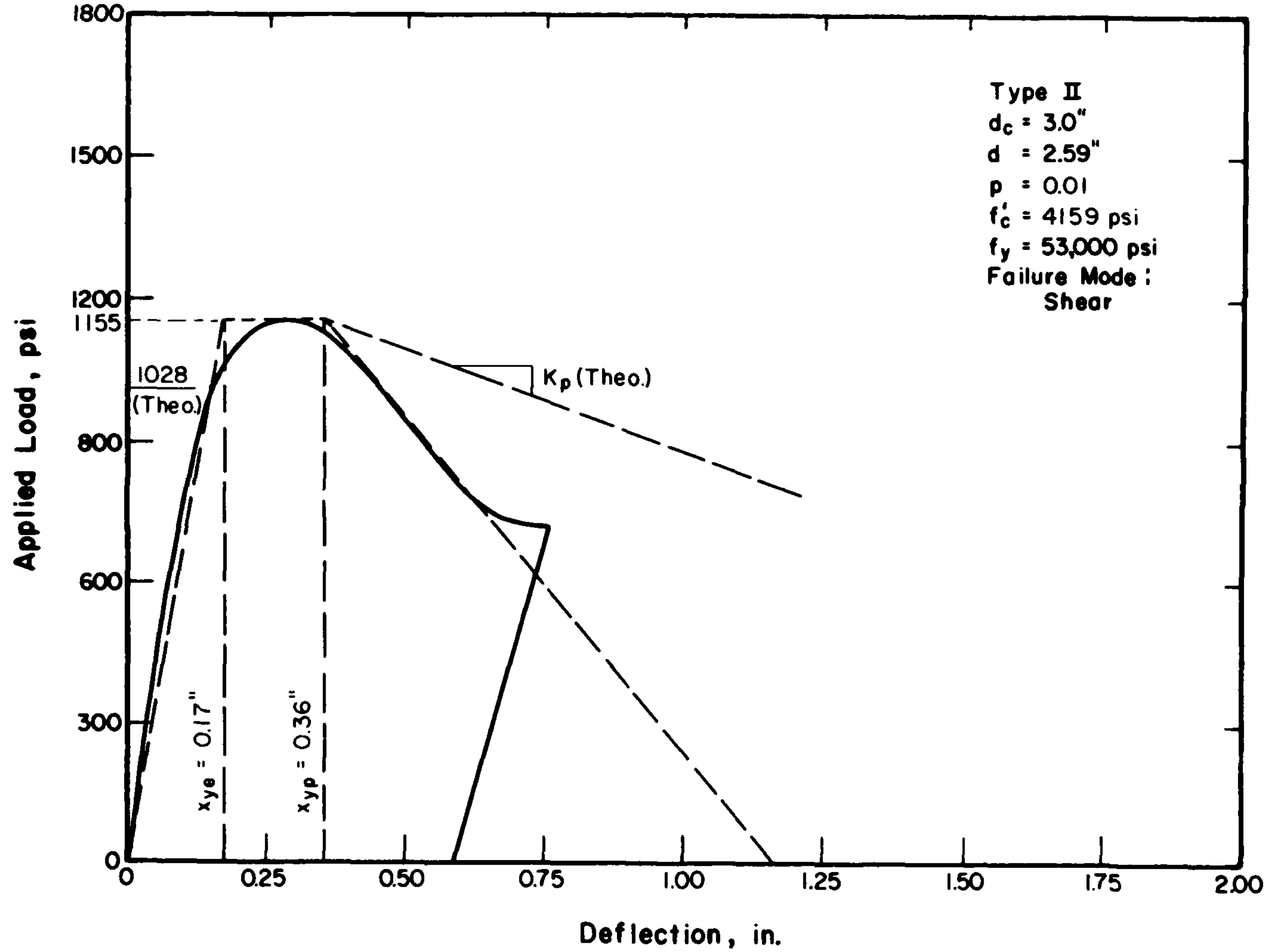

FIG. 35 LOAD-DEFLECTION CURVE FOR SLAB NO. 39

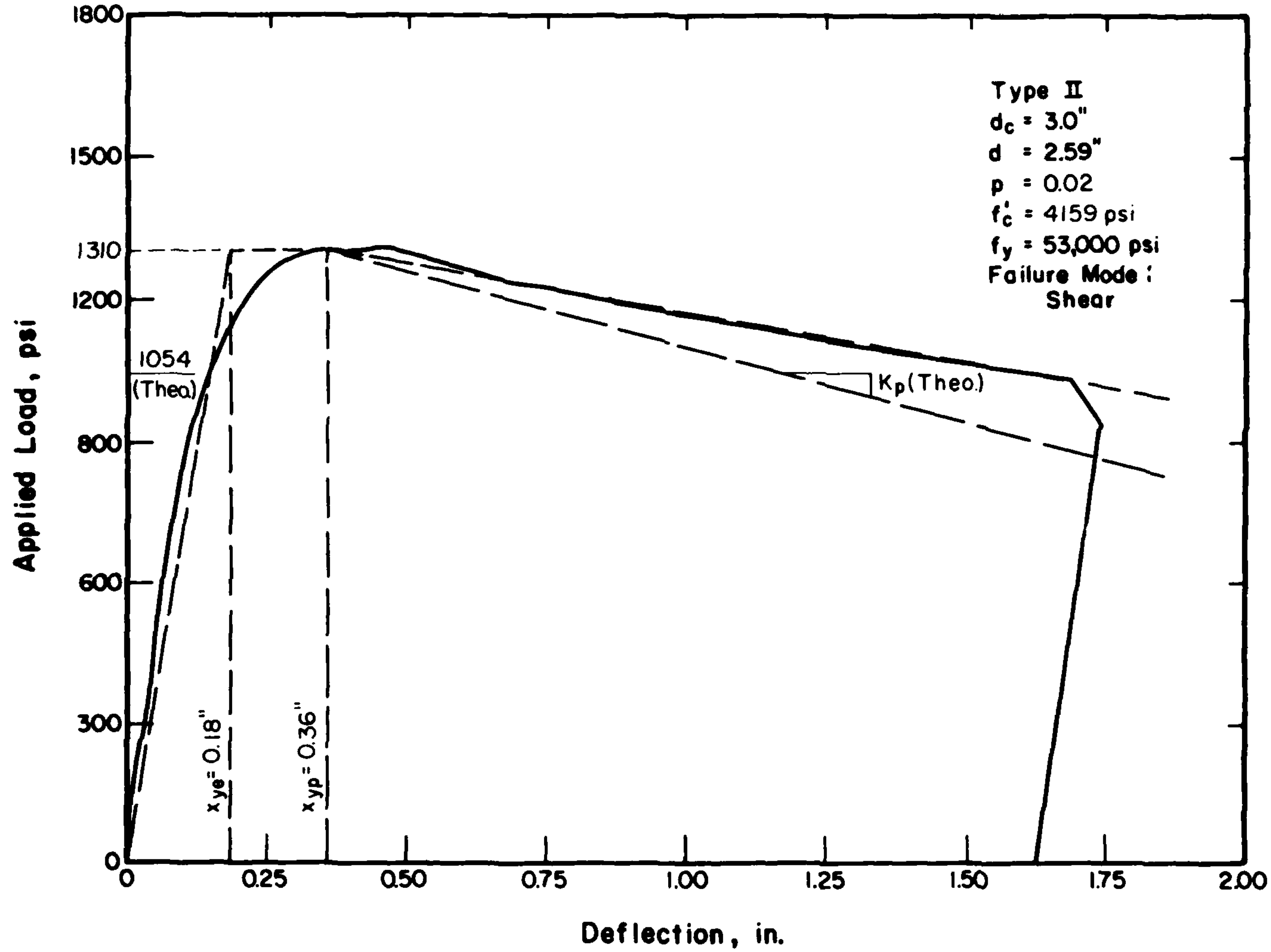

FIG. 36 LOAD-DEFLECTION CURVE FOR SLAB NO. 40

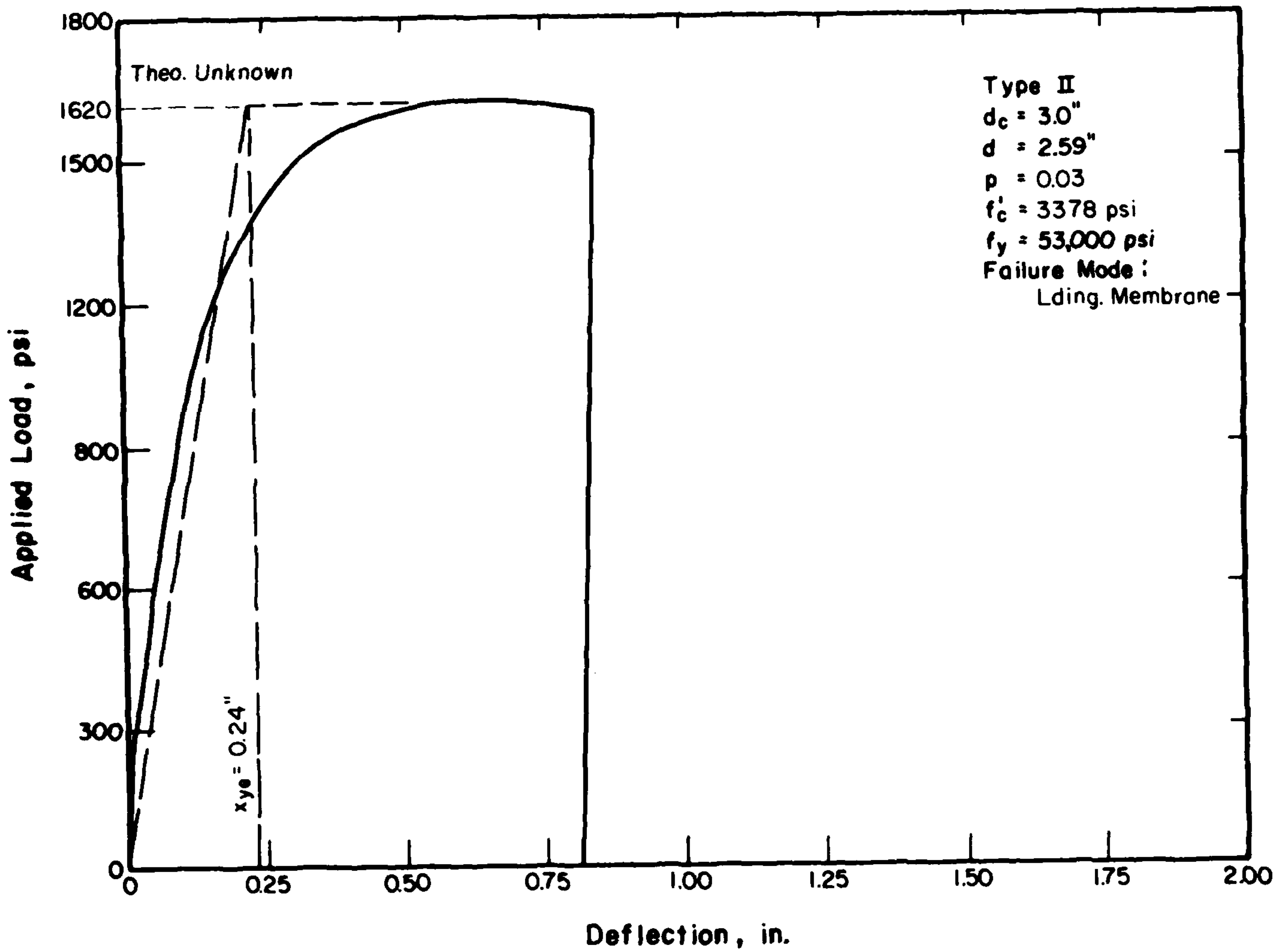

FIG. 37 LOAD-DEFLECTION CURVE FOR SLAB NO. 41

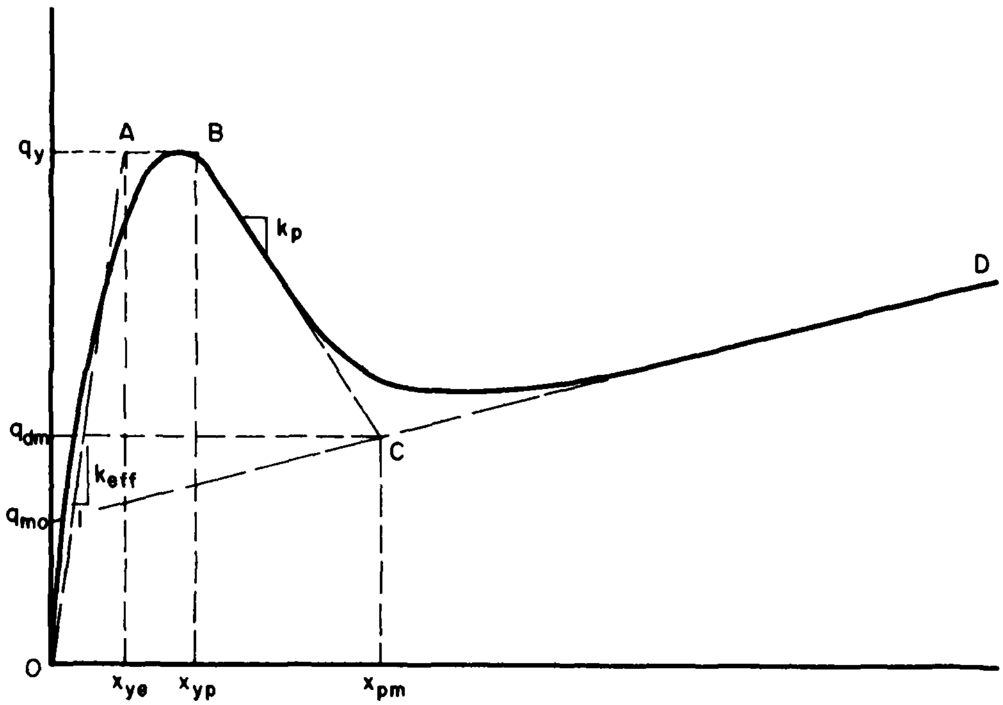

FIG. 38 IDEALIZED LOAD-DEFLECTION CURVE

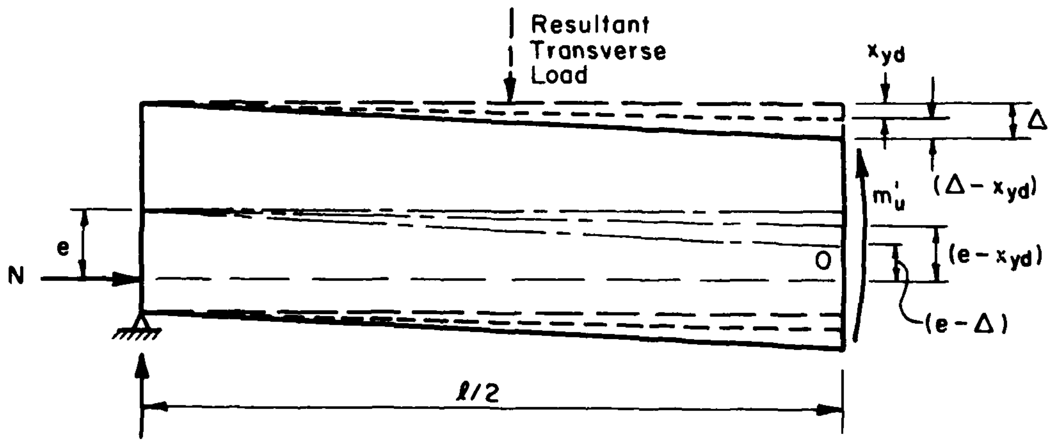

FIG. 39 EFFECT OF DEFLECTION ON MOMENT AUGMENTATION BY ECCENTRIC APPLICATION OF LATERAL RESTRAINT

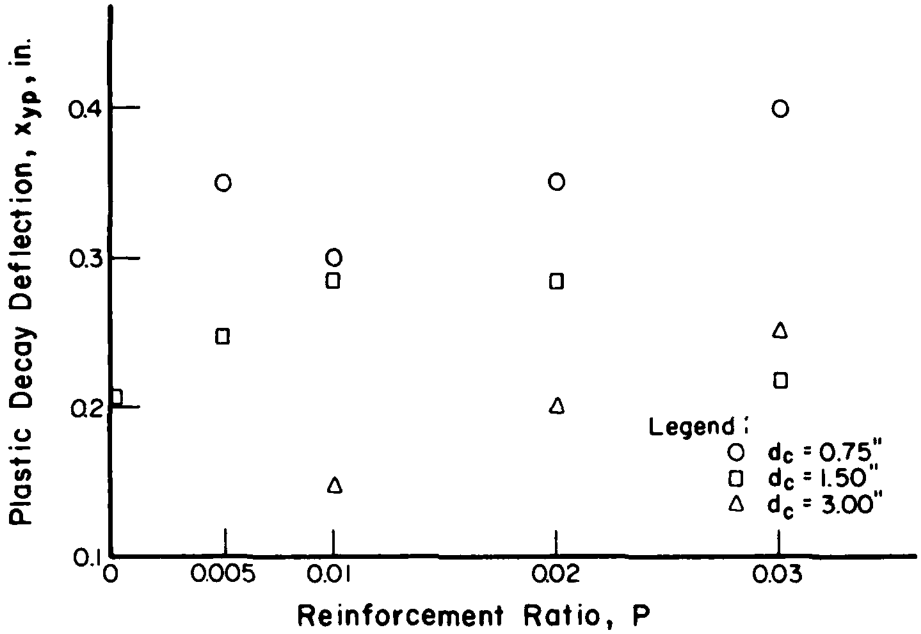

(a) For Type I Slabs

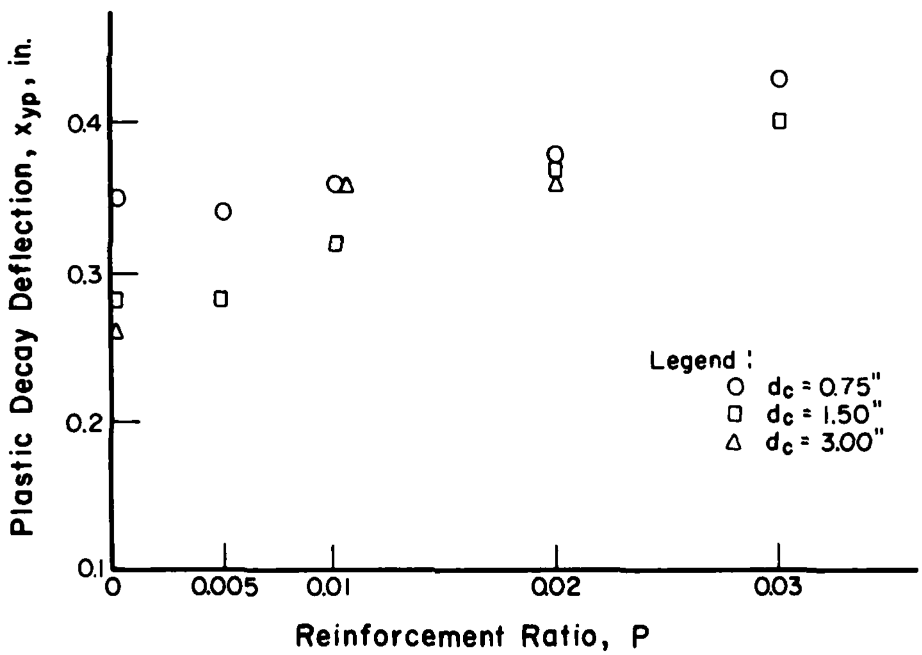

(b) For Type II Slabs

FIG. 40 EFFECT OF REINFORCEMENT RATIO ON PLASTIC DECAY DEFLECTION

References

1. Brotchie, John F; Jacobson, Ammon; and Okubo, Sadaji - "Effect of Membrane Action on Slab Behavior", Aug. 1965, Report R65-25 prepared by Mass. Inst. of Tech. for U.S. Naval Civil Engineering Laboratory.

2. Haltiwanger, J. D.; Hall, W. J.; and Newmark, N. M. - "Approximate Methods for the Vulnerability Analysis of Structures Subjected to the Effects of Nuclear Blast", June 15, 1976, Report No. U-275-76, N. M. Newmark Consulting Engineering Services, Urbana, Illinois.

3. Newmark, N. M. and Haltiwanger, J. D. - "Air Force Design Manual - Principles and Practices for Design of Hardened Structures", Dec. 1962, AFSWC-TDR-62-138.

Appendix

EXCERPTS FROM REFERENCE 1

For convenient reference, Chapter II and selected tables and figures from Ref. 1 are reproduced on the pages that follow. Ref. 1 is:

"Effect of Membrane Action on Slab Behavior" by John F. Brotchie, Ammon Jacobson, and Sadaji Okubo, Aug. 1965, Report R65-25, prepared by Massachusetts Institute of Technology for the U.S. Naval Civil Engineering Laboratory.

This reproduction is made with the permission of Dr. Warren H. Shaw, Head, Civil Engineering Department, USNCEL.

CHAPTER II

EXPERIMENTAL INVESTIGATION

SUMMARY

The experimental phase of the project consisted of the testing of 45 square slabs, of plain and reinforced concrete, under uniform loading. Form parameters varied were slab thickness, and reinforcement ratio; and boundary conditions considered were: fixed; simply supported; and restraint to axial displacement (elongation) only. The slabs were tested in a highly rigid steel frame, under incremental hydrostatic loading. Measurements were made of deflection at the center of the slab and near the supports, at each loading increment to failure. In the case of slabs which were restrained against elongation only, the restraining forces around the edge were also measured.

2.1 SLAB SPECIMENS

2.1.1 Form parameters:

The span in each case was 15" x 15"

Slab thicknesses used were 0.75", 1.5", and 3", resulting in span depth ratios of 20, 10 and 5.

Overall plan dimensions were 15.75" x 15.75" and 29" x 29".

Lower reinforcement only was used and was distributed uniformly and equally in each direction.

Reinforcement ratios were 0%, 0.5%, 1%, 2%, and 3%.

2.1.2 Boundary conditions:

The boundary conditions considered were as follows:

I. Restrained at edges against axial elongation only, at approximate level of reinforcement, by 24 cells (15.75" x 15.75" slabs).

II. Same external restraint condition as I but with added resistance to internal shear in the slab at the support (15.75" x 15.75" slabs)

III. Same as I but with level of restraining force at middle surface of the slab (one slab only, 15.75" x 15.75" slab)

IV. Clamped plate - continuous over support and restrained at the edge by Talurit plastic putty, and on the top and bottom faces, by the top plate and base plate respectively. (29" x 29" slabs)

V. Simply supported on 0.75" diameter roller bearings (15.75" x 15.75" slabs)

Further details are given in Table 1 and Fig. 1.

2.1.3 Materials and preparation:

A technique for modeling reinforced concrete structures with small scale reinforced mortar, or micro concrete, was developed in the Civil Engineering Models Laboratory at M.I.T., and has been utilized in the slab design.

Reinforcement consisted of spherodized bright annealed round wires to specification C 1040 with well defined yield zone varying from 53,000 to 60,000 psi for different wire gauges as given in Table 1.

Wire sizes used were 13g for 0.75" slabs, 10g for 1.5" slabs and 5g for 3" slabs. The wire was annealed at 1200°F for 20 minutes.

Reinforcement was held in position by light spot welds or wire ties. Steel bearing surfaces were cast into the slabs at restrained edges. Moulds were of steel for the 15.75" x 15.75" slabs and of treated aluminum for the 29" x 29" slabs, and were fabricated with a high degree of rigidity. All surfaces were accurately machined.

The slabs were cast of micro concrete. High early strength Velo type III cement was used, with water cement ratios of 0.70-0.72. The aggregate was New Jersey fine mortar sand graded between sieve sizes 8 and 200, so that the concrete is modeled to a scale of the order of 1:10.

Slabs were cured for 19 days at 95 to 100% humidity and a temperature of 70 to 75°F. They were removed and allowed to air dry for one day before testing. Concrete cylinders of the same mix were cured similarly and tested the same day as the slabs. Concrete strengths were of the order of 4000 to 5000 psi as given in Table 1. A range of cylinder sizes from 1" diameter to 3" diameter were tested to check on scale effect.

2.2 TEST APPARATUS

2.2.1 Restraining load cells

The lateral restraining force at the edge of the slab (15.75" x 15.75") was provided by 24 steel load cells (Figs. 1 and 2) each 2" wide, of variable thickness, and 7.5" long. Twelve of these were wired with electrical resistance strain gauges for measuring the restraining force. The load cells were distributed uniformly around the edge of the slab, with the live cells located on two adjacent sides. The live cells were calibrated individually, from 0 to 12,000 lbs, and were temperature compensated.

2.2.2 Restraining frame

The steel restraining frame (Figs. 2 and 3) was designed for essentially complete lateral rigidity, and also vertical rigidity. The main component is a box frame welded from 12" x 1.5" and 12" x 1" plates, and a 4" x 3" solid edge strip. A 1.5" thick, ribbed top plate provides the action to vertical loading and is connected to the box frame by 4 - 2" HT bolts. All bearing surfaces are accurately machined.

2.2.3 Loading system

Loading is provided through a neoprene membrane by hydraulic fluid. The fluid was stored in a reservoir from which it was pumped into the loading membrane cell. Two pumps of different capacities were used to allow accurate adjustment of the load and predetermined loading rates.

2.2.4 Measurements

Slab deflections were measured at the center and near two edges with 0.001" dial type deflection gauges. On the unrestrained slabs, lateral displacements of the edge were similarly measured. Measurements were recorded to the nearest 0.001" inches.

Applied uniform loading was measured on the relevant two of a series of six Master Test pressure gauges (accuracy: 0.25% of maximum reading) with ranges 0-20 psi, 0-60 psi, 0-100 psi, 0-200 psi, 0-1000 psi, and 0-2000 psi.

Restraining forces in each of the twelve load cells were recorded automatically on a multi-channel oscillograph recorder.

2.3 PROCEDURE

Slabs were tested at the rate of approximately two per week over a 24 week period between April and October, 1964.

Testing occurred 20 days after pouring of the slab, and one day after removal from the humidity room.

Loading increments were applied by means of hand pumps at approximately constant rate of slab deflection, between readings.

Load, deflection, and restraining forces were recorded for each loading increment to failure.

Cracking of the slab was recorded by visual observation, and on photographic film.

The loading system was designed with a high reaction modulus to enable the unstable portions of the load deflection and load restraining force curves to be accurately followed, and to provide sensitivity to slab deformation and safety at high pressures.

TABLE I

SLAB DETAILS

Slab No.	Slab Thick-ness t(inches)	Type of Restraint	Reinforce-ment Ratio p (%)	Effect-ive Depth d(inches)	Gauge of Steel Wire	Distance of Restraint from Bottom of Slab (inch)	Concrete Strength f'_c (psi)	Overall Size of Slab (ins)
4	0.75	I	1.0	0.56	No. 13 (0.0915"D)	3/16	4261	15.75 x 15.75
5	"	I	0	0.75	-	"	3509	"
6	"	I	0.5	0.56	No. 13	"	4528	"
7	"	I	2.0	0.56	"	"	4413	"
8	"	V	1.0	0.56	"	"	4413	"
9	"	V	3.0	0.56	"	"	4043	"
10	"	I	3.0	0.56	"	3/16	4043	"
11	1.5	I	0	1.50	-	3/8	4365	"
12	"	V	1.0	1.22	No. 10 (0.1350"D)	"	4223	"
13	"	I	1.0	1.22	"	3/8	4223	"
14	"	I	2.0	1.22	"	"	4585	"
15	"	V	3.0	1.22	"	"	3473	"
16	"	I	3.0	1.22	"	3/8	3473	"
17	"	I	0.5	1.22	"	"	3554	"
18	3	I	0	3.00	-	1/2	3421	"
19	"	V	1.0	2.59	No.5 (0.2070"D)	"	2925	"
20	"	I	1.0	2.59	"	"	2925	"

TABLE I (cont.)

Slab No.	Slab Thick-ness t(inches)	Type of Restraint	Reinforce-ment Ratio p (%)	Effect-ive Depth d(inches)	Gauge of Steel Wire	Distance of Restraint from Bottom of Slab (inch)	Concrete Strength f'_c (psi)	Overall Size of Slab (ins)
21	3	I	2.0	2.59	No.5 (0.2070"D)	1/2	3341	15.75 x 15.75
22	"	I	3.0	2.59	"	"	4123	"
23	"	V	3.0	2.59	"	"	4123	"
24	"	I	0.5	2.59	"	1/2	3551	"
25	3	III	0	3.00		1 1/2	4387	"
26	"	I	0	3.00		1/2	4387	"
27	1.5	II	0	1.50		3/8	4205	"
28	"	II	0.5	1.22	No. 10	"	4774	"
29	"	II	1.0	1.22	"	"	4487	"
30	"	II	3.0	1.22	"	"	4510	"
31	"	II	2.0	1.22	"	"	3620	"
32	0.75	II	0	0.75		3/16	4721	"
33	"	II	0.5	0.56	No. 13	"	4721	"
34	"	II	1.0	0.56	"	"	5041	"
35	"	II	2.0	0.56	"	"	5041	"
36	"	II	3.0	0.56	"	"	5540	"
37	3	II	0	3.00		1/2	3738	"
38	"	II	0.5	2.59	No. 5	"	3738	"
39	"	II	1.0	2.59	"	"	4159	"
40	"	II	2.0	2.59	"	"	4159	"
41	"	II	3.0	2.59	"	"	3378	"

TABLE I (cont.)

Slab No.	Slab Thickness t (inches)	Type of Restraint	Reinforcement Ratio p (%)	Effective Depth d(inches)	Gauge of Steel Wire	Distance of Restraint from Bottom of Slab (inch)	Concrete Strength f'_c	Overall Size of Slab (ins)
42	0.75	IV	0	0.75			5057	29" x 29"
44	0.75	IV	0	0.75			4321	"
45	1.5	IV	0	1.50			4273	"
46	0.75	IV	1.0	0.56	No. 13		5491	"
47	1.5	IV	1.0	1.22	No. 10		4565	"
48	0.75	IV	2.0	0.56	No. 13		4870	"
49	1.5	IV	2.0	1.22	No. 10		4619	"

Notes.

1) All slabs span 15" x 15"

2) All slabs are square and are uniformly and isotropically reinforced, resulting in four-fold symmetry.

3) Restraint types

I : restraint to elongation at approximate level of reinforcement by 24 restraining cells.
II : same as I but with shear reinforcement.
III : same as I but with restraint at middle depth.
IV : clamped: slab continued approximately 7" into support all around.
V : simple support: zero lateral restraint

4) Wire properties: C1040 spherodized annealed

Gauge		Yield	Ultimate
13 gauge wire	:	60. ksi	74.7 ksi
10 gauge wire		55. ksi	70.0 ksi
5 gauge wire	:	53. ksi	70.3 ksi

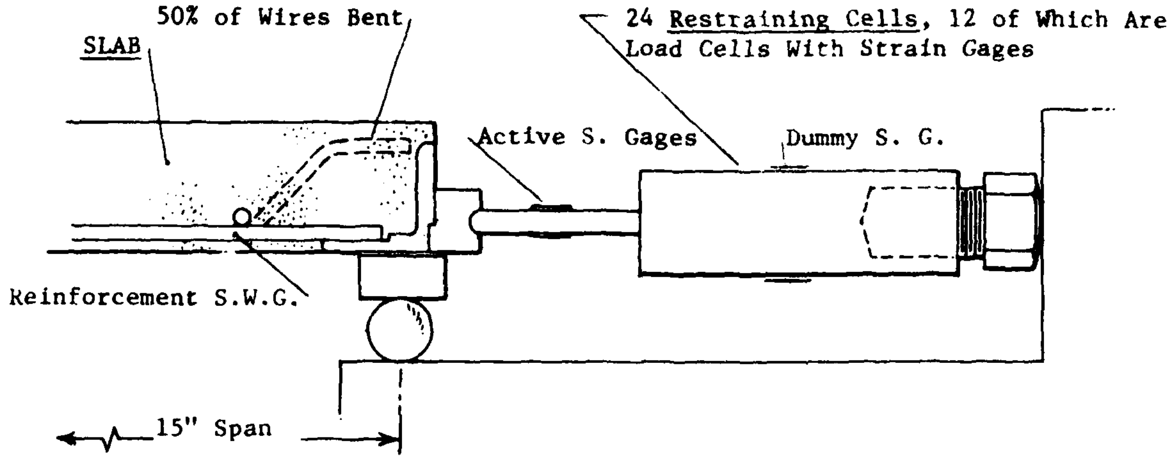

(a) DETAIL FOR SLABS TYPE II

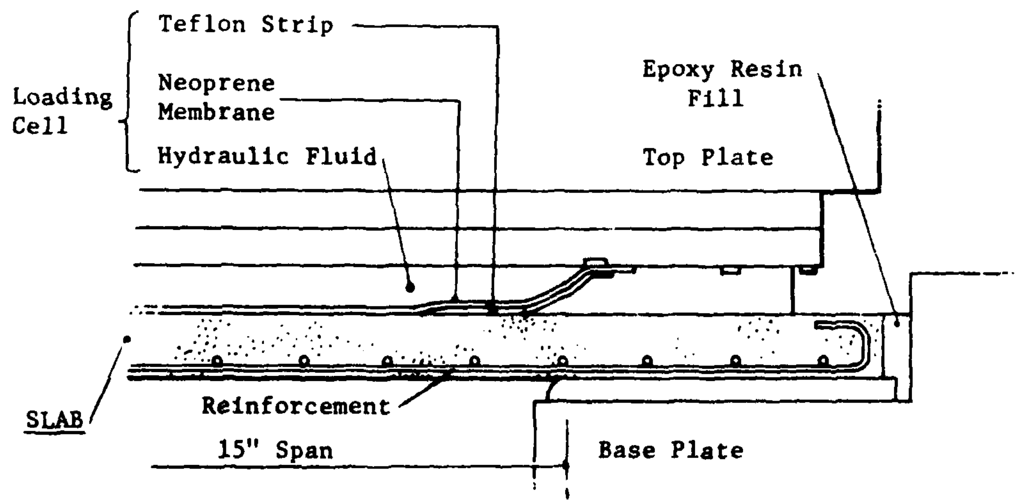

(b) DETAIL FOR SLABS TYPE IV

FIGURE 1: SLAB SPECIMENS - EDGE DETAILS

NOTE:

12 of the Restraining Cells
Are Load Cells (L.C. #1 - #12).

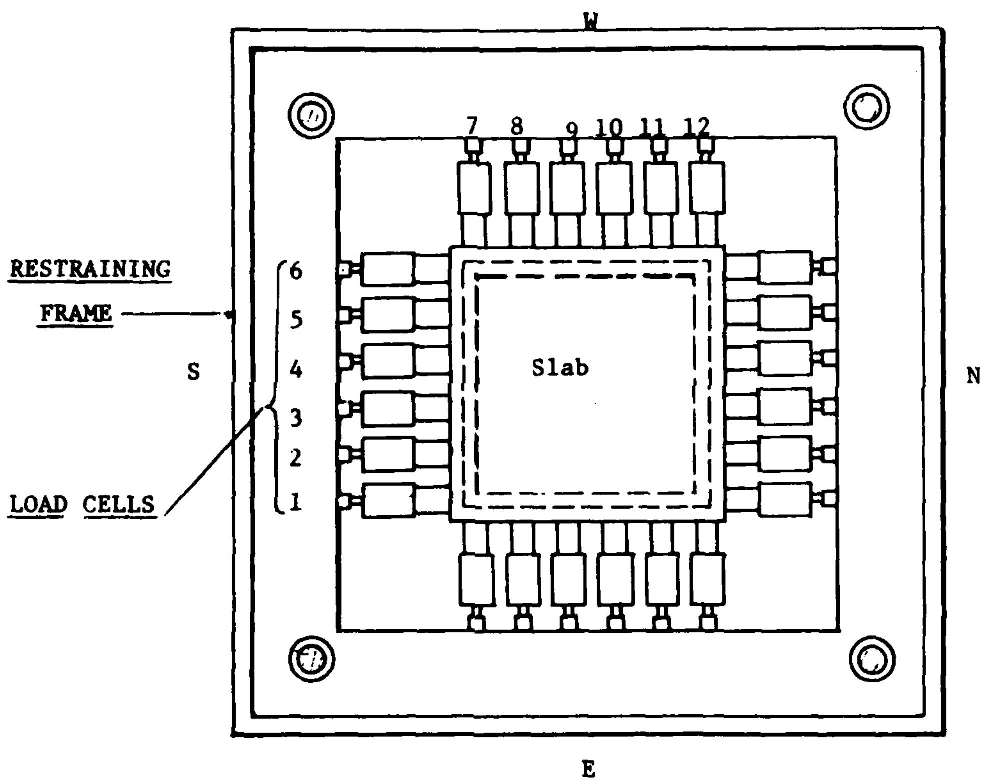

PLAN

FIGURE 2: RESTRAINING LOAD CELLS
- ARRANGEMENT IN RESTRAINING FRAME.

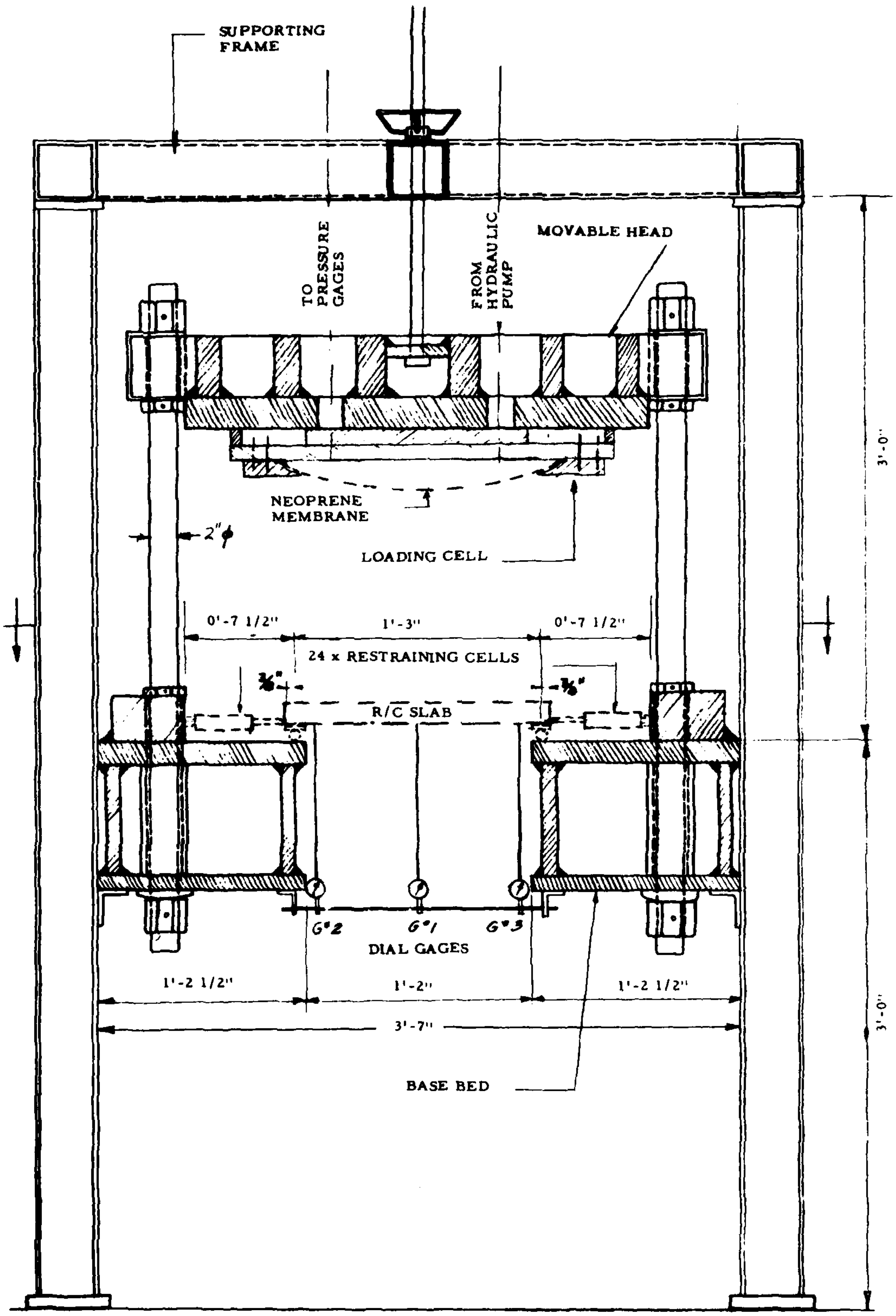

ELEVATION

FIG. 3: TESTING FRAME

DISTRIBUTION LIST

DEPARTMENT OF DEFENSE

Assistant to the Secretary of Defense
Atomic Energy
ATTN: Executive Assistant

Defense Advanced Rsch. Proj. Agency
ATTN: TIO

Defense Intelligence Agency
ATTN: DB-4C2, B. Morris
ATTN: RDS-3A
ATTN: DB-4C3
ATTN: DB-4C1

Defense Nuclear Agency
ATTN: DDST
ATTN: STSP
2 cy ATTN: SPSS
4 cy ATTN: TITL

Defense Technical Information Center
12 cy ATTN: DD

Field Command
Defense Nuclear Agency
ATTN: FCPR
ATTN: FCTMOF

Field Command
Defense Nuclear Agency
Livermore Division
ATTN: FCPRL

Interservice Nuclear Weapons School
ATTN: TTV

Joint Strat. Tgt. Planning Staff
ATTN: JLTW-2
ATTN: XPFS
ATTN: JSTPS/JLA, R. Haag
ATTN: NRI-STINFO Library

NATO School (SHAPE)
ATTN: U.S. Documents Officer

Undersecretary of Defense for Rsch. & Engrg.
ATTN: Strategic & Space Systems (OS)

DEPARTMENT OF THE ARMY

BMD Advanced Technology Center
Department of the Army
ATTN: ATC-T
ATTN: 1CRDABH-X

BMD Systems Command
Department of the Army
ATTN: BMDSC-H, N. Hurst

Chief of Engineers
Department of the Army
ATTN: DAEN-MCE-D
ATTN: DAEN-RDM

Construction Engineering Rsch. Lab
Department of the Army
ATTN: CERL-SOI-L

DEPARTMENT OF THE ARMY (Continued)

Deputy Chief of Staff for Rsch., Dev., & Acq.
Department of the Army
ATTN: DAMA-CSS-N

Engineer Studies Center
Department of the Army
ATTN: DAEN-FES, LTC Hatch

Harry Diamond Laboratories
Department of the Army
ATTN: DELHD-N-P
ATTN: DELHD-I-TL

U.S. Army Armament Material Readiness Command
ATTN: MA Library

U.S. Army Ballistic Research Labs
ATTN: DRDAR-BLT, A. Ricchiazzi
ATTN: DRDAR-BLE, J. Keefer
ATTN: DRDAR-BLV
ATTN: DRDAR-BLT, C. Kingery
ATTN: DRDAR-BLT, W. Taylor

U.S. Army Communications Command
ATTN: Technical Reference Division

U.S. Army Engineer Center
ATTN: ATZA

U.S. Army Engineer Div., Huntsville
ATTN: HNDED-SR

U.S. Army Engineer Div., Ohio River
ATTN: ORDAS-L

U.S. Army Engineer School
ATTN: ATZA-DTE-ADM
ATTN: ATZA-CDC

U.S. Army Engr. Waterways Exper. Station
ATTN: Library
ATTN: WESSA, W. Flathau
ATTN: WESSS, J. Ballard
ATTN: F. Brown

U.S. Army Foreign Science & Tech. Ctr.
ATTN: DRXST-SD

U.S. Army Material & Mechanics Rsch. Ctr.
ATTN: Technical Library

U.S. Army Materiel Dev. & Readiness Cmd.
ATTN: DRXAM-TL

U.S. Army Missile Command
ATTN: RSIC
ATTN: DRDMI-XS

U.S. Army Mobility Equip. R&D Cmd.
ATTN: DRDME-WC
ATTN: DRDME-HT, A. Tolbert

U.S. Army Nuclear & Chemical Agency
ATTN: Library

DEPARTMENT OF THE ARMY (Continued)

U.S. Army War College
ATTN: Library

U.S. Military Academy
ATTN: R. La Frenz

DEPARTMENT OF THE NAVY

David Taylor Naval Ship R&D Ctr.
ATTN: Code 1740, R. Short
ATTN: Code 1700, W. Murray
ATTN: Code 177, E. Palmer
ATTN: Code L42-3

Naval Construction Battalion Center
ATTN: Code L51, W. Shaw
ATTN: Code L51, R. Odello
ATTN: Code L51, J. Crawford
ATTN: Code L51, S. Takahashi

Naval Explosive Ord. Disposal Fac.
ATTN Code 504, J. Petrousky

Naval Facilities Engineering Command
ATTN: Code 09M22C

Naval Ocean Systems Center
ATTN: Code 4471
ATTN: Code 013, E. Cooper

Naval Postgraduate School
ATTN: Code 0142 Library
ATTN: Code 1424 Library

Naval Research Laboratory
ATTN: Code 8403, R. Belsham
ATTN: Code 2627
ATTN: Code 8440, F. Rosenthal

Naval Sea Systems Command
ATTN: SEA-06J, R. Lane
ATTN: SEA-09G53

Naval Ship Engineering Center
ATTN: SEC-6105D
ATTN: Code 09G3

Naval Surface Weapons Center
ATTN: Code R10
ATTN: Code R14
ATTN: Code U401, M. Kleinerman
ATTN: Code F31

Naval Surface Weapons Center
ATTN: Tech. Library & Info. Services Branch

Naval War College
ATTN: Code E-11 (Tech. Service)

Naval Weapons Center
ATTN: Code 266, C. Austin
ATTN: Code 233

Naval Weapons Evaluation Facility
ATTN: Code 10

Office of Naval Research
ATTN: Code 715

DEPARTMENT OF THE NAVY (Continued)

Strategic Systems Project Office
Department of the Navy
ATTN: NSP-43

DEPARTMENT OF THE AIR FORCE

Aerospace Defense Command
Department of the Air Force
ATTN: XPX

Air Force Armament Laboratory
ATTN: DLYV, J. Collins

Air Force Institute of Technology
ATTN: Library
ATTN: Commander

Air Force Weapons Laboratory
Air Force Systems Command
ATTN: DES-C, R. Henny
ATTN: DE, M. Plamondon
ATTN: SUL
ATTN: DES-G, S. Melzer
ATTN: DED

Ballistic Missile Office
Air Force Systems Command
ATTN: DEB

Ballistic Missile Office
Air Force Systems Command
ATTN: MNNH
ATTN: MMH

Deputy Chief of Staff
Research, Development, & Acq.
Department of the Air Force
ATTN: R. Steere

Deputy Chief of Staff
Logistics & Engineering
Department of the Air Force
ATTN: LEEE

Foreign Technology Division
Air Force System Command
ATTN: NIIS Library

Headquarters Space Division
Air Force Systems Command
ATTN: DYS

Headquarters Space Division
Air Force Systems Command
ATTN: RSS, D. Dowler

Rome Air Development Center
Air Force Systems Command
ATTN: RBES, R. Mair
ATTN: Commander
ATTN: TSLD

Strategic Air Command
Department of the Air Force
ATTN: NRI-STINFO Library

U.S. Air Force Academy
ATTN: DFCEM, W. Fluhr

DEPARTMENT OF ENERGY

Department of Energy
Albuquerque Operations Office
ATTN: CTID

Department of Energy
ATTN: Document Control for OMA/RD&T

Department of Energy
Nevada Operations Office
ATTN: Mail & Records for Technical Library

DEPARTMENT OF ENERGY CONTRACTORS

Lawrence Livermore Laboratory
ATTN: Document Control for J. Thomsen
ATTN: Document Control for Tech. Info. Dept. Lib.
ATTN: Document Control for R. Dong

Los Alamos Scientific Laboratory
ATTN: Document Control for M/5632, T. Dowler

Oak Ridge National Laboratory
ATTN: Document Control for Central Research Lab.

Sandia Laboratories
ATTN: Document Control for A. Chabai

OTHER GOVERNMENT AGENCIES

Department of the Interior
Bureau of Mines
ATTN: Technical Library

Department of the Interior
U.S. Geological Survey
ATTN: D. Roddy

Federal Emergency Management Agency
ATTN: Hazard Eval. & Vul Red. Div., G. Sisson

NASA
ATTN: R. Jackson

U.S. Nuclear Regulatory Commission
ATTN: R. Whipp for Div. of Sec. for L. Shao

DEPARTMENT OF DEFENSE CONTRACTORS

Acurex Corp.
ATTN: J. Stockton

Aerospace Corp.
ATTN: L. Selzer
2 cy ATTN: Technical Information Services

Agbabian Associates
ATTN: C. Bagge
ATTN: M. Agbabian

Analytic Services, Inc.
ATTN: G. Hesselbacher

Applied Theory, Inc.
2 cy ATTN: J. Trulio

ARTEC Associates, Inc.
ATTN: S. Gill

DEPARTMENT OF DEFENSE CONTRACTORS (Continued)

AVCO Research & Systems Group
ATTN: W. Broding
ATTN: Library A830

BDM Corp.
ATTN: T. Neighbors
ATTN: Corporate Library

BDM Corp.
ATTN: R. Hensley

Bell Telephone Labs.
ATTN: J. White

Boeing Co.
ATTN: Aerospace Library
ATTN: R. Dyrdahl
ATTN: J. Wooster
ATTN: R. Holmes

California Institute of Technology
ATTN: T. Ahrens

California Research & Technology, Inc.
ATTN: K. Kreyenhagen
ATTN: Library

California Research & Technology, Inc.
ATTN: D. Orphal

Civil Systems, Inc.
ATTN: J. Bratton

University of Denver, Colorado Seminary
ATTN: Sec. Officer for J. Wisotski

EG&G Washington Analytical Services Center, Inc.
ATTN: Library
ATTN: Director

Electric Power Research Institute
ATTN: G. Sliter

Electromechanical Sys. of New Mexico, Inc.
ATTN: R. Shunk

Eric H. Wang, Civil Engineering Rsch. Fac.
ATTN: N. Baum
ATTN: D. Calhoun

Franklin Institute
ATTN: Z. Zudans

Gard, Inc.
ATTN: G. Neidhardt

General Dynamics Corp.
ATTN: K. Anderson

General Electric Company—TEMPO
ATTN: DASIAC

General Research Corp.
ATTN: B. Alexander

H-Tech Labs, Inc.
ATTN: B. Hartenbaum

DEPARTMENT OF DEFENSE CONTRACTORS (Continued)

IIT Research Institute
ATTN: A. Longinow
ATTN: Documents Library

J. H. Wiggins Co., Inc.
ATTN: J. Collins

Kaman AviDyne
ATTN: Library
ATTN: E. Criscione

Kaman Sciences Corp.
ATTN: D. Sachs
ATTN: Library

Karagozian and Case
ATTN: J. Karagozian

Management Science Associates
ATTN: K. Kaplan

Martin Marietta Corp.
ATTN: G. Fotieo
ATTN: A. Cowan

Martin Marietta Corp.
ATTN: J. Donathan

University of Massachusetts
ATTN: W. Nash

McDonnell Douglas Corp.
ATTN: R. Halprin

Merritt CASES, Inc.
ATTN: Library
ATTN: J. Merritt

Mitre Corp.
ATTN: Director

Nathan M. Newmark Consult. Eng. Svcs.
ATTN: N. Newmark
ATTN: J. Haltiwanger
ATTN: W. Hall

University of New Mexico
ATTN: G. Triandafalidis

University of Oklahoma
ATTN: J. Thompson

Pacifica Technology
ATTN: G. Kent
ATTN: R. Allen

Physics International Co.
ATTN: Technical Library

University of Pittsburgh
ATTN: M. Willims, Jr.

DEPARTMENT OF DEFENSE CONTRACTORS (Continued)

R & D Associates
ATTN: R. Port
ATTN: C. MacDonald
ATTN: J. Lewis
ATTN: Technical Information Center

Rand Corp.
ATTN: A. Laupa
ATTN: Library
ATTN: C. Mow

Science Applications, Inc.
ATTN: Technical Library

Science Applications, Inc.
ATTN: S. Oston

Science Applications, Inc.
ATTN: D. Maxwell

Science Applications, Inc.
ATTN: W. Layson
ATTN: G. Binninger

Southwest Research Institute
ATTN: W. Baker

SRI International
ATTN: G. Abrahamson

Systems, Science & Software, Inc.
ATTN: Library

Teledyne Brown Engineering
ATTN: J. Ravenscraft

Terra Tek, Inc.
ATTN: Library

Tetra Tech, Inc.
ATTN: Library
ATTN: L. Hwang

Texas A & M University System
ATTN: H. Coyle

TRW Defense & Space Sys. Group
ATTN: Technical Information Center
ATTN: A. Feldman
2 cy ATTN: P. Dai

TRW Defense & Space Sys. Group
ATTN: E. Wong
ATTN: G. Hulcher

Weidlinger Assoc., Consulting Engineers
ATTN: J. McCormick
ATTN: M. Baron

Weidlinger Assoc., Consulting Engineers
ATTN: J. Isenberg

Westinghouse Electric Corp.
ATTN: W. Volz